ARGININE AVAILABILITY IN CHRONIC KIDNEY DISEASE

By

GIN-FU CHEN

A DISSERTATION PRESENTED TO THE GRADUATE SCHOOL
OF THE UNIVERSITY OF FLORIDA IN PARTIAL FULFILLMENT
OF THE REQUIREMENTS FOR THE DEGREE OF
DOCTOR OF PHILOSOPHY

UNIVERSITY OF FLORIDA

2009

To my Mom for giving me life and love, and to my wife for love and patience

ACKNOWLEDGMENTS

This work would not have been possible without the love and support of many people. I would like to acknowledge these people who have made an impression on my life and career.

Most importantly, I would like to take some time to thank my mentor, Chris Baylis. I stress the word “mentor” and additionally call her a friend. Three years ago I found myself lost and reached out through a single e-mail. Her simple response to that e-mail will change my life forever. In three years under her guidance I have learned how to become a better scientist, student, presenter, teacher, mentor, and person. She will always hold a special place, not only in my career, but also in my life. My goal is to make her proud one day as a successful scientist.

I would like to thank my past and present lab members. When I joined the lab in 2006, You-Lin Tain showed me everything I needed to know about transitioning into the lab and showed me the work ethic needed to succeed. Jennifer Sasser is probably the sweetest human being I have ever met. Not only is she an excellent mother, scientist, and person, she will be my friend, and gossip partner, forever. Harold Snellen is the lab teddy bear and friend. These past years would not have been as enjoyable without you and your surfing videos. Natasha Moningka, or the little one, has help make these past years fly by, with her interesting conversations and her friendship in and out of lab. Bruce Cunningham crawls out of his cave every so often to bless us with his presence and golf stories. I will always cherish his friendship and rounds of golf. I would be remised to not say a special thanks to the Hungarians, Laszlo, Andrea, Mickey, and Andras. In the year they were in our lab I have developed more than any other point in my career. They will always be special to me and I miss them dearly. One day we will

meet up again, maybe in Hungary. Finally, a brief acknowledgment to those who have been a part of the Baylis lab during my time there: Cheryl Smith, Annette Kirabo, Leslie White, and Mark Cunningham…thanks for the friendship.

I would like to thank my committee. Charles Wood has been a mentor to me for my entire graduate career. I enjoyed out many interactions and looked forward to the wonderful Christmas potlucks. I have also known Charles Wingo since my first year in graduate school and he has always shown me respect and guidance. Sergey Zharikov played a significant role not only in my research but also as a friend. He has taught me as a scientist but has always treated me as a colleague and equal. Mark Segal has always shown me respect and never failed to acknowledge my presence. The impact of these gestures has more impact on a person's career and development is greater than one can imagine.

I would like to thank my friends and family. I have made very strong bonds and lifelong friendships these past 6 years. I will always remember the countless potlucks and cooking competitions. We have been through beach parties, weddings, and births. To my mother, a special thanks and dedication for sticking with her kids in times of hardship. Even through disappoints and pains she is a bright beacon for her desires and dreams to see her kids succeed. I would like to acknowledge my brothers and sister for never hassling and judging me. Finally, I would like to thank and dedicate this dissertation to my wife. For eight years she has shown great patience and love throughout the entire process. Although there were occasional periods of frustration she has always been a calming and loving presence. Also a quick and loving acknowledgement to my puppies.

Finally, I would like to acknowledge the precious animals that were sacrificed in all the studies. Without them discovery would not be possible. I owe a large debt to these gentle creatures for all they have allowed me to accomplish.

TABLE OF CONTENTS

page

ACKNOWLEDGMENTS 4

LIST OF TABLES 11

LIST OF FIGURES 12

ABSTRACT 15

CHAPTER

1 INTRODUCTION 17

Chronic Renal Disease and End-Stage Kidney Disease 17
Nitric Oxide Deficiency in CKD 18
Substrate Deficiency 19
L-Arginine 19
Endogenous Synthesis 19
Argininosuccinate Synthase and Argininosuccinate Lyase 20
Synthesis in CKD 21
Transport 22
Cationic Amino Acid Transporter 22
Transport in CKD 24
Metabolism of L-Arginine 25
Arginase 25
Arginase in CKD 26
ADMA: Endogenous Nitric Oxide Synthase Inhibitor 27
Synthesis and Metabolism 27
ADMA in CKD 28
Specific Aims 29
The 5/6 Ablation/Infarction Model 29
Puromycin Aminonucleoside 30
Fawn Hooded Hypertensive Rats 30
Aims 31
Specific Aim 1 31
Specific Aim 2 32
Specific Aim 3 32
Specific Aim 4 32

2 GENERAL METHODS 37

Surgical 5/6 Ablation/Infarction 37
Metabolic Cage Collection 38
Protein Quantification 39
Bradford Assay 39

Lowry Method 39
Tissue Harvest 40
NO_2^- + NO_3 Assay (NOx) 40
TBARS 41
Hydrogen Peroxide 42
Plasma and Urine Citrulline 42
L-Arginine/ADMA/SDMA Measurements 43
Creatinine Clearance 44
Renal Plasma Flow 44
Kidney Histology 45
Dehydration and Infiltration 45
Embedding 46
Sectioning 46
Periodic Acid-Schiff Staining (PAS) 46
Scoring Glomerulosclerosis 47
Western Blot 47
Tissue Homogenization 47
Tissue Fractionation 48
Sample Preparation 48
Gel Preparation 48
Loading and Electrophoresis 49
Transfer 49
Ponceau Staining 50
Probing 50
Densitometry Analysis 51
Tissue DDAH Activity 51
Tissue Arginase Activity 53

3 *IN VIVO* RENAL ARGININE RELEASE IS IMPAIRED THROUGHOUT DEVELOPMENT OF 5/6 ABLATION/INFARCTION CHRONIC KIDNEY DISEASE 55

Introduction 55
Methods 56
In Vivo Renal Uptake of Citrulline 57
Renal Function 58
Calculations 58
Citrulline 58
L-Arginine Measurements 59
Western Blot 59
Histology 60
Statistics 60
Results 61
Discussion 62

4 REDUCED ARGININE AVAILABILITY IN PUROMYCIN AND 5/6 ABLATION INFARCTION INDUCED CHRONIC KIDNEY DISEASE DUE TO TRANSPORTER DYSFUNCTION 75

Introduction 75
Methods 76
Renal Function 77
Histology 78
Western Blot 78
CAT1 and PKC-α Western Blot 79
Arginase Assay 80
L-Arginine 80
Citrulline 81
Plasma and Urinary NOx 81
Statistics 81
Results 81
Discussion 83

5 ARGININE/ADMA SYNTHESIS AND METABOLIC PATHWAYS IN FAWN-HOODED HYPERTENSIVE RATS: A MODEL OF SPONATENOUS CHRONIC KIDNEY DISEASE; IMPACT OF DISEASE ATTENUATION ON ARGINASE 96

Introduction 96
Methods 97
Renal Function 98
Histology 98
Western Blot 99
Arginase Assay 100
DDAH Activity Assay 100
L-Arginine/ADMA/SDMA Measurements 100
Citrulline 101
Plasma and Tissue Oxidative Stress Measures 101
Tissue NOx 101
Statistics 101
Results 102
Discussion 103

6 ADMA ABUNDANCE AND REGULATION IN PUROMYCIN AND 5/6 ABLATION/INFARCTION INDUCED CHRONIC KIDNEY DISEASE 114

Introduction 114
Methods 115
Plasma L-Arginine/ADMA/SDMA 115
Oxidate Stress 115
Western Blot 116
DDAH Activity 116
Statistics 116

Results 117
Discussion 118

7 SUMMARY AND PERSPECTIVES 126

Summary 126
Aim 1 126
Aim 2 127
Aim 3 127
Aim 4 128
Connecting the Pathways 128
Spanning Animal Models of CKD 130
Limitations of Our Studies 132
Clinical Implications and Future Directions 133
Maintained Plasma L-Arg 133
L-Arginine Supplementation 134
Citrulline Supplementation 135
Mechanisms of ANGII Regulation of Arginase 138
Human L-Arg Deficiency 138
Final Thoughts 139

LIST OF REFERENCES 145

BIOGRAPHICAL SKETCH 164

LIST OF TABLES

Table		page
2-1	Western blot antibody list.	54
3-1	Physiological data and renal function for 5/6 ablation infarction CKD	70
3-2	Citrulline and L-Arginine concentrations in plasma and renal cortex citrulline	71
3-3	Effect of citrulline infusion on renal plasma flow (RPF) and resulting renal citrulline delivery	72
3-4	Proximal tubule uptake mechanisms of citrulline.	73
3-5	Urinary excretion of citrulline and L-Arginine factored for body weight at baseline and during citrulline infusion	74
4-1	Functional data for puromycin induced CKD	88
5-1	Functional data taken at time of sacrifice for FHH rats	108
5-2	L-Arginine/citrulline/ADMA concentrations and kidney cortex NOx concentrations	108
6-1	Measures of oxidative stress in puromycin CKD	122
6-2	Plasma concentrations of L-Arginine, ADMA, and SDMA	122

LIST OF FIGURES

Figure		page
1-1	Nitric oxide production in patients and animals with CKD/ERKD	34
1-2	Mechanisms of nitric oxide deficiency	35
1-3	Pathways of L-arginine synthesis and metabolism.	36
3-1	Renal uptake of citrulline and release of L-Arginine at baseline and during citrulline infusion	67
3-2	L-Arginine and citrulline A-V correlations.	68
3-3	Argininosuccinate synthase and lyase protein expression.	69
4-1	Timeline of PAN chronic kidney disease progression	89
4-2	Argininosuccinate synthase (ASS) and lyase (ASL) protein abundance	90
4-3	L-Arginine transporter and PKC-alpha protein abundance	91
4-4	L-Arginine metabolizing enzyme abundance and activity	93
4-5	Kidney cortex CAT and cellular fractions of PKC-α expression	95
5-1	Body weight, urine protein excretion and renal pathology	109
5-2	Arginine synthesizing enzyme abundance measured by western blot	110
5-3	Arginase protein abundance measured by western blot.	111
5-4	ADMA synthesizing and metabolizing enzyme abundance	112
6-1	Tissue abundance of L-Arginine methylating enzyme	123
6-2	Abundance and activity of AMDA metabolizing enzymes	124
6-3	ADMA in stages of 5/6 ablation/infarction chronic kidney disease	125
7-1	Regulation of L-Arginine and nitric oxide synthesis	141
7-2	Indices of disease severity in various CKD models	142
7-3	Plasma citrulline as a marker of renal injury	143
7-4	Renal DDAH activity and plasma ADMA values in various CKD models	144

LIST OF ABBREVIATIONS

ADMA	Asymmetric dimethylarginine
A/I	Ablation/infarction
ANG	Angiotensin
Arg	Arginine
ASS	Argininosuccinate synthase
ASL	Argininosuccinate lyase
A-V	Arterial-Venous
BP	Blood pressure
BW	Body Weight
CCr	24 hour clearance of creatinine
CKD	Chronic kidney disease
CVD	Cardiovascular disease
DDAH	Dimethylarginine dimethylaminohydrolase
ESKD	End-stage kidney disease
FHH	Fawn-Hooded Hypertensive
GFR	Glomerular filtration rate
GSI	Glomerulosclerosis Index
NO	Nitric oxide
NOS	Nitric oxide synthase
PAH	Para aminohippurate
PAN	Puromycin aminonucleoside
PNOx	Plasma nitrite plus nitrate levels
PRMT	Protein arginine methyltransferase
RPF	Renal plasma flow

ROS	Reactive oxygen species
SD	Sprague-Dawley
SHR	Spontaneously hypertensive rats
SDMA	Symmetric dimethylarginine
UNOxV	24hr urinary nitrite plus nitrate levels
UpV	24hr urinary protein excretion

Abstract of Dissertation Presented to the Graduate School
of the University of Florida in Partial Fulfillment of the
Requirements for the Degree of Doctor of Philosophy

ARGININE AVAILABILITY IN CHRONIC KIDNEY DISEASE

By

Gin-Fu Chen

December 2009

Chair: Chris Baylis
Major: Medical Sciences--Physiology and Pharmacology

Chronic kidney disease (CKD) affects over 26 million Americans and numbers are increasing every year. The mechanism of CKD progression to end-stage kidney disease (ESKD) is unknown but patients have shown reductions in nitric oxide (NO) production. The reduction in NO are hypothesized to increase endothelial dysfunction and further accelerates progression of renal injury. We studied the possible mechanisms of NO deficiency in various models of CKD, focusing on possible reduced NO synthase (NOS) substrate (L-arginine, L-Arg). The kidney is the major organ for circulating L-Arg synthesis, utilizing citrulline conversion by argininosuccinate synthase (ASS) and lyase (ASL). In a remnant kidney model we have shown that renal L-Arg release is impaired in early, moderate, and severe CKD. This is due to reduced renal citrulline delivery or uptake and ASS expression in the injured kidney. We have also shown in the remnant model and a podocyte injury induced model (puromycin aminonucleoside, PAN) that the protein abundance of the transporter involved in L-Arg secretion is reduced in addition to impaired uptake by endothelial cells. This would result in reduced L-Arg available to NOS within the endothelial cell. In addition, we found increased arginase activity and abundance, which metabolizes L-Arg into urea, in a model of spontaneously developing

CKD (Fawn hooded hypertensive rats). This would result in increased consumption of L-Arg and less available for NO production. The increased arginase was blocked by attenuating renal damage with angiotensin receptor blockade and resulted in higher plasma L-Arg concentrations. Lastly, the L-Arg that is able to enter the cell must then compete with endogenous NOS inhibitors, specifically asymmetric dimethylarginine (ADMA), for NOS. Enzymes that metabolize ADMA are highly abundant in the kidney and liver. We have found in the remnant model and in our PAN model, increased plasma ADMA levels and decreased renal activity of the enzymes responsible of ADMA metabolism.

Our studies, for the first time, demonstrate that L-Arg deficiency is present in various models and stages of CKD and this may partially explain the reduction in NO seen in patients and animals with CKD. Logically these data suggest a novel pathway for potential therapeutic intervention in the treatment of CKD.

CHAPTER 1
INTRODUCTION

Chronic Renal Disease and End-Stage Kidney Disease

As of 2007, approximately 20 million Americans had some evidence of chronic kidney disease (CKD) and are at risk to develop end-stage kidney disease (ESKD). Another 20 million are at increased risk for developing kidney disease (5). Older individuals are at higher risk and as the baby-boomers age the number of Americans with kidney disease is expected to increase significantly. Approximately 485,000 Americans have been diagnosed with ERKD and require ongoing, expensive and life-altering treatments, including frequent dialysis treatments or kidney transplantation, to stay alive. The annual cost of treating all ERKD patients is currently over $32 billion in America alone and the number of Americans with ERKD is expected to grow to 785,000 by 2020.

More than 1.6 million individuals worldwide underwent treatment for ERKD and the prevalence of CKD has increased 20-30% over the past decade and worldwide incidence of ERKD is projected to increase 5-8% each year (40). Nearly 1 million people die each year from complications from ERKD worldwide mostly from cardiovascular diseases (CVD) (46). These numbers are staggering and soon the cost associated with treatment of these patients will become unbearable. The annual costs to treat kidney disease are more than one quarter (27.6 percent) of Medicare's expenditures, and this will increase in the years to come (5).

Our challenge is stop the progression of CKD and to prevent the development of CVD and not just to treat those who have progressed to ERKD. To accomplish this we must study the common mechanisms found in patients and animals models of this

disease and understand the basic physiological mechanisms behind them. Many of these have already been addressed, including the role of the renin-angiotensin system, oxidative stress, and inflammation. Interestingly, these all have a common pathway in reducing nitric oxide (NO) bioavailability.

Nitric Oxide Deficiency in CKD

NO is an important messenger molecule in many physiological and pathophysiological processes. First discovered as an endothelium derived relaxing factor due to its role in smooth muscle relaxation, it is now known to have a plethora of actions including cellular proliferation, platelet aggregation, and cellular adhesion. NO is synthesized in many cell types including the vascular endothelium via NO synthase (NOS). There is a significant amount of evidence that chronic NOS inhibition causes systemic and glomerular hypertension, glomerular ischemia, glomerulosclerosis, and proteinuria (205). Thus, normal NO synthesis is necessary for normal renal function and health.

Net NO deficiency develops as a result of CKD both in patients and in animal models (15, 142, 143, 192) (Figure 1-1). This is measured as total urinary and plasma NOx (NO_2+NO_3), the stable oxidation products of NO. NO is produced throughout the body and one likely site of reduced NO synthesis is the endothelium, due to the endothelial dysfunction. The reduction in NO and associated endothelial dysfunction increases the incidence of CVD seen in CKD (46, 165). Most likely this increased cardiovascular risk due to CKD accelerates the progression of CKD into ERKD, thus creating a vicious cycle. Although no clinical evidence is available, animal studies also implicate intrarenal NO deficiency in CKD as a major factor in causing progression in various models (41-43, 161, 185, 205).

There are many ways by which net NO deficiency could develop, including reduced substrate (L-Arginine), reduced NOS abundance or activity, increased endogenous NOS inhibitors, or increased NO scavenging by reactive oxygen species (ROS) (Figure 1-2).

Substrate Deficiency

The major focus of this dissertation is on the possibility of reduced availability of L-Arginine (L-Arg), which may result from 1) reduced endogenous production, 2) impaired delivery of L-Arg to NOS and/or 3) diversion of L-Arg through other metabolic pathways. In addition to reducing NO production secondary to substrate limitation, L-Arg deficiency (by any mechanism) causes the neuronal (nNOS) and inducible NOS (iNOS) to become superoxide generators (21, 197).

L-Arginine

L-Arg is a “semi-essential” amino acid meaning that dietary intake is not required for the maintenance of an adult’s healthy appearance, normal eating pattern, reproductive capability, or nitrogen balance (108). This is due to the ability of a healthy adult to synthesize endogenous L-Arg at a rate sufficient for normal function. Under stress conditions however, L-Arg can become an essential amino acid (196). Plasma L-Arg is maintained constant in normal states by a delicate balance between its synthesis and metabolism.

Endogenous Synthesis

The source of endogenously produced circulating L-Arg is predominately via kidney synthesis and protein turnover. Approximately 60% of net L-Arg synthesis in the adult occurs in the kidney (196). The liver contains high levels of L-Arg synthesizing enzymes but utilizes the L-Arg for the urea cycle, the major pathway for the

detoxification of ammonia. Citrulline is the substrate for endogenous L-Arg synthesis and is derived primarily from glutamine metabolism in the small intestine, although some foods have high levels of citrulline (33). Citrulline is transported in the blood to the kidney and into the endothelium for conversion to L-Arg by argininosuccinate synthase (ASS) (57) and argininosuccinate lyase (ASL) (57, 106, 175, 196). Windmueller and Spaeth have shown that up to 85% of citrulline released by the small intestines is metabolized by the kidneys (193). Citrulline can be delivered to the proximal tubule via filtration then taken up by transporters located on the apical side, recently shown to be B(0)AT1 and b(0,+)AT (101), or by peritubular uptake by transporters on the basolateral membrane or organic anion transporter (OAT1) (109).

Argininosuccinate Synthase and Argininosuccinate Lyase

ASS is a cytosolic enzyme that catalyzes citrulline + aspartate + ATP into argininosuccinate + pyrophosphate + AMP. ASL catalyzes the reversible breakdown of argininosuccinate into Arg + fumarate. This enzyme exists in almost all organisms and is ubiquitously expressed with high levels in the liver and kidney (57). The ASS gene is well conserved between all organisms and resides on chromosome 9 (22) and the ASL gene is located on chromosome 7 (110).

Regulation of ASS and ASL expression occurs at the transcriptional level since there is no known post-translational modification. In the liver, glucocorticoids, glucagon and glutamine increase ASS and ASL expression while insulin, growth hormone and oleic acid reduce expression (57). Starvation increases expression of ASS and ASL presumably as a response to reduced citrulline (61). *In vivo* rates of L-Arg synthesis in healthy adults are limited primarily by the amount of citrulline produced by other organs rather than by the renal L-Arg biosynthetic capacity (38). In other words L-Arg synthesis

is usually substrate (citrulline) limited. The site of L-Arg synthesis in the kidney is the proximal tubule where expression of ASS and ASL is the largest (86). Although the entire proximal tubule synthesizes L-Arg, the early portion has the greatest activity of L-Arg synthesis and there is a progressive decline towards the straight segment. L-Arg synthesized in the convoluted portion is transported out into the peritubular capillaries and exits the kidney into the general circulation via the renal vein. In contrast, the majority (64%) of L-Arg from the proximal straight tubules is converted into urea and the remaining is released into the blood (86).

In normal conditions the rate of renal L-Arg synthesis is dependent on the rate of citrulline delivery to the proximal tubules. Levillain et al showed that L-Arg synthesis was proportional to extracellular citrulline concentration in isolated tubules up to 432µM (physiological range is ~60µM) (86). Dhanakoti et al demonstrated, *in vivo*, that increasing circulating concentrations of citrulline by 4 fold increased renal uptake and increased L-Arg synthesis by a similar extent (38). The healthy kidney was very sensitive to all the citrulline delivered to it, consistent with findings in humans (166).

In addition to the kidney, the vascular endothelium contains the necessary enzymes to synthesize L-Arg (52, 150, 157) by recycling the citrulline generated during local NO synthesis and, possibly, by uptake of circulating citrulline via neutral amino acid transporters (195).

Synthesis in CKD

In humans and experimental animals with CKD, plasma citrulline concentration is substantially elevated (13, 160). This probably does not reflect either increased citrulline intake/synthesis or decreased renal clearance since normally there is little or no urinary excretion of citrulline (38), and is presumed to reflect decreased renal conversion to L-

Arg. There is little information on the regulation of ASS or ASL enzymes in CKD. Chan et al reported marked reductions in renal L-Arg synthesis (even when factored for total kidney mass) whereas liver ASS activity was unchanged in nephrectomy induced CKD (27). Moradi et at showed a reduction in total renal ASS and ASL abundance in 5/6 nephrectomy due to failure of the remaining renal mass to increase expression (103). Tizianello et al showed a ~60% reductions in renal L-Arg production in patients with nondiabetic induced CKD (166). In contrast, Bouby et al suggested that renal L-Arg synthesis was maintained in moderate 5/6 ablation/infarction CKD due to a combination of proximal tubular hypertrophy (leading to increased L-Arg biosynthetic capacity), increased GFR to remnant nephrons (delivering more citrulline to the tubule for utilization by ASS and ASL), and increased plasma citrulline (increasing both filtration and peritubular delivery of citrulline) (18). The reason behind these opposing results is unknown and needs to be further studied. Additionally, there is no information on the endothelial activity/abundance of the ASS/ASL enzymes in clinical or experimental CKD.

Transport

Cationic Amino Acid Transporter

L-Arg that is produced by the proximal tubule must be secreted into the circulation and then taken up by endothelial cells to the site of NOS. Intracellular concentrations of L-Arg in endothelium are in the mM range, far in excess of the Km of eNOS; however, exogenous L-Arg boosts NO production *in vivo* (the “arginine paradox”). One possibility is that there are micro compartments within the cell and that intracellular L-Arg is not fully available to the membrane-bound eNOS, which therefore must rely on extracellular L-Arg entry via transporters. Transport in most cell types is via a system y+ , high

affinity, and sodium-independent transporter. System y+ is widely expressed and exhibits Km values for L-Arg of 80-100μM and is pH independent (30). Cationic amino acid transporter (CAT) has been shown to be the major transporter for L-Arg and function in L-Arg secretion by the proximal tubules and uptake by the vasculature. There are three members of the CAT family (CAT1, 2B, and 3) that conform to system y+. CAT1 has the highest affinity for L-Arg, while CAT2B (which is inducible in response to immune/inflammatory stimuli)(29) has a lower affinity and is more sensitive to pH changes (30). CAT3 activity in rat and mouse studies has shown very low activity in overexpressing cells (54). CAT3 is most abundant in the brain but shown to be expressed in the kidney at the message level (194).

Studies demonstrate that the primary endothelial cell L-Arg transporter, CAT1, co-localizes and interacts with eNOS in the membrane caveolus (100), providing a potential explanation to the "arginine paradox". Venema and colleagues have confirmed the findings of Block and colleagues that there is a stimulatory protein-protein interaction between caveolar CAT1 and eNOS (88). Overexpression of CAT1 in cells stimulated NO release but the increased NO was not due to increased transport of L-Arg. However, Zani and Bohlen reported that *in vivo*, lysine induced inhibition of L-Arg transport by CAT1, produced substantial and rapid falls in vascular NO production (204), indicating a role for L-Arg uptake in supplying substrate for endothelial NO synthesis. Interestingly Racusen et al has shown that lysine induces acute renal failure through tubular obstruction.(125). Perhaps the inhibition of NO release seen by Zani is due to reduced L-Arg synthesis by the injured kidney due to lysine and not solely from competitive inhibition? Additionally, studies have indicated that approximately 50% of

whole body NO synthesis in healthy adult humans is derived from circulating L-Arg (23), highlighting the importance of cellular uptake mechanisms.

These contrasting studies maybe due to compartmentalization of L-Arg into two separate pools shown in human endothelial cells and human umbilical endothelial cells. Simon et al (152) suggested one pool (pool I) was depleted by extracellular lysine inhibition; implying that transport from extracellular L-Arg was necessary. The second pool was not exchangeable with the extracellular space but was still accessible to eNOS. This pool originates from intracellular formation (from citrulline, pool IIA) and protein turnover (pool IIB).

Transport in CKD

One puzzling finding in CKD and ERKD patients is that plasma L-Arg levels are normal (13, 142, 143). A reduction in the rate at which L-Arg is transported from plasma into the endothelial cells might maintain plasma L-Arg levels and mask an intracellular L-Arg deficiency.

Schwartz et al studied glomerular and aortic L-Arg uptake, CAT1 and CAT2 mRNA expression, and CAT1 protein in rats with 5/6 nephrectomy CKD and observed decreases in glomerular and aortic L-Arg transport *in vitro* in CKD tissues versus shams (145). L-Arg transporter protein abundance was decreased, although not reflected by changes at the gene level demonstrating that posttranscriptional modifications can decrease CAT1 protein expression in CKD. Furthermore, posttranslational inhibition of CAT1 has been demonstrated by activation of protein kinase C (PKC)-alpha in porcine aortic endothelial cells (PAEC). Specifically, translocation of PKC-alpha to the plasma membrane induces phosphorylation of the CAT1 transporter, which inhibits transport activity in PAEC (80). Of note, angiotensin II (ANGII), a primary culprit in many forms of

CKD, stimulates multiple PKC isoforms (68). ANGII plays a major role in the pathogenesis of CVD and CKD.

L-Arg supplementation does not improve arterial endothelial function or reduce the rate of progression of renal failure in adults or children with CKD (12, 32, 36, 207). This could be due to the inability of administered L-Arg to be transported to the eNOS due to CAT defects described above.

Metabolism of L-Arginine

L-Arg that is produced by the proximal tubule and secreted into the circulation is subject to metabolism. L-Arg is a highly promiscuous amino acid and is involved in multiple pathways (Figure 1-3). Agamatine production via L-Arg decarboxylase makes up a small portion of L-Arg flux and the role of agamatine is not clearly understood although it may have actions as a neurotransmitter and endogenous inhibitor of NOS (47, 89). Creatine synthesis represents a sizable fraction of total body L-Arg usage. An average adult excretes about 1.5g of creatinine per day (184) and to maintain creatine homoeostasis this must be match by equimolar synthesis of creatine which requires about 2.3g of L-Arg per day (19, 23). L-Arg used in creatine synthesis is substantial but is a fixed amount. L-Arg utilization by NOS is comparatively low since the Vmax of NOS for L-Arg is low in comparison to arginase and NOS only accounts for about 1% L-Arg flux in normal adults (23).

Arginase

The most significant metabolism of L-Arg is via arginases, which are constitutively present and can also be induced in many different cell types. Arginase is metalloenzyme with two distinct isoforms (I and II) sharing 60% sequence homology. Arginase induction leads to extracellular matrix (ECM) proliferation and fibrosis

secondary to proline synthesis as well as cell proliferation secondary to polyamine synthesis in vascular smooth muscle and endothelial cells (90, 91, 190). In addition, since increased arginase activity decreases substrate availability to NOS and lowers NO production; the decreased NO exacerbates cell proliferation and ECM accumulation (7, 90). Arginases consume large quantities of L-Arg in the production of urea, proline and polyamines. In liver L-Arg is rapidly utilized by arginase I, a cytosolic enzyme, and recycled within the urea cycle (196). Arginase I is responsible for the majority of total body arginase activity. A deficiency in arginase I in humans and mice is associated with increased plasma L-Arg (hyperargininemia) and results in ammonia accumulation and early mortality (31, 60). The kidney contains arginase II and vascular endothelial cells contain both isoforms (20, 90, 135). Arginase II is also a substantial consumer of whole body L-Arg since plasma L-Arg increases 2 fold in the arginase II knock out mouse (151), however there is no distinguishable phenotype from wild-type. Arginase II is a mitochondrial enzyme. The signaling pathway for arginase regulation is not clearly understood although there is a potential role of the Jak-stat pathway and cAMP in the induction and activation of arginase within vascular smooth muscle cells (189).

Arginase in CKD

Arginase plays a role in the pathogenesis of a variety of diseases. Endothelial dysfunction associated with aging has been linked the vascular arginase. Inhibition of arginase with a specific inhibitor, (S)-(2-boronoethyl)-L-cysteine, HCl (BEC), in old rats results in significant vascular relaxation and both arginase isoforms are increased in blood vessels of old rats (14). Additionally, vascular arginase activity is increased in experimental hypertension in rats and the Apo-E knockout mouse model of atherosclerosis (37, 66, 134, 135, 206) and arginase “inhibition” (somewhat non

selective) restored endothelial NO synthesis and attenuated injury. Both arginase I and II are upregulated in the vasculature of Dahl salt-sensitive rats on high-salt (66) and in spontaneously hypertensive rats (SHR) (37).

Development of CVD involves structural changes in the blood vessels that include accumulation of extracellular matrix proteins such as collagen (136). Since collagen requires proline synthesis by arginase (90, 190), vascular expression of arginase is likely to be elevated during vascular remodeling in cardiovascular disease. In collaborative studies with Dr Sid Morris (University of Pittsburgh) our lab has previously found that levels of mRNAs for both arginase II and I were elevated by approximately 5 fold in the aorta of Sprague Dawley (SD) rats with DOCA/salt-induced hypertension and CKD. Furthermore, this was accompanied with increases in “in vitro” arginase activity in aorta. The exact mechanisms of increased arginase are unknown; however enhanced formation of ROS is a common finding in many vascular disorders. There is evidence of potential redox-sensitive responsive elements in the arginase I promoter region (70).

ADMA: Endogenous Nitric Oxide Synthase Inhibitor

Anther potential mechanism of reduced NO production is the accumulation of endogenous inhibitors. L-Arg that is released by the kidneys and enters the cell must compete with endogenous inhibitors of NOS. Therefore, the endogenous NOS inhibitor, asymmetric dimethylarginine (ADMA) is another potential method of regulation in NOS activity.

Synthesis and Metabolism

Arginine residues within proteins are methylated by protein arginine N-methyltransferase (PRMT) to form methylarginines: N^{W}-monomethyl-L-arginine (L-NMMA), ADMA, and symmetric dimethylarginine (SDMA) (172). L-NMMA and ADMA,

but not SDMA are competitive inhibitors of NOS isoenzymes. There are nine PRMT isoenzymes identified and classified as either types I or II (10, 116) with PRMT1 being the dominant form. Both types of PRMT can catalyze the formation of L-NMMA as an intermediate. PRMT-I leads to the formation of ADMA, whereas PRMT-II produces SDMA.

Metabolism of ADMA is via dimethylarginine dimethylaminohydrolase (DDAH) and exists in two isoforms, DDAH1 and DDAH2, which have 62% similarity and 95% homology between rat and human, respectively (73). Both DDAHs have distinct tissue distributions but seemingly similar activity. DDAH1 is mainly located in nNOS predominant tissues, whereas DDAH2 is found in tissues with high eNOS expression (84). However, both DDAHs are widely expressed and not confined to NOS-expressing cells. *In vitro*, DDAH inhibition decreases NO production in endothelial cells (95). DDAH1 overexpression reduces plasma and tissue ADMA levels and enhances tissue NOS activity both in vitro and in vivo (35, 62) and ADMA levels are attenuated in DDAH2 overexpressing transgenic mice (50).

Due to its ability to competitively inhibit NOS metabolism of L-Arg it is important to consider ADMA in the context of L-Arg availability and we often refer to the ratio of L-Arg to ADMA. It may be this ratio, either through increased ADMA or reduced L-Arg, or both, that is altered in disease states.

ADMA in CKD

Baylis et al has previously found reduced L-Arg to ADMA ratio in CKD and ERKD patients and in a rat chronic glomerulonephritis CKD model (185, 200). Elevated plasma ADMA level has also been reported in the presence of various CKD models and is a risk factor for CVD in man (172).

Type I PRMT protein gene expression was increased in 5/6 nephrectomized rats (98), and it is possible that increased PRMT1 expression may contribute to increased ADMA synthesis in CKD. DDAH expression and/or activity can be inhibited by tumor necrosis factor alpha (58), IL-1 beta (168), homocysteine (156), glycated bovine serum albumin (201), and erythropoietin (139) . All of the above pathways provoke oxidative stress and these effects could be prevented by antioxidants (139, 156, 201), suggesting DDAH may be downregulated by oxidative stress (75) which is prevalent in most models of CKD.

Specific Aims

The major goal of this dissertation was to address the question whether or not there is an L-Arg deficiency in CKD. As discussed previously, this field is controversial and not fully resolved. To do this we used various animal models of CKD and to fully understand the reasoning behind the experiments performed we must understand the basics of the disease models.

The 5/6 Ablation/Infarction Model

The remnant rat model of CKD is obtained with a surgical 50% reduction in total renal mass and approximately 80% reduction in functional renal mass. This is obtained by removal (ablation) of a kidney and ligation (infarction) of the some of the branches to the remaining kidney (5/6 A/I). The remnant kidney undergoes a series of functional changes including increased single nephron glomerular filtration rate (SNGFR), and progressive reductions in GFR and renal plasma flow (RPF). It is associated with hypertension, proteinuria, and structural changes including epithelial cell protein reabsorption droplets, foot process fusion, mesangial expansion, and progressive glomerulosclerosis (124). There is a parallel reduction in renal synthesis of NO and

decline of renal function (2). This model is associated with increased activation of the renin angiotensin system (96).

Puromycin Aminonucleoside

Puromycin aminonucleoside (3'-Amino-3'-Deoxy-N,N-dimethyladenosine) (PAN) is an antibiotic derived from *Streptomyces alboniger* bacterium. PAN specifically injures the glomerular podocyte and produces a model of nephrotic syndrome, which can progress into CKD.

Studies by Anderson et al (3) elucidated the mechanism of progression from acute to chronic injury. PAN injected rats show overt nephrotic syndrome and impaired glomerular filtration, which is due to a reduction in the glomerular capillary ultrafiltration coefficient. Histology of the kidney shows a disappearance of glomerular epithelial cell foot processes and reduced filtration slit diaphragms (Phase I). In Phase II the animals showed a reduction in proteinuria, restored renal function, and improved histology. However, there was a presence of glomerular capillary hypertension and reductions in the ultrafiltration coefficient continued but to a lesser degree. Thus, Anderson et al concluded that glomerular hypertension thus may explain the development of glomerular sclerosis and renal failure long after an episode of acute glomerular injury (3). The rate and severity of injury can be exacerbated by multiple injections (41, 45).

Fawn Hooded Hypertensive Rats

The Fawn Hooded (FH) rat was derived from the German Brown rat and is a model for the human platelet storage pool disease (81). At 3 to 5 weeks of age there are no renal lesions but male FH hypertensive (FHH) rats show increased blood pressure as early as 5 weeks and have focal and segmental glomerulosclerosis at 9-13 weeks (~5% of total glomeruli). They begin to die spontaneously around 47 weeks and

at ~1 year male rats reach end-stage (79). The development of the disease model is linked to several genes, termed renal failure genes (Rf) (99, 123).

The response of the interlobular arteries and afferent arterioles to increased renal perfusion pressure and ANGII infusion is significantly reduced in FHH rat. Thus, changes in blood pressure are not well buffered and rises in systemic pressure are easily transferred into the glomeruli (179). FHH have a low afferent arteriolar resistance when compared to other hypertensive rat models (180).

Aims

The first aim was to establish what occurs in different stages of CKD in terms of renal uptake of citrulline and production of L-Arg. Based on findings from the first aim we formulated the second aim to determine how CKD might impair the ability of the kidney to secrete the synthesized L-Arg into the circulation, and the ability of the vasculature to transport the L-Arg into the endothelium for NOS utilization. The third aim of this dissertation was to determine if there are alternate pathways of L-Arg metabolism, other than NOS, that is being activated by CKD and thus diverting L-Arg away from NO production. Specifically, we looked at the changes in arginase enzyme abundance/activity in different tissues in disease states. Finally, I will incorporate studies on ADMA abundance and metabolism in the models of CKD since the abundance of L-Arg is most accurately described as the ratio of L-Arg to ADMA. This dissertation is divided into 4 aims in hopes of determining the extent of substrate deficiency in CKD.

Specific Aim 1

Determine the ability of the kidney to take up citrulline and release L-Arg at various stages of CKD at baseline and with exogenous citrulline supplementation. This aim is

discussed in Chapter 3. We used the 5/6-ablation/infarction model studied at early, moderate, and severe injury. At each stage we measured the arterial-renal vein difference of citrulline and L-Arg in an acute surgical setting. We calculated the renal extraction of citrulline and the secretion of L-Arg. In Chapter 3, 4, and 5 we used protein quantification techniques to measure the abundance of L-Arg synthesizing enzymes in the kidney cortex and other organs.

Specific Aim 2

Determine the impact of CKD on L-Arg transporter abundance and regulatory enzyme abundance. In Chapter 5 using protein quantification we measured the abundance of CAT1 and PKC-α in the 5/6 A/I stages, and moderate and severe PAN injury. These measurements were made in both the membrane bound fractions and the soluble fractions of the aorta and the kidney cortex.

Specific Aim 3

Determine the changes in arginase abundance and activity in CKD. This is discussed in Chapter 5 along with the impact of attenuating hypertension and CKD on L-Arg metabolism via AT1 blockade. In the FHH rats we determined the abundance of renal and aortic arginase abundance and activity in response to a high protein diet and treatment with an ANGII receptor antagonist. This combined with plasma measurements of L-Arg allowed us to propose a potential alternate benefit of ANGII blockade on renal and cardiovascular disease. We also measured arginase abundance and activity in Chapters 4 in PAN injury.

Specific Aim 4

Determine the impact of various models of CKD on ADMA abundance and metabolism. The role of ADMA is discussed in Chapters 4 and 6, in all three models of

CKD that we have studied. We measured the abundance of ADMA by HPLC and the renal activity of DDAH by looking at ADMA conversion to citrulline.

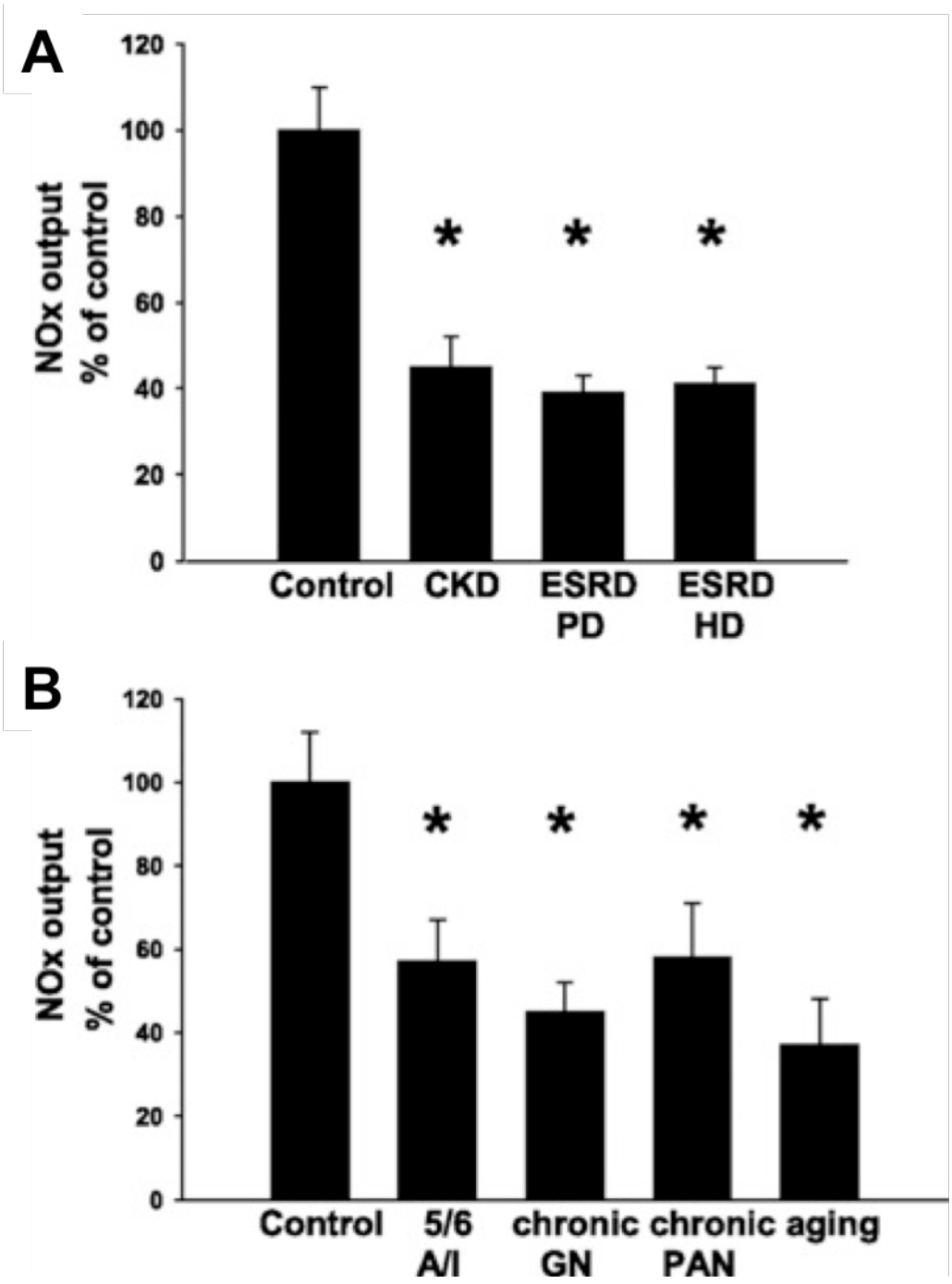

Figure 1-1. Nitric oxide production in patients and animals with CKD/ERKD. Total NO production measured by urinary excretion of stable metabolites. NO production is shown (A) in patients with residual renal function and no renal function undergoing dialysis and in (B) various animal models of CKD including 5/6 ablation/infarction, chronic glomerulonephritis, chronic puromycin aminonucleoside, and normal aging. Figure from review by Baylis (8)

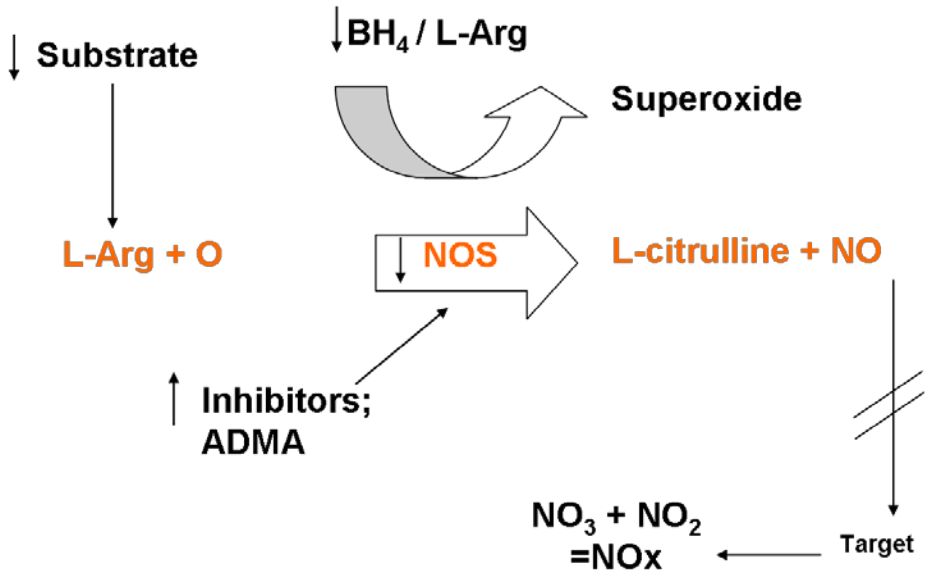

Figure 1-2. Mechanisms of nitric oxide deficiency. Multiple pathways of NO deficiency include reduced L-arginine delivery to NOS, increased NOS inhibitors, reduced coenzyme abundance (tetrahydrobiopterin), reduced NOS abundance/activity, or increased superoxide scavenging of NO.

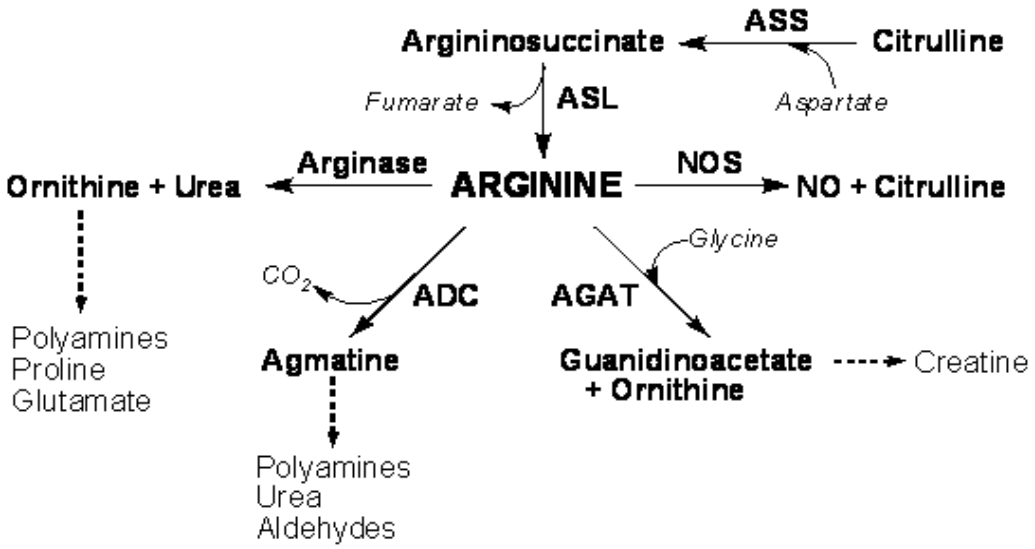

Figure 1-3. Pathways of L-arginine synthesis and metabolism. L-arginine is synthesized from citrulline via ASS and ASL enzymes and then metabolized by several pathways. These include NO synthesis through NOS, replenishing creatine by AGAT, agmatine synthesis by ADC, and by arginase to produced polyamines and proline.

CHAPTER 2
GENERAL METHODS

All animal procedures were approved by the Institutional Animal Use and Care Committee (IACUC) at the University of Florida.

Surgical 5/6 Ablation/Infarction

Renal mass was removed under isofluorane general anesthesia using full sterile technique. Rats were fasted overnight prior to surgery. When the animal was anesthetized (not responsive to toe pinch) the right and left flanks were shaved and scrubbed three times by alternating a betadine solution (1:1 with alcohol) and alcohol. The animal was placed on the surgical table (with heating pad) with its left flank up and a sterile drape was placed over the surgical site. Anesthesia was delivered through a nose cone and was monitored closed by monitoring breathing patterns and occasional toe pinches. A one-inch incision was made along the left flank below the floating rib. The kidney was exposed by gently pulling the fat surrounding it and was kept moist with sterile saline. The renal vein and artery were exposed and carefully separated to avoid bleeding. We exposed the renal artery branches and clamped each on individually and observed the blanching of the left kidney to obtain a combination of approximately 2/3-blood flow infarction. When the combination was obtained we tied off those branches with 6-0 silk ligatures. The kidney was gently placed back into the body and the surgical site was closed off with 3-0 silk sutures and surgical staples. Betadine solution was applied to the closed wound.

The animal was flipped to expose the right flank and again a one-inch incision was made below the floating rib but further towards the spine (since the

right renal artery and vein are shorter vs. the left). The kidney was exposed by gently pulling the fat, although this is a bit more difficult than the left side since the attachment seems more prone to tearing. The kidney was decapsulated and the renal artery and vein was tied off with 4-0 silk and cut between the kidney and the tie. The kidney was removed and the fat and vessels were returned into the body and the surgical site was closed off with 3-0 silk sutures and surgical staples. Betadine solution was applied to the closed wound.

The animal was taken off anesthesia and placed into a recovery cage with a heating pad underneath. A subcutaneous injection of buprenorphine was given immediately after surgery and again at approximately 12 hours post. Animals were monitored closely and returned to conventional housing within 24 hours of the surgery.

Metabolic Cage Collection

The metabolic cage was used to collect urine for measurements in multiple assays. Animals were weighed and placed into the metabolic cage, individually housed, and given only free access to filtered water. A funnel with filters to prevent feces contamination was placed underneath the wire bottom cage and urine was collected into pre-weighed closed containers containing 200µl of 4% boric acid (to prevent bacterium contamination). Animals were kept in the cages overnight (approximately 16 hours). Prior to removal we used a spray bottle containing filtered water to spray the inside of the funnel (exactly 10 sprays) to collect any urine residue and to correct for any evaporation. The animals were weighed again and returned to their conventional housing and given food and water. The containers containing urine were weighed and the previous weight

was subtracted and factored for time to obtain the volume excreted per 24 hours. The urine was transferred to a 15ml conical tube and spun (300 rpm for 10min) to remove any debris. Urine was aliquoted into 1.5ml tubes and stored at -80ºC for later analysis.

Protein Quantification

Bradford Assay

This assay was used for urinary protein concentrations. The Bradford reagent (Biorad) was purchased and instructions were followed as directed. Dye reagent was prepared by diluting 1 pat Dye Reagent Concentrate with 4 parts distilled water then filtered through Whatman #1 filter to remove particulates. The diluted dye reagent was stored up to 1 month at 4ºC. Standard scale was prepared by diluting bovine serum albumin (BSA) to concentrations of 500, 250, 125, 62.5, and 31.25µg/ml. Urine was diluted 1:4 with deionized water; higher dilutions were used for diseased states. In a 96-well clear plate 10µl of the standard or sample was pipetted into each well in triplicates. The diluted dye reagent (200µl) was added to each standard and sample and placed on a plate mixer at low speed for 10min at room temperature. Any bubbles were popped. The plate was read on a spectrophotometer (Magellan) reading absorbance at 595nm.

Lowry Method

Lowry assay materials were purchased at Biorad and manufacturer instructions were followed. Samples were dilute 1:50 and the 6 standards were prepared by serial dilution (0, 0.1, 0.2, 0.4, 0.8, and 1.6 mg/ml). Then 5µl of the samples or standards were added to a 96 well plates. Solution A was prepared (4

ml of solution A + 80 µl of Reagent S) and shook for 5min. The following was pipetted into each well using multi-tip pipette:

25µl of Solution A – 5min shake, and then 200µl of Solution B – 7min shake.

Plate was run on a spectrophotometer (Magellan) for absorbance at 750nm.

Tissue Harvest

Tissue harvesting was done in isofluorane-anesthetized rats. The level of anesthesia was monitored by responsiveness to a tail pinch. The animal was placed on the surgical table and an incision was made along the midline of the abdomen to minimize bleeding. A 20-gauge butterfly was inserted into the abdominal aorta at the bifurcation and clamped in place. Blood pressure was measured through the catheter and then a blood sample was taken (usually 5ml). The vasculature was perfused with 60ml ice-cold PBS at 25ml/min and the vena cava vented. Blood was spun at 3,000rpm for 10min and plasma was stored at -80ºC. For frozen tissue harvesting for western blot etc, tissues were harvested on ice and snap frozen in liquid nitrogen and then stored at -80ºC until analysis. For histology the perfused tissue was cut into a thin slice then stored in the 10% formalin for 48 hours at 4ºC. Kidneys were weighed (wet weight) after removal of fat and dissected into renal cortex and medulla. The thoracic aorta was cleaned of adventitia carefully without stripping the endothelium.

NO_2^- + NO_3 Assay (NOx)

NOx levels were measured in metabolic cage collected urine and plasma taken from rats placed on a 24hour low nitrate diet. Tissue NOx was measured in tissue homogenized in TBS buffer and filtered. The NOx levels were measured with Griess reaction according to Stuehr et al. (155) using the nitrate reductase

enzyme which reduced NO_3^- to NO_2^-. Prior to assay, urine and plasma were filtered through a 10,000 molecular weight cut-off filter (Millipore) by centrifugation at 14,000g for 60min at 4ºC. Briefly, 125µl of samples plus 100µl of HEPES/ammonium formate (1:1) were mixed with 25µl of nitrate reductase, incubated for 60 minutes at 37ºC. After the incubation, samples were centrifuged (2000rpm for 15min) and 100µl of supernatant was transferred into a 96-well plate. Griess reagent was made by 1:1 (V/V) mixed 1% sulfanilamide with 0.1% naphthylethylene diamine. 150µl of Griess reagent was added into each well. Samples were incubated for 15 minutes at room temperature. Absorbance was determined at a wavelength of 543 nm spectrophotometrically (Magellan). All chemicals for NOx assay were from Sigma (St Louis, MO, USA). A standard curve was constructed ranged from 0-400µM.

TBARS

Tissue homogenized in a TBS buffer and plasma was measured for thiobarbituric acid reactive substances (TBARS) using an OXItek TBARs Kit (ZeptoMetrix, Buffalo NY)). In glass tubes 100µl of the sample was added to 100µl SDS solution and mixed. Then 2.5ml TBA/Buffer Reagent was added to each tube, covered with a marble and incubated at 95°C for 60min. The samples were cooled to room temperature in an ice bath for 10min and centrifuged at 3000rpm for 15min. The absorbance of the supernatant was read at 532nm using a spectrophotometer (Magellan). A standard curve ranging from 0nmol/ml to 10nmol/ml MDA content was used.

Hydrogen Peroxide

Plasma hydrogen peroxide (H_2O_2) was measured using an Amplex Red Hydrogen Peroxide/Peroxidase Assay Kit (Molecular Probes, Eugene OR) according to manufacturer instructions.

Plasma and Urine Citrulline

This is a modification of the DDAH activity protocol shown later and developed by Tain et al (164). Since the endpoint for the DDAH protocol is citrulline content we utilized the same reagents. Plasma (50µl) was diluted 1:4 with filtered water and urine (5µl) was diluted 1:50. Samples were pre-incubated with urease (100U/ml homogenate) at 37°C in a water bath for 15 min. An equal volume of 4% sulfosalicylic acid was added to each sample to deproteinate and centrifuged at 3000g for 10min. Then the sample supernatant was added to separate eppendorf tubes. A series of standards were made by serial dilutions of a citrulline standard (100µM stock) to make 7 standards (100µM, 50µM, 25uM, 12.5µM, 6.25µM, 3.125µM, 0µM). Equal amount of color mixture (one part oxime reagent is mixed with 2 parts of antipyrine/H_2SO_4 reagent, made fresh) was added to each sample/standard. The oxime reagent was made by 0.8 g of diacetyl monoxime (Fisher AC403300250, 25g) in 100 ml of 5% (v/v) acetic acid (Fisher A38212) (stored in dark bottle covered in foil at 4° C for up to 3 weeks). The antipyrine/H2SO4 solution was made with 0.5g antipyrine (Sigma A5882, 25g) into 100 ml of 50% sulfuric acid (Sigma 258105, 500ml) (stored at room temperature indefinitely).

The samples/standards were vortex and incubated at 60°C for 110 min in the dark. Following incubation the samples/standards were placed at -20°C for

10 min to stop the reaction. All samples/standards were loaded into 96-well plate (200µL/well) in triplicates and the absorbance read by spectrophotometer (Magellan) analysis at 466 nm.

L-Arginine/ADMA/SDMA Measurements

Plasma and urine L-Arg, ADMA, and SDMA were measured using reverse-phase HPLC with the Waters AccQ-Fluor fluorescent reagent kit as we described previously (163). Tissue homogenates were prepared as described later (Tissue Homogenization). Samples were prepared by mixing 60µl of plasma or 10µl of urine with 5µl of 23.8 µM N-omega-propyl-L-arginine as internal standard (Cayman, Ann Arbor, Michigan), and 350µl of borate buffer (pH=9). This was placed on an unconditioned Oasis MCX column (Waters, Milford, MA) then washed with 1 ml borate buffer, 3x1 ml H2O, and 1 ml MEOH. The sample was eluted with 1ml NH4OH/ H2O /MEOH (10:40:50), dried under nitrogen gas, then reconstituted with 30µl H_2O. Recovery was approximately 85%. Twenty microliters of the samples was mixed with 60µl borate buffer and 20µl of AccQ Fluor reagent (Waters, Milford, MA). 50µl of mixture was injected onto a Luna 150 x 3 mm C-18 reversed-phase column (Phenomenex, Torrance, CA). A flow rate of 1.3 ml/min was attained with a PerkinElmer Series 200 Pump, and intensity was measured using a series 200 fluorescent detector, EX 250/EM 395 (PerkinElmer Life and Analytical Sciences, Shelton, CT). Standards contained concentrations of L-Arg in the range of 200µM to 3.12µM. ADMA and SDMA standard range was 8µM to 0.125µM

Creatinine Clearance

Plasma was prepared using the method of Tsikas et al (167) with a few modifications. Plasma (80µl) was precipitated in acetonitrile at 4 times its volume and then centrifuged at 15,000 g for 15 min and dried under N_2 at 45^{o}C. The dried sample was dissolved in glass-distilled water at half of its original sample volume and then centrifuged for 10 minutes at 15,000xg. Urine samples were diluted 1:200 and then prepared using the method of Tsikas et al (167). Creatinine was measured by HPLC using the chromatographic method of George et al (48). Creatinine was eluted on a 3.9x150 mm Waters AccQ-Tag C18 column in a 20mM potassium dihydrogen phosphate pH 7.4 isocratic mobile phase, followed by a 60/40 buffer/acetonitrile 12 minute column wash out and then a 5 minute reequilibration in 100% Buffer (20mM potassium dihydrogen phosphate buffer pH 7.4). Creatinine was then measured with a Perkin Elmer series 200 HPLC with series 200 UV detector.

Creatinine clearance (CCr) was calculated using the following formula: Urinary creatinine concentration (mg%) x urine flow rate (ml/min) / plasma creatinine concentration (mg%) = CCr (ml/min) and factored for body weight (per 100g).

Renal Plasma Flow

The estimated renal plasma flow (RPF) was measured with perfusion of para-aminohippurate (PAH) (freely filtered and not reabsorbed) and collection of arterial, renal vein plasma, and timed urine from the bladder. For plasma, 20µl was diluted in 400µl of filtered water immediately after collection and added to 200µl of 9.3% TCA to precipitate out proteins, DNA, and RNA, and stored at 4°C

until assay was run. Urine was diluted with filtered water according to flow rate (more diluted with reduced flow rate). Standards were made from a 20mg% PAH stock to obtain 5 standards (0.2, 0.1, 0.05, 0.025, and 0%). In a clear 96-well plate 120µl of the standards/samples were added to each well in triplicates. Then 40µl of 1N HCl was added to each well followed by 40µl of $NaNO_3$ solution (0.1%) and incubated for 3min. Then 40µl of NH_4 sulfamate (0.5%) was added to each well followed by another 3min incubation. Finally, 40µl of coupling reagent (0.1% n-(1-naphtyl) ethylenediamine dihydrochloride acs reagent) was added and incubated for 10min prior to reading absorbance on a spectrophotometer (Magellan) at 540nm.

RPF was calculated with the following formula: Urinary PAH x urine flow rate (ml/min) / arterial plasma PAH – renal vein plasma PAH = RPF (ml/min) for one kidney flow.

Kidney Histology

The left kidney was cut along the transverse axis at the time of harvest and fixed in 10% formalin for 48 hours then processed as follows:

Dehydration and Infiltration

Formalin fixed sections were place into pre-labeled individual plastic cassettes and washed twice with distilled water to remove all formaldehyde. Samples were transferred into 70% ethanol for a brief storage then placed into the retort of a Leica paraffin machine (Leica, ASP300). The embedding process was automated and performed overnight using the following solutions and times: 70% ethanol 45min (tissue remains in this solution for several hours when doing

a delayed start), 90% ethanol 45min, 4 absolute alcohol cycles and 3x60min, 3 xylene cycles 45, 60, and 75min, and 3 paraffin cycles 60min each.

Embedding

Following completion of tissue embedding samples were placed immediately into paraffin reservoir in blocking machine to prevent hardening of the paraffin. Tissue sections were placed cut side down onto a metal mold and melted paraffin was poured onto the tissue up to the inside edge of the mold. The mold was moved to a cold surface and allowed to set and harden for ~5 min then removed from mold. Blocks were placed at -20°C overnight and store at room temperature until sectioning.

Sectioning

Tissue blocks were placed on ice face down for 20 min before cutting. Slicing was done using a microtome (Leica, RM2125). The block was planed down until the entire tissue face was exposed and then 5µm sections were sliced. The sections were moved to a distilled water bath set at 55∞C and pick up onto Superfrost slides (Fisher) with two sections per slide. Slides were placed at an angle to allow excess water to drain off. Sections were stored at room temperature until staining.

Periodic Acid-Schiff Staining (PAS)

PAS Staining was done with a kit (Sigma, 395B) according to manufacturer instructions. Slides were deparaffinized and hydrated as follows: xylene 2x10min, 100% ethanol 2x10min, 95% ethanol 2x3min, 70% ethanol 3min, distilled water 2x5min. Hydrated sections were incubated in Periodic Acid solution for 5 minutes at room temp and washed with distilled water 3x3min. Then slides were

immersed in Schiff's reagent for 15 minutes at room temp and washed in running tap water for 5 minutes. Each slide was counterstained with Hematoxylin solution, Gill No. 3 for 90 seconds then rinsed in running tap water till water ran clear. Sections were dehydrated as follows: 70% ethanol 2min, 95% ethanol 2min, 100% ethanol 2x2min, then xylene 2x1min. Slides were then mounted in toluene/xylene based mounting media (Cytoseal).

Scoring Glomerulosclerosis

PAS stained sections were analyzed for glomerulosclerosis under a light microscope (Olympus). Up to one hundred glomeruli were scored blindly based on the following scale: 0=healthy glomeruli, +1=<25% damage, +2=25-50% damage, +3=51-75% damage, +4=>75% damage. Data was represented as percent of healthy glomeruli calculated by: Total Glomeruli observed – (#of+1)+(#of+2)+(#of+3)+(#of +4)/Total Glomeruli observed. A glomerulosclerosis index score (GSI) was calculated using the following equation: (#of+1)+ 2(#of+2)+ 3(#of+3)+ 4(#of +4)/Total Glomeruli observed. This formula was established by Raij et al (126).

Western Blot

Tissue Homogenization

Tissue was homogenized in a 20mM Tris base lysis buffer (pH 7.4) containing 5mM EDTA, 10mM EGTA, 2mM DTT, 1mM Na_3VO_4, 0.1% PMSF, 0.1% leupeptin, 0.1% aprotinin, 1% Triton X-100, 2.5mM Na^+ pyrophosphate, and 1mM ß-glycerophosphate. Homogenization was done mechanically on ice in three 10-second intervals with 10-second rest periods. The homogenate was

centrifuged at 11,000rpm for 10min at 4°C and supernatant was collected. Protein content of each sample was determined by Lowry method.

Tissue Fractionation

This method was obtained from studies performed by Schwartz et al (145) since the antibodies needed for this method were obtained from them. Flash frozen tissue was homogenized in a lysis buffer of PBS containing 0.01% Triton X-100, 0.1% SDS and protease inhibitors (1 mM phenylmethylsulfonyl fluoride, 4.5 µM leupeptin, 5 µM aprotinin). Samples were mechanically homogenized on ice and left on ice for 45min. Homogenates were centrifuged at 15,000 rpm for 10 min at 4°C and lysates were removed as the cytosolic fraction. The membrane fraction was obtained by adding to the pellet an equal volume of lysis buffer supplemented by Tween 20 (0.25%) to solubilize. The protein content of each sample was determined by Lowry method.

Sample Preparation

Samples were diluted with lysis buffer and 2x loading buffer (100mM Tris base, 4% sodium dodecyl sulfate (SDS), 0.25 bromophenol blue, 20% glycerol) to obtain desired concentrations. Samples were boiled for at least 2 minutes and stored at 4°C until loading.

Gel Preparation

The gel pouring system was purchased from Biorad. Gels (separating gel) used in all the experiments were either 7.5% or 12% acrylamide. The recipes for both concentrations are as follows: 7.5% separating gel (10ml): 4.8ml filtered water, 2.5ml 30% acrylamide mix (Sigma), 2.5ml 1.5M Tris Base (pH 8.8), 100µl 10% SDS, 7µl TEMED (tetramethylethylenediamin), and 100µl 10% APS

(ammonium persulfate). For 12% separating gel (10ml) reduced water to 3.3ml and 30% acrylamide mix increased to 4ml.

The stacking gel (5% acrylamide) was prepared with the following recipe (4ml): 2.85ml filtered water, 0.66ml 30% acrylamide mix, 0.5ml 0.5M Tris Base (pH 6.8), 40µl 10% SDS, 4µl TEMED, and 40µl 10% APS.

APS was added just prior to gel pouring. The separating gel was added leaving about ½ inch for the stacking gel. Bubbles were removed with water-saturated isobutanol (500µl). When gel had hardened the isobutanol was poured off and the top of the gel was washed with filtered water to remove remaining residue. APS was added to the stacking gel mixture and added to the top of the glass plate setup and the plastic comb was placed into the stacking gel at an angle to prevent bubbles. The gels were allowed to harden at room temperature and stored in a moist seal bag at 4°C until needed (no longer than 2 days).

Loading and Electrophoresis

Gels were placed into the electrophoresis apparatus (Biorad) according to manufacturer instructions. Running buffer (25mM Tris Base, 0.25mM glycine, 0.5% SDS) was added into the apparatus and gel combs were removed in submerged buffer to prevent well collapse. Samples, controls, and ladders were loaded with the appropriate volumes and run for 1 hour and 5 min at 200V at room temperature.

Transfer

After electrophoresis was complete we transferred the protein to a nitrocellulose membrane in a semi-dry transfer apparatus (Trans-Blot BD, BioRad). The membrane was cut to fit the gel and soaked in transfer buffer

(47.9mM Tris Base, 38.6mM glycine, 0.04% SDS, 20% methanol) along with the gel for no less than 15 minutes. Extra thick blot paper was soaked in transfer buffer for 5 min. The gel sandwich was assembled in the Trans-Blot in the following order (bottom to top): Base (anode plate assembly), extra thick blot paper, nitrocellulose membrane, acrylamide gel, extra thick blot paper, and cathode plate assembly with latches. Special attention was paid to prevent capture of bubbles between layers. The gels were transferred at 0.18A for 1 hour and 45 min at room temperature.

Ponceau Staining

When transfer was complete the membranes were washed with filtered water briefly and Ponceau reagent (Sigma, P3504) was added to the membranes for 10 min on a shaker. The stain was removed and the membranes were washed 3x with filtered water and placed between plastic sheets to prevent drying. A photograph was taken using the Versa Doc imaging system (BioRad) and the total protein density was measured by Quantity One Analysis software (BioRad). Using the box feature a rectangle of fixed area was drawn within the edges of the Ponceau stain for each lane and the densitometry was calculated after subtraction of background. The stain was washed off with TBS.

Probing

Probing of the membranes for specific proteins was done by following a general protocol regardless of protein: 1) blocking, 2) incubation with primary antibody specific for protein of interest, 3) one 15min wash followed by two 5min washes, 4) incubation with secondary antibody for 1hour at room temperature, and finally 5) one 15min wash followed by three 5min washes.

The exact antibodies used along with blocking solution, the concentration and incubation time for the primary and secondary, and the wash buffer and times are shown in Table 2-1 for each protein of interest.

Densitometry Analysis

After the final wash the membranes were placed between plastic sheets to prevent drying. Bands of interest were visualized using SuperSignal West Pico reagent (Pierce, Rockford, IL) and quantified by densitometry (VersaDoc imaging system and Quantity One Analysis software, Bio-Rad), as integrated optical density (IOD) after subtraction of background. The IOD was factored for Ponceau red staining to correct for any variations in total protein loading and for an internal standard. The protein abundance was represented as IOD/Ponceau Red/Std. We used Ponceau red method for standardization because in some situations β-actin may change.

Tissue DDAH Activity

This method was developed by Tain et al (164) and utilized formation of citrulline from exogenous ADMA addition. Tissue was homogenized in a sodium phosphate lysis buffer (0.1 M phosphate buffer, pH = 6.5) made from stock solutions: A) 0.2 M NaH_2PO_4 and B) 0.2 M Na_2HPO_4. Solution A (34.25 ml) was mixed with B (15.75 ml) and dilute with dH_2O to make final volume of 100 ml just prior to homogenization. The homogenates were centrifuged at 11,000 rpm for 10 min and supernatant was collected. Protein concentrations were determined with Lowry method and the homogenate was adjusted to 20 mg/ml by adding the lysis buffer.

Samples were pre-incubated with urease (100U/ml homogenate) at 37°C in a water bath for 15 min. The samples were separated into two sets of 100µl each. To one set 400µl of lysis buffer was added (baseline) and to the second 400µl of 1mM ADMA in lysis buffer. Both sets were incubated in 37°C water bath for 45 min. After incubation 500µL of 4% sulfosalicylic acid was added to each sample to deproteinate and centrifuged at 3000g for 10min. Then 300µL of the sample supernatant was added to separate eppendorf tubes. A series of standards were made by serial dilutions of a citrulline standard (100µM stock) to make 7 standards (100 µM, 50 µM, 25uM, 12.5 µM, 6.25 µM, 3.125 µM, 0 µM). Equal amount of color mixture (one part oxime reagent is mixed with 2 parts of antipyrine/H_2SO_4 reagent, made fresh) was added to each sample/standard. The oxime reagent was made by 0.8 g of diacetyl monoxime (Fisher AC403300250, 25g) in 100 ml of 5% (v/v) acetic acid (Fisher A38212) (stored in dark bottle covered in foil at 4° C for up to 3 weeks). The antipyrine/H2SO4 solution was made with 0.5g antipyrine (Sigma A5882, 25g) into 100 ml of 50% (v/v) sulfuric acid (Sigma 258105, 500ml) (stored at room temperature indefinitely).

The samples/standards were vortex and incubated at 60°C for 110 min in the dark. Following incubation the samples/standards at -20°C for 10 min to stop reaction. All samples/standards were loaded into 96-well plate (200µL/well) in triplicates and the absorbance read by spectrophotometer (Magellan) analysis at 466 nm. The citrulline concentration of the baseline set was subtracted from the ADMA containing samples to obtain µM of L-Cit formed per gram protein per minute. Endogenous content of citrulline was determined by the baseline set.

Tissue Arginase Activity

Arginase activity in liver and kidney cortex was determined by measuring the rate of urea production in the homogenate using α-isonitrosopropriophenone (9% in absolute ethanol) as previously described (208). Tissue was mechanically homogenized in filtered 50mM Tris-HCl (pH = 7.5) containing 0.1mM EDTA, 0.1mM EGTA, and protease inhibitor cocktail. The protein content was measured by Lowry assay and the samples were diluted to contain 2mg protein/100µl. Then 100µl of the homogenate was removed and added to 150µl 50mM Tris-HCl+10mM $MnCl_2$ (pH = 7.5) and the arginase was activated by heating the sample at 56°C for 10min. L-Arg (0.5M in water) was added to the samples (100ml) and incubated at 37°C for 60min. The reaction was stopped by addition of 800µl H2SO4:H3PO4:H2O (1:3:7) solution. Finally the α-isonitrosopropriophenone (50µl) was added to each sample and boiled for 45min. Sample were transferred to a 96-well clear plate and placed in the dark for 10min at room temperature prior to measuring absorbance at 550nm (Magellan). The arginase activity was represented as µmol urea formed/g protein/unit time.

Table 2-1. Western blot antibody list. The incubation times for each primary antibody is overnight at 4°C. The blocking reagent for most antibodies are 5%-NFM dissolved in the wash buffer. Primary antibodies are dissolved into blocking solution for all antibodies, arginase I is 1% NFM 1%BSA TBS-T 0.1%. Secondary antibodies are all diluted in blocking buffer. Wash buffer is represented with % Tween-20. SC- Santa Cruz, BD- BD Transduction Laboratories, Gotoh- Developed by Dr Mori, Dr Morris- Gift from Dr Sid Morris, Schwartz- Developed and gifted by Dr Doron Schwartz. TBS- Tris buffered saline, NFM- Non fat milk, MW- molecular weight

Protein	Source	Type	Gel%	Conc	2°	Source	Conc	Wash BF	MW (kDa)
ASS	Gotoh	Rabbit	12	1:2000	Goat	BioRad	1:3000	TBS-0.1%	46
ASL	Gotoh	Rabbit	12	1:2000	Goat	BioRad	1:3000	TBS-0.1%	51
ArgI	Morris	Chick	12	1:10000	Goat	Upstate	1:5000	TBS-0.5%	40
ArgII	SC	Rabbit	12	1:3000	Goat	BioRad	1:3000	TBS-0.5%	40
CAT1	Schwartz	Rabbit	7.5	1:500	Goat	BioRad	1:3000	TBS-0.5%	90
PKC-α	BD	Mouse	7.5	1:1000	Goat	BioRad	1:3000	TBS-0.5%	82
PRMT1	Upstate	Rabbit	12	1:2000	Goat	BioRad	1:3000	TBS-0.05%	43
DDAHI	SC	Goat	12	1:500	Donkey	SC	1:2000	TBS-0.05%	30
DDAHII	SC	Goat	12	1:100	Donkey	SC	1:2000	TBS-0.05%	34

CHAPTER 3
IN VIVO RENAL ARGININE RELEASE IS IMPAIRED THROUGHOUT DEVELOPMENT OF 5/6 ABLATION/INFARCTION CHRONIC KIDNEY DISEASE

Introduction

There is a net NO deficiency in patients and animals with CKD and ERKD (2, 15). There are multiple possible causes of NO deficiency in renal disease, one of which is a reduced availability of the rate limiting NOS substrate, L-Arg, since the kidney is an important site of L-Arg synthesis (38, 196). Renal L-Arg synthesis requires citrulline, made primarily in the small intestine, which is taken up into the kidney and converted by argininosuccinate synthase (ASS) and argininosuccinate lyase (ASL)(38, 196) into L-Arg. The L-Arg is then released into the circulation via the renal vein and is taken up into cells and utilized in several pathways including NO synthesis (196).

In normal healthy adults L-Arg is a non-essential amino acid since endogenous production is sufficient for metabolic needs (196). A significant fraction (approximately 40%) of ingested L-Arg mainly undergoes catabolism (196); thus, the majority of circulating L-Arg used for other organ metabolic processes is provided by renal production and protein turnover (196). Citrulline does not undergo significant hepatic uptake and is therefore available for renal L-Arg synthesis (193). In normal individuals citrulline is rate limiting for renal L-Arg synthesis(38) and citrulline supplementation stimulates L-Arg synthesis leading to increases in plasma L-Arg (49).

Man and animals with renal disease show increases in plasma citrulline correlating with decreased renal function (26). This is probably caused by a reduction in renal uptake and utilization of citrulline rather than increased citrulline production or intake. However, the effect of renal disease on renal L-Arg production is controversial with reductions in renal L-Arg production being reported in man and rats with CKD (27, 166)

as well as maintained L-Arg production in the rat with CKD and in man with ERKD (18, 82).

In this study we have undertaken a systematic evaluation of renal citrulline uptake and L-Arg synthesis during the evolution of the 5/6-ablation/infarction (A/I) model of CKD. In *in vivo* studies we measured the renal uptake of citrulline and release of L-Arg in controls and in early, moderate and severe stages of CKD studied under baseline conditions and during acute citrulline supplementation. We also measured the abundance of various enzymes that influence L-Arg metabolism and breakdown.

Methods

Male Harlan Sprague Dawley rats were housed in conventional cages and given free access to normal chow and water. Urine was collected overnight (16 hours) in metabolic cages with animals given free access to water only. Urine protein excretion (UpV) was measured by Bradford method (BioRad, Hercules, CA). After baseline UpV was measured, the rats were fasted overnight and underwent 5/6 A/I surgeries. Under full sterile conditions the animal was anesthetized with isofluorane and the left and right flank was shaved. An incision was made under the floating rib and the left kidney was exposed. Using 6-0 silk, branches of the renal artery were ligated to achieve ~2/3 infarction of the left kidney. The right kidney was removed after ligation of the renal vein and artery. Sham animals had both kidneys exposed but no ligation or ablation was performed. The animals were separated into 4 groups: Sham (n=11), 1-2 weeks post injury (early, n=11), 4-5 weeks post injury (moderate, n=7), and 10-12 weeks post injury (severe, n=17). UpV and body weight (BW) were measured every 2 weeks starting 1 week after A/I injury. All experiments were approved by the University of Florida Institutional Animal Care and Use Committee.

In Vivo Renal Uptake of Citrulline

Animals were anesthetized with inactin (120mg/kg BW) via IP injection. Body temperature was monitored through a rectal probe and regulated by a heated surgical table and lamp. The left femoral artery was cannulated, and baseline arterial blood was taken and spun for plasma. Red blood cells were reconstituted with artificial plasma (2.5% Bovine serum albumin and 2.5% γ globulin in lactated Ringer's solution) at a volume equal to plasma removed and restored to the rat via femoral vein catheter. Blood pressure (BP) was monitored via the femoral artery catheter. The trachea was cannulated, and a constant flow of oxygen was streamed across to maintain BP. The bladder was catheterized and a timed baseline urine sample was collected following a brief recovery time. Sham animals had the right ureter ligated and cut upstream of the ligation to allow for single kidney urine collection via the bladder. The left renal vein was cannulated without obstruction of normal blood flow. Artificial plasma was infused into the femoral vein at 1% BW/ hour for the first 20min of surgery then reduced to 0.15% BW/ hour for the remainder of the experiment. Baseline renal plasma flow (RPF) was measured by infusing p-aminohippuric acid (PAH, 1.3mg/ml for sham, 0.22mg/ml for all A/I groups) in 0.9% saline at 1.2ml/100gBW/hour into the femoral vein following a 0.5ml bolus PAH injection. After 40min equilibration, a 20min urine sample was taken with midpoint blood taken from the femoral artery and renal vein to determine renal extraction of PAH. A bolus of 100mM citrulline was given and the infusion was switched to contain 30mM citrulline, while adjusting saline concentration to maintain osmolarity. After 40min equilibration, urine was collected for 20min with midpoint blood samples from the femoral artery and renal vein. Hematocrit was measured and plasma taken for

analysis of PAH, L-Arg and citrulline; red blood cells were then reconstituted with artificial plasma and returned to the rat. Following the final blood draw, the kidneys were perfused blood free with PBS, and the kidney was harvested. Part of the kidney was fixed for histology, see below, and the remainder divided into cortex and medulla and flash frozen then stored at -80°C for later analysis, see below.

Renal Function

PAH concentration was established using a colorimetric assay previously described (137) to calculate left kidney RPF. Total creatinine clearance (CCr) was calculated using timed urine samples and plasma collected at the beginning of the acute surgery was analyzed for creatinine by HPLC as described in Chapter 2-Creatinine Clearance.

Calculations

Total renal uptake of citrulline was calculated as renal citrulline delivery (single kidney RPF x Arterial Citrulline concentration) minus citrulline outflow (RPF x Venous Citrulline concentration) minus urinary citrulline excretion, and then multiplied by number of kidneys (2 for sham, 1 for CKD). Total renal release of L-Arg was calculated as renal vein L-Arg outflow (RPF x Venous L-Arg concentration) minus renal L-Arg delivery (RPF x Arterial L-Arg concentration) minus urinary L-Arg excretion, and then multiplied by number of kidneys (2 for sham, 1 for CKD).

Citrulline

Renal cortex homogenate, plasma, and urine citrulline were measured by a colorimetric assay employing acidic diacetylmonoxime (121) modified by us and described previously (164).

L-Arginine Measurements

Plasma and urine L-Arg were measured using reverse-phase HPLC with the Waters AccQ-Fluor fluorescent reagent kit. Samples were prepared by mixing 60µl of plasma or 10µl of urine with 350µl of borate buffer (pH=9). This was placed on an unconditioned Oasis MCX column (Waters, Milford, MA) then washed with 1 ml borate buffer, 3x1 ml H_2O, and 1 ml MEOH. The sample was eluted with 1ml NH_4OH/ H_2O /MEOH (10:40:50), dried under nitrogen gas, then reconstituted with 30µl H_2O. Recovery was approximately 85%. Twenty microliters of the samples was mixed with 60µl borate buffer and 20µl of AccQ Fluor reagent (Waters, Milford, MA). 50µl of mixture was injected onto a Luna 150 x 3 mm C-18 reversed-phase column (Phenomenex, Torrance, CA). A flow rate of 1.3 ml/min was attained with a PerkinElmer Series 200 Pump, and fluorescence intensity was measured using a series 200 fluorescent detector, EX 250/EM 395 (PerkinElmer Life and Analytical Sciences, Shelton, CT). Standards contained concentrations of L-Arg in the range of 200µl to 3.12µM. This method was adapted from Heresztyn et al (53).

Western Blot

Western blot analysis was made as described previously (163). Briefly, measurement was conducted on kidney cortex (100µg total protein) loaded on 12% polyacrylamide gels. Rabbit polyclonal antibodies (developed by Dr Masataka Mori, Kumamoto University, Kumamoto)(203) against ASS and ASL were used at 1:2000 dilutions, overnight incubations. A goat anti-rabbit IgG-HRP secondary antibody (Bio-Rad, 1:3000 dilution, one hour incubation) was used for detection. Bands of interest were visualized using SuperSignal West Pico reagent (Pierce, Rockford, IL) and quantified by densitometry (VersaDoc imaging system and Quantity One Analysis

software, Bio-Rad), as integrated optical density (IOD) after subtraction of background. The IOD was factored for Ponceau red staining to correct for any variations in total protein loading and for an internal standard (rat liver). The protein abundance was represented as IOD/Ponceau Red/ Int Std.

Histology

Kidney histology was prepared as previously described in Chapter 2-Kidney Histology. The left kidney was cut along the transverse axis and fixed in 10% formalin for 48 hours then paraffin embedded. Sections were cut at 5µm onto Superfrost/Plus microscope slides (Fisher Scientific). Slides were deparaffinized and rehydrated in xylene and serial alcohol incubations and stained with Periodic Acid Schiff (PAS, Sigma, St Louis, MO) followed by hematoxylin as the secondary stain. Up to one hundred glomeruli were scored blindly based on the following scale: 0=healthy glomeruli, +1=<25% damage, +2=25-50% damage, +3=51-75% damage, +4=>75% damage. A glomerulosclerosis index score (GSI) was calculated using the following equation: (#of+1)+ 2(#of+2)+ 3(#of+3)+ 4(#of +4)/ total glomeruli observed.

Statistics

One-way ANOVA combined with Newman-Keuls post hoc test was used for statistical evaluation of mean values across groups. Paired t-test with a two-tailed P value was used to compare between baseline and citrulline infusion. Linear regression was used to determine relationship between two parameters; p values and goodness of fit (r^2) are shown. All graphs and statistics were done with Prism 4 software (GraphPad Software, Inc., San Diego, CA). Values are reported as means ± SE with $P<0.05$ was considered statistically significant.

Results

As shown in Table 3-1, both BW and functional renal mass fell with 5/6 A/I and there was a progressive increase in proteinuria and glomerular damage with increasing time after surgery. At sacrifice, all CKD groups had elevated BP and a reduced CCr.

Baseline plasma citrulline values were significantly and progressively increased in CKD rats compared to shams (Table 3-2). Citrulline infusion increased plasma concentrations of citrulline in all animals and most markedly in CKD rats. Baseline plasma L-Arg concentrations were not different in any group and citrulline infusion only increased plasma L-Arg in shams and 1-2 week animals (Table 3-2). At the termination of the study, after citrulline infusion, the renal cortex content of citrulline was increased at all stages of CKD.

Baseline RPF was reduced in all CKD groups (Table 3-3). Citrulline infusion resulted in an increased RPF to the sham rats but had no effect on RPF in any CKD group. The decline in RPF due to CKD resulted in reduced delivery of citrulline to the kidneys at baseline, despite increased plasma citrulline concentrations. With citrulline infusion there were increases in renal delivery of citrulline in all groups, although the magnitude of increase was less in all CKD groups vs. shams.

At baseline, total renal uptake of citrulline at 1-2 weeks post injury was higher than in shams but as CKD developed renal citrulline uptake fell below sham values (Figure 3-1A). Citrulline infusion increased the total renal citrulline uptake in shams (~13 fold) and, to a lesser extent in 1-2 week animals (~2 fold) but had no impact on citrulline uptake as CKD developed. Citrulline uptake by the kidney was predominately via filtered citrulline reabsorption in shams (Table 3-4). However, at early injury the basolateral uptake was the major site. At baseline, total renal release of L-Arg was diminished

(Figure 3-1B) at all stages of renal injury. Citrulline infusion significantly increased the total renal L-Arg release in shams, but did not improve L-Arg release in the injured kidney.

Baseline urinary citrulline excretion was low and similar apart from a transient increase at 1-2 weeks of injury vs. shams (Table 3-5). Citrulline infusion had no effect on urinary citrulline excretion compared to baseline in any group. Baseline L-Arg excretion was slightly higher only at 10-12 weeks CKD vs. sham. Citrulline infusion increased L-Arg excretion in shams but had no impact at any CKD stage (Table 3-5).

As shown in Figure 3-2A, there is ~1:1 correlation between renal citrulline uptake and L-Arg output in the sham rats. At 1-2 weeks post injury the relationship is blunted (~4:1, Figure 3-2B) and there is no relationship between citrulline uptake and L-Arg production at the later stages of CKD (Figure 2C and D).

Renal ASS abundance was reduced at all stages of CKD vs. sham (Figure 3-3A). ASL density was unchanged at 1-2 weeks after injury, was elevated at 4-5 weeks then restored to sham values at 10-12 weeks (Figure 3-3B).

Discussion

Using the 5/6 A/I model of CKD we found that in the presence of substantial injury both renal citrulline uptake and renal citrulline to L-Arg conversion were impaired compared to rats with normal kidney function. In fact, the renal L-Arg production was impaired quite early, before significant structural damage was evident. Thus, the renal production of L-Arg was markedly reduced in this CKD model over a wide range of injury.

Renal L-Arg synthesis requires the delivery of an adequate supply of citrulline and we observed a reduction in renal citrulline delivery at all stages of injury progression.

This was due to such large reductions in RPF that the increases in plasma citrulline (routinely seen in CKD and also seen here) were unable to compensate to maintain citrulline delivery. Not surprisingly, renal citrulline uptake was below sham levels at moderate and severe injury although we observed mildly increased citrulline uptake early after 5/6 A/I. Exogenous citrulline infusion resulted in increased renal delivery of citrulline in all groups. However, while renal uptake of citrulline was greatly increased in sham animals there was only a slightly increase in early CKD and no stimulation of uptake at moderate and severe injury.

Cellular uptake of citrulline is by a number of L amino acid carrier systems. There are sodium independent transporters in the nervous system (141) and sodium dependent transporters in rat endothelial cells (193). In the kidney, Mitsuoka et al (101) identified B(0)AT1 and b(0,+)AT, sodium independent and dependent transporters of citrulline on the apical membrane of cultured rat renal proximal tubular cells. On the basolateral side of the proximal tubules, sodium independent transporters are present and OAT1 is the primary basolateral transporter (109). Giusto et al demonstrated a reduction in basolateral OAT1 following renal ischemia/reperfusion injury in rats (39). As shown in Table 3-4, the majority of the citrulline taken up into the normal (sham) kidney is delivered by filtration, as also reported by Munger et al (107). With the 5/6 A/I surgery there is an immediate and persistent fall in GFR, leading to declines in citrulline delivery by filtration. Our findings are consistent with an initial increase in citrulline transport capacity by the hypertrophying remnant, which is rapidly lost as injury progresses. In the normal kidney we found that exogenous citrulline infusion caused a huge increase in renal uptake of citrulline, suggesting a large reserve capacity of citrulline transport. The

blunted increase seen early in the injury progression as well as the failure of administered citrulline to boost renal citrulline uptake as CKD advances, is also suggestive of loss of citrulline transport capacity with disease progression.

Our findings are different to those of Bouby et al, who using the same injury model, found no change in citrulline uptake at 4-6 weeks post injury (18). In their study the delivery of citrulline was well maintained by a 3-fold increase in plasma citrulline with only ~30% reduction in RPF, whereas our animals showed >85% reduction in RPF and only a 2-fold increase in plasma citrulline 4-5 weeks post injury. Obviously the rate of CKD progression was much greater in our study, for reasons unknown.

According to Brosnan and colleagues, citrulline delivery is the limiting determinant of rate of renal L-Arg synthesis in the normal rat kidney (38). Our findings support this since we observed a ~1:1 relationship between citrulline uptake and L-Arg production in the shams both under baseline conditions and after exogenous citrulline. However, exogenous citrulline did not significantly improve L-Arg release at any stage of CKD and despite increased citrulline uptake at 1-2 weeks (Figure 1). This implicates a defect in the renal machinery for citrulline to L-Arg conversion, i.e. in the ASS and ASL located in the proximal convoluted tubules of the rat kidney (86). This is supported by our finding of reduced renal cortical ASS protein abundance at all stages of CKD, which coupled with loss of functional renal mass means an overall loss of renal ASS activity. The renal cortical ASL protein abundance was unchanged in early injury but increased above sham values at moderate injury. Given the loss of functional renal mass, this means a fall or little change in renal ASL activity. Moradi et al, showed, in studies at 6 weeks in the milder 5/6 nephrectomy CKD model, no change in ASS/ASL protein abundance in

whole kidney, but when factored for viable renal mass there was a reduction in total abundance of ASS/ASL (103). Although protein abundance may not always reflect activity, our present observations suggest that there is a direct correlation in the 5/6 A/I model.

Again, our findings conflict with those of Bouby et al who reported unchanged renal L-Arg production at 4-5 weeks post 5/6 A/I and maintained L-Arg to citrulline conversion in isolated proximal convoluted tubules (18). Again, these differences presumably reflect the much milder level of injury in this earlier study. In addition, with 270 min of unilateral ischemia reperfusion reduced L-Arg release was reported despite increased citrulline uptake (122), reminiscent of our findings at 1-2 weeks post 5/6 A/I. Studies by Chan et al, confirm our findings with a report of reduction in ASS/ASL activity in rat kidney cortex homogenates from rats with advanced CKD (8-10 weeks) due to 5/6 A/I (27). Finally, in clinical studies in patients with non-diabetic CKD with ~25% residual renal function, there was ~65% reduction in both citrulline uptake and L-Arg release versus hypertensives with normal renal function (166).

Consistent with our findings regarding renal L-Arg release, citrulline infusion increased RPF only in sham animals. Although indirect, this suggests that the increased L-Arg release, seen in shams, result in a functional vasodilation presumably through increased NO synthesis. Studies with perinatal citrulline supplementation in female spontaneous hypertensive rats (SHRs) showed increased renal NO levels compared to untreated SHRs (78).

Despite clear evidence of impaired L-Arg release by the damaged, 5/6 A/I kidney, there is no reduction in circulating L-Arg values. A similar result was reported by Chan

et al (27) in the rat with CKD and by Tizianello et al (166) in man with CKD. Furthermore, plasma L-Arg levels in CKD and end-stage patients are relatively normal (13, 142, 143). This maintenance of a normal plasma L-Arg in the face of significant renal disease could reflect: 1. That circulating L-Arg is not determined by renal L-Arg synthesis. 2. CKD loss of renal L-Arg production is compensated for by increased L-Arg synthesis in other locations (e.g. endothelium). 3. Compensation by alternate L-Arg sources such as dietary intake/changes in GI absorption and/ or increased protein turnover. 4. Reduced endothelial uptake creates intracellular L-Arg deficiency but leaves a deceptively normal plasma L-Arg (198). 5. Compensatory decrease in whole-body L-Arg catabolism (24, 25). Resolution of these important questions will improve our ability to manage CKD.

In regards to L-Arg synthesis by other locations, our data suggests that citrulline supplementation increases plasma L-Arg concentrations through non-renal pathways. During citrulline infusion the early CKD group showed a significant increase in plasma L-Arg despite reduced renal L-Arg release. This may reflect the ability for the endothelium to produce L-Arg since it contains the necessary enzymes (52, 195).

In conclusion, this study demonstrates that renal L-Arg release is reduced over a range of CKD severity in the 5/6 A/I rat, due both to reduced citrulline uptake and to reduced ASS/ASL activity in the renal cortex. Our acute citrulline infusion data suggest that citrulline supplementation will not increase renal L-Arg release in cases of established renal injury. While the established dogma holds that the kidney is a primary source for endogenous L-Arg production, plasma L-Arg is relatively maintained in CKD. The precise reasons for this remain to be defined.

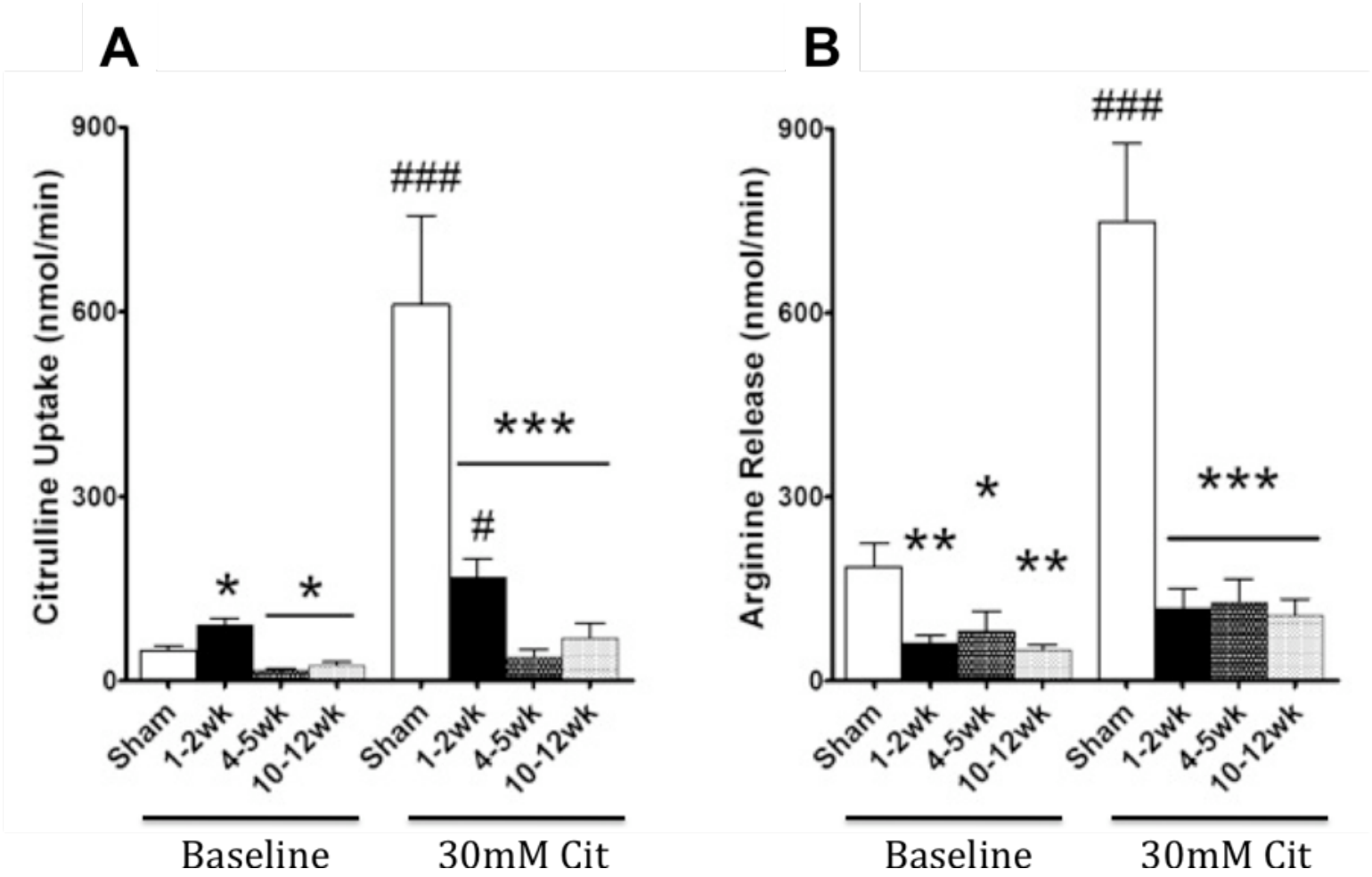

Figure 3-1. Renal uptake of citrulline and release of L-Arginine at baseline and during citrulline infusion. (A) Total renal uptake of citrulline. (B) Total renal L-Arg release. Statistics comparing each injury to sham were done with one-way ANOVA. * $p<0.05$, ** $p<0.01$, *** $p<0.001$ vs. sham. Statistics comparing baseline vs. infusion were done with paired T-Test. # $p<0.05$, ### $p<0.001$ vs. group baseline.

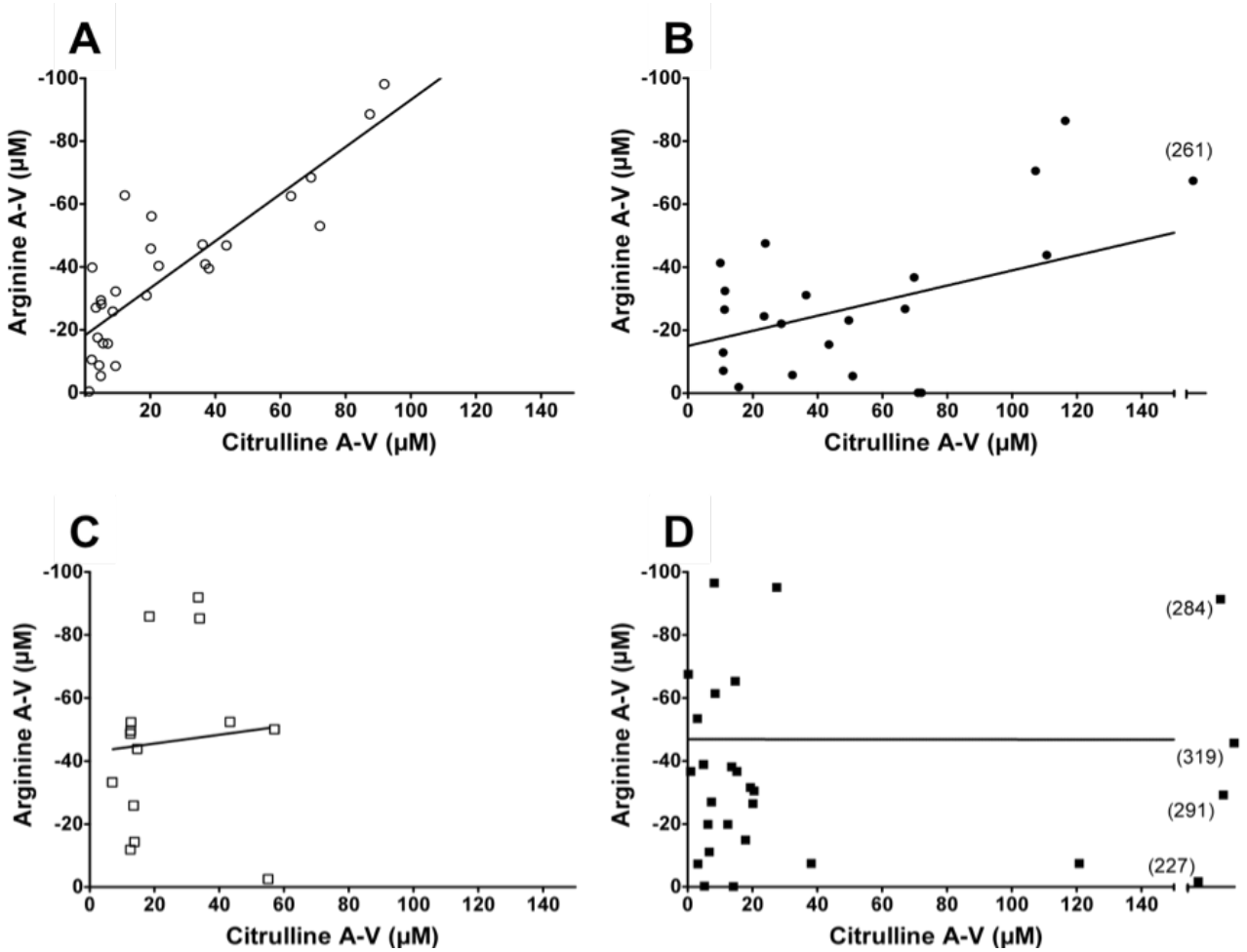

Figure 3-2. L-Arginine and citrulline A-V correlations. Correlation between the citrulline A-V difference and L-Arg A-V difference (shown as a negative number reflecting net L-Arg release by the kidney, into the renal vein) in (A) shams (r^2=0.8143, p<0.0001), (B) 1-2 weeks (r^2=0.4925, p=0.0026), (C) 4-5 weeks (r^2=0.1336, NS), and (D) 10-12 weeks (r^2=0.00007, NS) post injury. Scale is set from 0 to 150 on the x-axis, samples laying outside this range are shown on the extended axis with exact values in parenthesis. Linear regression analysis was performed on each correlation to obtain the r^2 and p-values shown.

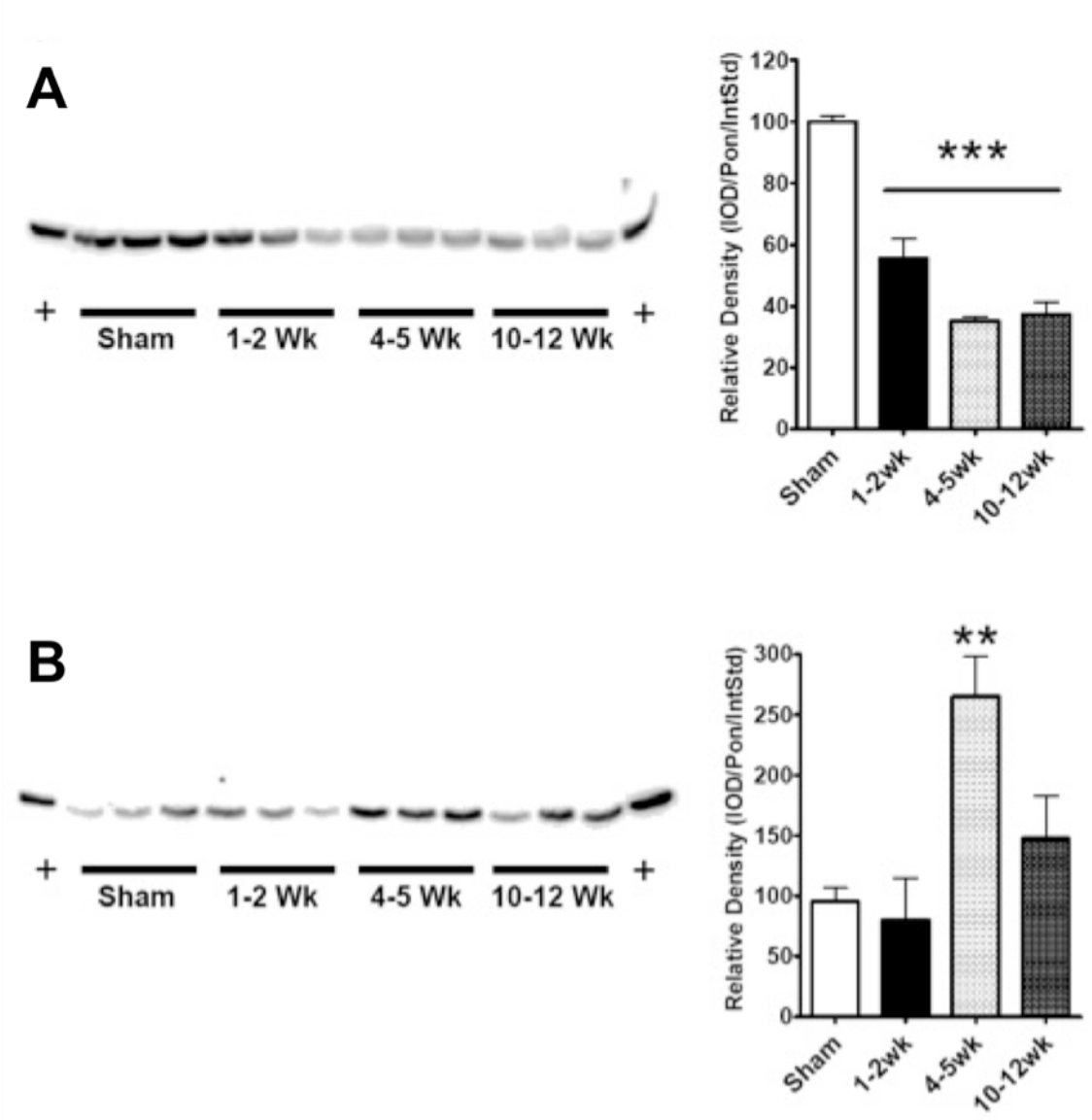

Figure 3-3. Argininosuccinate synthase and lyase protein expression. Renal cortex (A) ASS and (B) ASL protein expression per mg total protein shown with density analysis and representative blot. Protein blots are shown with equal protein loading in each lane and densitometry is represented in graphs; n=6 per group. Statistics comparing each injury to sham were done with a One-way ANOVA. * $p<0.05$, ** $p<0.01$, *** $p<0.001$ vs. sham.

Table 3-1. Physiological data and renal function for 5/6 ablation infarction CKD. Urine protein excretion (UpV) is based on 16-hour overnight collection. Mean arterial pressure (MAP) was taken at time of acute surgery via femoral artery catheter. Functional renal mass is based on 2 kidney weights in shams and single kidney minus scar tissue in A/I rats. Glomerulosclerosis Index (GSI) was measured on representative tissue sections stained with PAS. All values represented as mean±SE. Statistics were done with one-way ANOVA. * $p<0.05$, ** $p<0.01$, *** $p<0.001$ versus sham

	Sham	1-2 Weeks	4-5 Weeks	10-12 Weeks
Number	11	11	7	17
BW (g)	447±21	372±7**	378±8**	406±11*
UpV (mg/24h/ 100gBW)	8±2	21±3**	40±4***	93±24***
MAP (mmHg)	114±3	132±9**	148±3***	154±4***
Functional Renal Mass (g)	3.32±0.09	1.88±0.12***	1.76±0.16***	2.12±0.05***
GSI	0.09±0.01	0.25±0.05	0.76±0.25*	1.31±0.16***
Total CCr (ml/min/100gBW)	0.72±0.08	0.37±0.05***	0.23±0.05***	0.21±0.04***

Table 3-2. Citrulline and L-Arginine concentrations in plasma and renal cortex citrulline. Citrulline is measured in plasma and tissue using a colorimetric assay. L-Arg concentrations are measured via HPLC. Statistics comparing each injury to sham were done with one-way ANOVA. * p<0.05, ** p<0.01, ***p<0.001. Statistics comparing baseline vs. infusion were done with paired T-Test. NS: no significant difference.

	Sham	1-2 Weeks	4-5 Weeks	10-12 Weeks
Plasma Citrulline (μM)				
Baseline	61±3	107±8***	120±3***	153±5***
Cit Infusion	145±8	349±24***	393±18***	478±64***
	p<0.01	p<0.001	p<0.001	p<0.001
Plasma L-Arg (μM)				
Baseline	65±6	71±5	62±8	70±5
Cit Infusion	114±10	110±10	66±8*	73±6*
	p<0.001	P<0.01	NS	NS
Renal Cortex (μM/g protein)				
Citrulline	8.5±1	26±7*	37±7**	27±5**

Tables 3-3. Effect of citrulline infusion on renal plasma flow (RPF) and resulting renal citrulline delivery. RPF was measured by PAH clearance at baseline and during citrulline infusion. Sham RPF is for two kidneys. Renal citrulline delivery was determined by RPF x Plasma Citrulline concentrations. Statistics comparing each injury group to sham were done with one-way ANOVA. ** p<0.01, *** p<0.001 versus sham. Statistics comparing baseline vs. infusion were done with paired T-Test. NS: no significant difference.

	Sham	1-2 Weeks	4-5 Weeks	10-12 Weeks
Total RPF (ml/min)				
Baseline	9.4±0.7	3.1±0.3***	1.3±0.3***	2.2±0.3***
Cit Infusion	14.2±0.9	2.6±0.7***	1.9±0.5***	2.0±0.3***
	p<0.01	NS	NS	NS
Total Renal Citrulline Delivery (nmol/min)				
Baseline	632±52	324±36**	150±31***	331±53**
Cit Infusion	2170±271	816±182***	586±166***	630±104***

Table 3-4. Proximal tubule uptake mechanisms of citrulline.

	Sham	1-2 Weeks	4-5 Weeks	10-12 Weeks
Citrulline Renal Uptake (nmol/min)	66±7	91±11	32±16	26±5
Filtered Citrulline (nmol/min)	50±4	28±4	16±3	11±2
Peritubular Uptake (nmol/min)	11±8	55±16	17±15	7±5
% Filtered Uptake	89±10	36±10	71±13	65±15

Table 3-5. Urinary excretion of citrulline and L-Arginine factored for body weight at baseline and during citrulline infusion. Statistics comparing each injury group to sham were done with one-way ANOVA. ** p<0.01, *** p<0.001 versus sham. Statistics comparing baseline vs. infusion were done with paired T-Test. NS: no significant difference.

	Sham	1-2 Weeks	4-5 Weeks	10-12 Weeks
Citrulline Excretion (pg/min/100gBW)				
Baseline	3.7±1.1	12.7±3.8***	1.3±0.1	4.8±1.1
Cit Infusion	4.2±1.1	10.0±2.7***	1.5±0.3	4.0±0.7
	NS	NS	NS	NS
Arginine Excretion (pg/min/100gBW)				
Baseline	0.7±0.2	0.6±0.1	0.3±0.1	1.2±0.3*
Cit Infusion	1.4±0.3	0.8±0.2	0.5±0.1	1.0±0.2
	p<0.01	NS	NS	NS

CHAPTER 4
REDUCED ARGININE AVAILABILITY IN PUROMYCIN AND 5/6 ABLATION INFARCTION INDUCED CHRONIC KIDNEY DISEASE DUE TO TRANSPORTER DYSFUNCTION

Introduction

There is a net NO deficiency in patients and animals with CKD and ERKD(2, 15). There are multiple possible causes of NO deficiency in renal disease, one of which is a reduced availability of the NOS substrate, L-Arg. L-Arg availability is the rate-limiting step in NO production by NOS, and the kidney is an important site of L-Arg synthesis (38, 196). Renal L-Arg synthesis requires citrulline, which is taken up into the kidney and converted by argininosuccinate synthase (ASS) and argininosuccinate lyase (ASL) into L-Arg (38, 196). In normal healthy adults L-Arg is a non-essential amino acid since endogenous production, much of which occurs in the kidney, is sufficient for metabolic needs (196).

Patients and animals with renal disease show increases in plasma citrulline correlating with decreased renal function (26). This is probably caused by a reduction in renal uptake and utilization of citrulline rather than increased citrulline production or intake. However, the effect of renal disease on renal L-Arg production is controversial with reports of reduction in patients with chronic renal insufficiency and in 5/6 nephrectomized rats (27, 166) and maintenance in renal 5/6 ablation/infarction rats (18). We have preliminary data showing that the renal release of L-Arg is impaired in 5/6 renal mass reduction-induced CKD due to both reduced citrulline uptake and reductions in renal cortex ASS expression (28).

L-Arg that is synthesized by the renal proximal tubules (86) must be secreted across the basolateral side of the cell, taken up into the peritubular blood and then

delivered to the endothelial cells. The major endothelial transporter for L-Arg is the system y+ cationic amino acid transporter (CAT). CAT1 is constitutively present on all endothelial cells and transports L-Arg into the cell for NOS consumption (30). There is substantial evidence that L-Arg transport is impaired in renal disease, due to the presence of circulating CAT inhibitors in ERKD (198, 199) and to reduction in CAT abundance in aorta and glomeruli of the renal mass reduction induced-CKD rats. Further, there is a negative regulation of CAT by PKC-α (147, 209, 210) in nephrectomized and hyperlipidemic rats. In addition to controlling endothelial uptake, CAT1 is also present on the basolateral side of proximal tubules and contributes to L-Arg efflux from the kidney for distribution throughout the body (51, 74).

In addition to utilization by NOS, there are alternate pathways of L-Arg metabolism, including the arginase pathway and vascular arginases are elevated in several disease models (196) and may divert L-Arg away from NOS leading to decreased NO production.

The goal of this project was to determine several aspects of L-Arg bioavailability in the puromycin aminonucleoside (PAN) model of CKD (41). We measured renal ASS/ASL abundance (as an indication of renal L-Arg synthesis), CAT1 abundance in kidney cortex (as a measure of proximal tubule L-Arg efflux), aortic CAT1 abundance (as a measure of endothelial L-Arg uptake) and arginase abundance and activity (as a possible competing pathway for L-Arg utilization).

Methods

All experiments were performed using male Sprague-Dawley rats in accordance with the National Institutes of Health Guide for the Care and Use of Laboratory Animals

and approved and monitored by the University of Florida Institutional Animal Care and Use Committee. Urine was collected overnight (16 hours) in metabolic cages with animals given free access to water only. Urine protein excretion (UpV) was measured by Bradford method (BioRad, Hercules, CA). After a baseline urine collection, rats were randomly separated into 3 groups (n=8/group): Control (Saline vehicle), low dose (25mg/kg BW initial, 10mg/kg boosters), and high dose (50mg/kg BW initial, 20mg/kg BW boosters). The initial injection was given subcutaneously (SC) at week 0, and booster injections (SC) were given at weeks 2, 4, and 6. UpV was collected and monitored at weeks 1, 3, 5, 7, 9 and 11. Body weight (BW) was measured once per week. At week 11, rats were placed on a low nitrate diet 16 hours prior to urine collection and for three days prior to sacrifice. Rats were anesthetized with isofluorane, and mean arterial pressure (MAP) was measured via an abdominal aortic puncture then blood was collected, and plasma was stored at -80^{o}C. The organs were perfused with cold sterile PBS, the left kidney was removed, weighed and fixed in 10% formalin for histology, and the aorta, liver, and right kidney were harvested and flash frozen in liquid nitrogen and stored at -80^{o}C.

Renal Function

Week 11 overnight urine collected prior to sacrifice and plasma collected at sacrifice were analyzed for creatinine by HPLC. Plasma (80µl) was precipitated in acetonitrile at 4 times its volume and then centrifuged at 15,000 g for 15 min and dried under N_2 at 45 ^{o}C. The dried sample was dissolved in glass-distilled water at half of its original sample volume and then centrifuged for 10 minutes at 15,000xg. Urine samples (were diluted 1:200 and then prepared using the method of Tsikas et. al (167). Creatinine was measured by HPLC using the chromatographic method of George et al

(48). Creatinine was eluted on a 3.9x150 mm Waters AccQ-Tag C18 column in a 20mM potassium dihydrogen phosphate pH 7.4 isocratic mobile phase, followed by a 60/40 buffer/acetonitrile 12 minute column wash out and then a 5 minute reequilibration in 100% Buffer (20mM potassium dihydrogen phosphate buffer pH 7.4). Creatinine was then measured with a Perkin Elmer series 200 HPLC with series 200 UV detector.

Histology

Kidney histology was prepared as previously described in Chapter 2-Kidney Histology. The left kidney was cut along the transverse axis and fixed in 10% formalin for 48 hours then paraffin embedded. Sections were cut at 5µm onto Superfrost/Plus microscope slides (Fisher Scientific). Slides were deparaffinized and rehydrated in xylene and serial alcohol incubations and stained with Periodic Acid Schiff (PAS, Sigma, St Louis, MO) followed by hematoxylin as the secondary stain. Up to one hundred glomeruli were scored blindly based on the following scale: 0=healthy glomeruli, +1=<25% damage, +2=25-50% damage, +3=51-75% damage, +4=>75% damage. A glomerulosclerosis index score (GSI) was calculated using the following equation: (#of+1)+ 2(#of+2)+ 3(#of+3)+ 4(#of +4)/ total glomeruli observed.

Western Blot

Western blot analysis was made as described previously (163) using 12% acrylamide gels. Measurements were conducted on kidney cortex, aorta, and liver homogenates. . Rabbit polyclonal antibodies (developed by Dr Masataka Mori, Kumamoto University, Kumamoto)(203) against ASS and ASL were used at 1:2000 dilutions, 1-hour incubation. Rabbit polyclonal arginase II antibody (Santa Cruz) was used at a dilution of 1:3000. A goat anti-rabbit IgG-HRP secondary antibody (Bio-Rad, 1:3000 dilution, one hour incubation) was used for detection. Chicken arginase I

antibody (gift from Dr. Sidney Morris) was used at 1:10000 and a goat anti-chicken IgG-HRP secondary antibody was used for detection. Bands of interest were visualized using SuperSignal West Pico reagent (Pierce, Rockford, IL) and quantified using the VersaDoc imaging system and Quantity One Analysis software (Bio-Rad), as integrated optical density (IOD) after subtraction of background. The IOD was factored for Ponceau red staining to correct for any variations in total protein loading and for an internal positive control (rat liver for ASS, ASL, and arginase I; rat kidney cortex for arginase II). The protein abundance was represented as IOD/Positive control/total protein by Ponceau red, relative to the HP group (set to 100).

CAT1 and PKC-α Western Blot

Flash frozen kidney cortex and aorta were fractionated into membrane and cytosolic fractions as previously described by Schwartz et al (145). Briefly, tissue was homogenized in a lysis buffer of PBS containing 0.01% Triton X-100, 0.1% SDS and protease inhibitors (1 mM phenylmethylsulfonyl fluoride, 4.5 µM leupeptin, 5 µM aprotinin). Samples were mechanically homogenized on ice and left on ice for 45min. Homogenates were centrifuged at 15,000 rpm for 10 min at 4°C and lysates were removed as the cytosolic fraction. The membrane fraction was obtained by adding to the pellet an equal volume of lysis buffer supplemented by Tween 20 (0.25%) to solubilize. The protein content of each fraction was determined by Lowry method. Homogenates (30µg) were run on 7.5% acrylamide gels. A polyclonal rabbit antibody was used to probe for CAT1 (developed by Schwartz et al) at 1:500. . A goat anti-rabbit IgG-HRP secondary antibody (Bio-Rad, 1:3000 dilution, one hour incubation) was used for detection. A mouse monoclonal antibody was used for PKC-α (BD Transduction

Laboratories, Lexington KY) at 1:1000, and anti-mouse secondary (1:1000) was used for detection.

Arginase Assay

Arginase activity in liver and kidney cortex was determined by measuring the rate of urea production in the homogenate using α-isonitrosopropriophenone (9% in absolute ethanol) as previously described.(208) Tissue was homogenized in 0.5 ml of lysis buffer containing 50 mM Tris-HCl (pH 7.5), 0.1 mM EDTA, 0.1 mM EGTA, and protease inhibitors (inhibitor cocktail Set III (Calbiochem)). Homogenates were incubated with L-Arg (0.5 M; pH 9.7) at 37^{o} C for 60 min. The hydrolysis reaction of L-Arg by arginase was stopped by adding 750 ml of an acid solution mixture (H_2SO_4:H_3PO_4:H_2O, 1:3:7).

L-Arginine

The concentration of L-Arg in plasma was measured using reverse-phase HPLC with the Waters AccQ-Fluor fluorescent reagent kit. Samples were prepared by mixing 60µl of plasma with 350µl of borate buffer (pH=9). This was placed on an unconditioned Oasis MCX column (Waters, Milford, MA) then washed with 1ml borate buffer, 3x1 ml H_2O, and 1ml MEOH. The sample was eluted with 1ml NH_4OH/ H_2O /MEOH (10:40:50), dried under nitrogen gas, then reconstituted with 30µl H_2O. Recovery was approximately 85%. Twenty microliters of the samples was mixed with 60µl borate buffer and 20µl of AccQ Fluor reagent (Waters, Milford, MA). 50µl of mixture was injected onto a Luna 150 x 3 mm C-18 reversed-phase column (Phenomenex, Torrance, CA). A flow rate of 1.3ml/min was attained with a PerkinElmer Series 200 Pump, and fluorescence intensity was measured using a series 200 fluorescent detector, EX 250/EM 395 (PerkinElmer Life and Analytical Sciences, Shelton, CT).

Standards contained concentrations of L-Arg in the range of 200µM to 3.12µM. This method was adapted from Heresztyn et al (53).

Citrulline

Plasma citrulline was measured by a colorimetric assay described previously (164).

Plasma and Urinary NOx

Total NO content (from NOx = NO_3^- + NO_2^-) was measured by Griess reaction (159) in plasma collected at week 11 sacrifice, urine collected at week 11 by metabolic cage and in kidney cortex homogenates prepared as previously described (163). Rats were kept on a low nitrate diet 16-hour prior to start of urine collection and 3 days prior to plasma collection.

Statistics

Repeated Measures-ANOVA combined with Bonferonni post hoc test was used for statistical evaluation for timeline of proteinuria and BW between groups. One-way ANOVA combined with Newman-Keuls post hoc test was used for statistical evaluation of mean values across groups. All graphs and statistics were done with Prism 4 software (GraphPad Software, Inc., San Diego, CA). Values are reported as means ± SE with $P<0.05$ was considered statistically significant.

Results

Both low dose and high dose PAN injected rats exhibited significant proteinuria throughout the study. High dose PAN led to protein excretions up to ~400mg/day/100g BW at week 9, and the low dose treated rats reached a peak at week 9 of 200mg/day/100gBW (Figure -41A). There was a fall in protein excretion at week 11 in the high dose group associated with a very low GFR (Table 4-1), while GFR was similar

to controls in the low dose group. BW of high dose PAN rats fell within 1 week of the first injection and remained low throughout the study, whereas low dose PAN animals had similar weight gain versus control until 11 weeks post injection (Figure 4-1B). Blood pressure increased dose dependently in the 2 PAN groups and renal pathology revealed significant injury in the low dose PAN and marked injury in high dose PAN kidneys. Significant renal hypertrophy was also evident in the high PAN dos group (Table 4-1).

Kidney cortex expression of ASS was significantly reduced only in the high dose group; while ASL was reduced in both PAN groups and was nearly undetectable in the high dose (Figure 4-2A and B). In contrast, there was no change in hepatic expression of ASS or ASL (Figure 4-2C and D). However, plasma L-Arg concentration was unchanged between low and high dose versus control (128±8 and 98±10 vs. 97±9μM, respectively). Plasma citrulline was intermediate in low dose PAN rats and was significantly elevated in the high dose PAN rats versus control ($p<0.05$; 138±15 and 160±23 vs. 89±10, respectively).

Membrane and cytosolic expression of CAT1 was markedly reduced in both PAN groups in the kidney cortex (Figure 4-3A and B) and PKC-alpha expression was increased in both membrane and cytosolic fractions of kidneys from high dose PAN treated rats (Figure 4-3C and D). Low dose PAN treatment resulted in increased PKC alpha only in the cytosolic fraction. Aortic expression of membrane bound CAT1 was reduced in both PAN groups and increased in the cytosolic fraction of high dose (Figure 4-3E and F). PKC-α was reduced in both PAN groups in both membrane and soluble fractions (Figure 4-3G and H).

Kidney cortex arginase II abundance and arginase activity were unchanged by PAN treatment (Figure 4-4A and B). Neither hepatic arginase abundance nor activity was different between groups (Figure 4-4C and D). Aortic expression of arginase was increased in low dose PAN but was comparable to sham levels in high dose PAN (Figure 4-4E). Arginase activity was not measured in the aorta due to lack of tissue.

Total NO production was measured by nitrate and nitrite (NOx) concentrations in the plasma and urine. There was a significant reduction in plasma NOx in the high dose group when factored for plasma creatinine, and urinary excretion of NOx was markedly reduced in both PAN groups (Table 4-1).

Renal cortex abundance of membrane CAT1 is reduced in the moderate and severe stages of 5/6 A/I (Figure 4-5A). PKC-α is increased in both the membrane and cytosolic fractions in the mild and moderate stages (Figure 4-5B and C).

Discussion

The novel findings of this study are that PAN induced CKD results in severity dependent reduction in renal ASS/ASL abundance. This together with the loss of renal CAT1 must mean a marked reduction in renal L-Arg synthesis and release, despite which, plasma L-Arg level is maintained. We also find loss of vascular (aortic) CAT1, which must lead to reduced L-Arg uptake from plasma and may account for the "deceptively" normal plasma L-Arg.

PAN selectively attacks the glomerular podocytes and when given acutely PAN produces nephritic syndrome. When followed by additional, lower doses this converts to a progressive model of CKD (14). In the present study we found that PAN injections resulted in a dose dependent renal injury. After 11 weeks of administration the high

dose kidneys were severely injured with GSI > 2.0 (GSI = 4.0 means total damage to every glomeruli) and had only ~20% residual renal function. The low dose PAN injections produced a significant but moderate renal injury that was without functional impairment.

During development of CKD, increases in plasma citrulline are invariably observed (87). Citrulline is the rate limiting substrate for L-Arg production and the increases in plasma citrulline suggest decreased renal uptake, which should result in decreased L-Arg production. With both levels of PAN-induced CKD there were significant reductions in renal ASS and ASL abundance, the enzymes required for conversion of citrulline to L-Arg, which also means reduction in renal L-Arg synthesis. In fact, the high dose group showed virtually no expression of renal ASL, which would prevent any renal L-Arg synthesis. These are the first studies in the PAN model of CKD although we have shown previously that renal uptake of citrulline and release of L-Arg is reduced in CKD due to 5/6 renal mass reductions by combined ablation/infarction. In that study, we also observed significant reduction in renal ASS which coupled with reduced citrulline delivery to the kidney, would contribute to the loss of L-Arg release (28).

Once synthesized in the renal proximal tubule, L-Arg would need to be secreted across the basolateral membrane in order to gain entry to the plasma. Specific transporters are required for L-Arg movement across membranes and Kizhatil et al has shown CAT1 localization on the basolateral side of renal epithelial cells (74). In the present studies we observed a reduction in renal cortical CAT1 abundance in the membrane (where the transporter is active). PKC-α is known to inhibit L-Arg transport by CAT1 via post-translational modifications that cause CAT1 to leave the membrane

(80, 132, 133, 147, 210). In these studies there was a significant increase in PKC-α in the kidney cortex of low dose PAN and a 20-fold increase in abundance in the high dose. This increase could explain the reduction in membrane bound CAT1 seen in our animals. This trend is also seen in the 5/6 A/I CKD; membrane bound CAT1 is reduced and PKC-α is increased about 30-fold in the cytosolic fractions.

CAT proteins are involved in the influx as well as the efflux of cationic amino acids (51) and CAT1 is the primary transporter for L-Arg in the vascular endothelium (29). We also saw a marked fall in the membrane bound CAT1 from aorta of both PAN models. There was an increase in cytosolic CAT1 expression in the aorta from the high dose implying transport of CAT1 away from the membrane. It was previously reported that protein abundance (but not mRNA) of aortic CAT1 was reduced in the 5/6-nephrectomy model (145). What caused the fall in aortic CAT1 in the present study is not clear in view of reduced PKC-α abundance in the aorta.

This brings us back to the puzzling finding that plasma L-Arg levels are usually normal in CKD and ERKD (142, 143), and are maintained in the present study. The contribution of kidney derived L-Arg to circulating levels is significant (196), and given our evidence suggesting that renal L-Arg production is impaired with PAN-CKD, the maintenance of normal plasma levels is puzzling. One possible reason could be that a reduction in L-Arg uptake occurs into the vasculature, which is supported by our finding that membrane aortic CAT1 falls in these models. In addition, we have previously shown that plasma from uremic patients contains factors that inhibit L-Arg entry into the endothelial cells (198, 199). Thus, reduced endothelial L-Arg uptake may camouflage renal l-Arg deficiency by allowing L-Arg to accumulate in plasma to apparently normal

values. Another observation is that L-Arg supplementation does not improve arterial endothelial function or reduce the rate of progression of renal failure in adults or children with CKD (12, 32, 36, 207). This could also reflect a failure of administered L-Arg to be transported to the endothelial NOS.

In addition to decreased renal synthesis another possible mechanism of L-Arg deficiency in CKD could be via increased metabolism by arginase. Arginase is activated by injury and is involved in repair processes (190). Increased vascular arginase levels have been reported in several models of hypertension and CKD and some workers suggest that this might divert L-Arg away from the NOS, leading to NO deficiency (7). In the present study we did see increased aortic arginase abundance in the low dose PAN model, and did not see any changes in renal or hepatic arginase abundance/ activity in either PAN groups. In the severe injury model, however, aortic arginase was comparable to control levels, perhaps reflecting the greater severity and more rapid progression of the disease (BP was much higher in these animals) such that attempt at repair had already occurred.

NO deficiency is a common finding in man and animals with renal disease, which contributes to the progression and the cardiovascular events (7). We see marked declines in total NO production in the present study as indicated by the falls in 24h NOx excretion, and in plasma NOx in the severe injury model. There are many possible mechanisms by which NO deficiency could occur but this study suggests that decreased renal L-Arg synthesis/release as well as decreased vascular uptake of L-Arg could contribute. Potential therapeutics to maintain renal L-Arg synthesis and transport

may shift the balance in favor of NO production and attenuate the progression of the systemic sequela of CKD.

Table 4-1. Functional data for puromycin induced CKD. MAP mean arterial blood pressure, CCr creatinine clearance factored for body weight, GSI glomerulosclerosis index, KW kidney weight factored for body weight, plasma NOx corrected for plasma creatinine, and 24-hour urinary NOx excretion. Statistics comparing each PAN group to controls were done with one-way ANOVA. * $p<0.05$, *** $p<0.001$vs. Controls. (ND not detectable)

Group	n	MAP (mmHg)	Total CCr (ml/min/100gBW)	GSI	KW/100g BW	Plasma NOx/Cr (µM/mg%)	Urine NOx (µmol/day)
Control	8	100±2	0.73±0.07	0.11±0.02	0.39±0.03	1.9±0.4	2.62±0.28
Low Dose	8	116±5*	0.66±0.09	1.04±0.28*	0.55±0.05	1.3±0.2	0.37±0.21
High Dose	8	134±8***	0.16±0.07***	2.19±0.34***	0.79±0.07***	0.8±0.3*	0.38±0.20

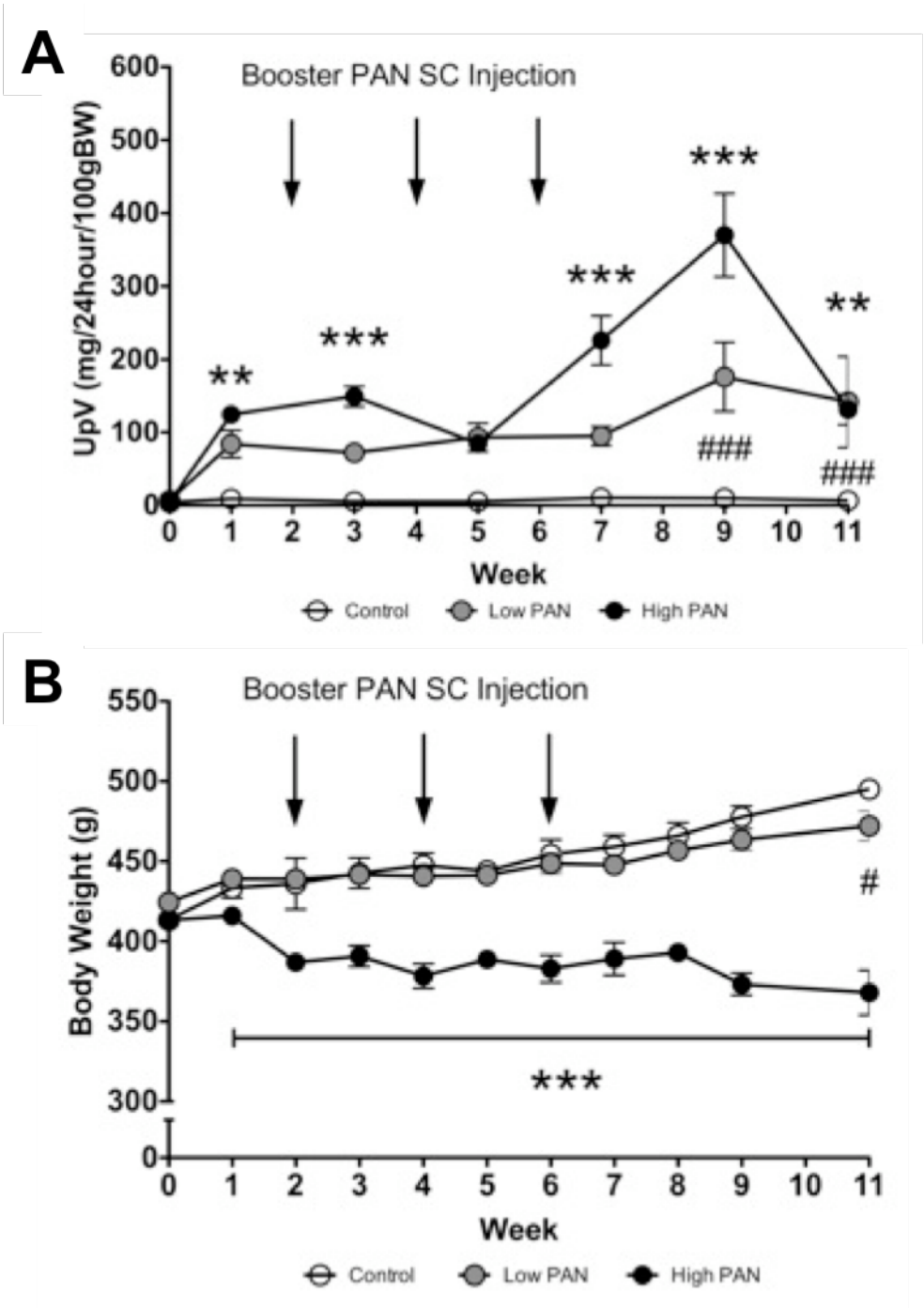

Figure 4-1. Timeline of PAN chronic kidney disease progression. (A) Urinary protein excretion and (B) body weight from baseline to 11 weeks post initial PAN injection. Values are mean ± SEM, ** $p<0.01$ and *** $p<0.001$ high dose PAN vs control, # $p<0.05$ and ### $p<0.001$ low dose PAN vs control.

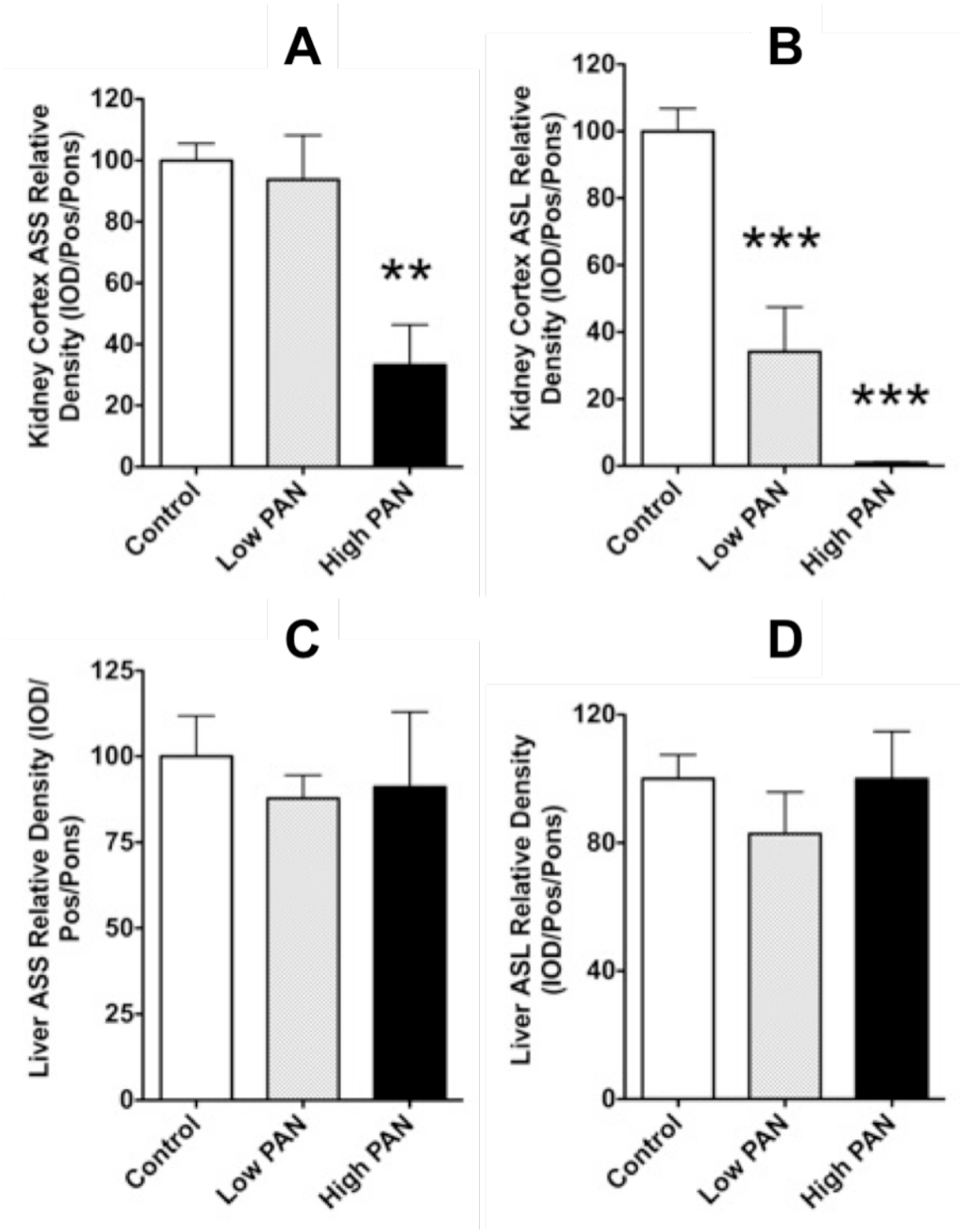

Figure 4-2. Argininosuccinate synthase (ASS) and lyase (ASL) protein abundance. Renal cortex expression of (A) ASS, (B) ASL and hepatic expression of (C) ASS, (B) ASL measured by Western blot (n=8 per group). Statistics comparing each PAN group to controls were done with one-way ANOVA. ** $p<0.01$, *** $p<0.001$vs. Controls.

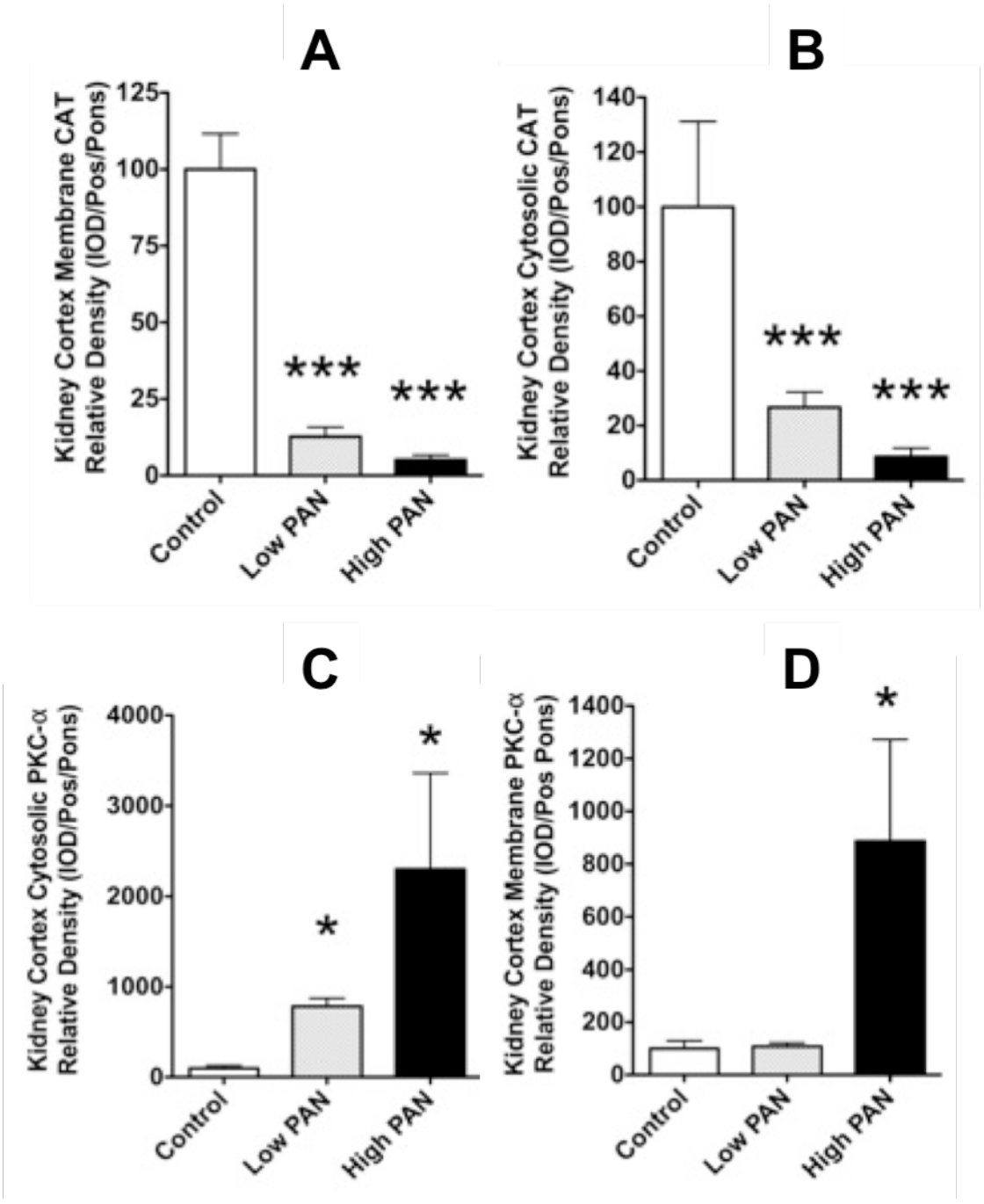

Figure 4-3. L-Arginine transporter and PKC-alpha protein abundance. Renal cortex expression of (A) membrane bound and (B) cytosolic CAT1, and (C) membrane PKC-α and (D) cytosolic PKC-α. Aortic expression of (E) membrane bound and (F) cytosolic CAT1, and (G) membrane PKC-α and (H) cytosolic PKC-alpha measured by Western blot (n=8 per group). Statistics comparing each PAN group to controls were done with one-way ANOVA. * $p<0.05$, ** $p<0.01$, *** $p<0.001$vs. Controls.

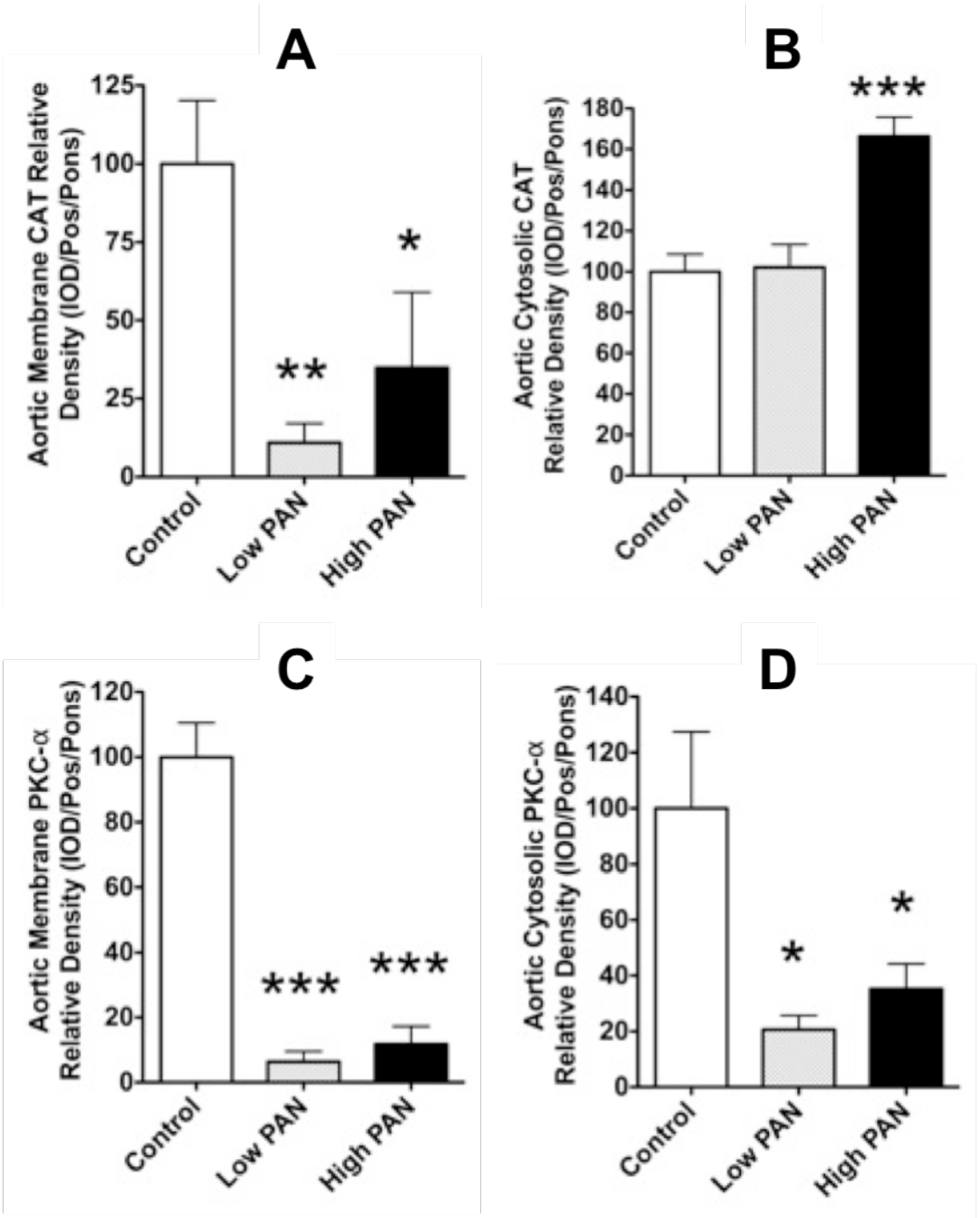

Figure 4-3. Continued

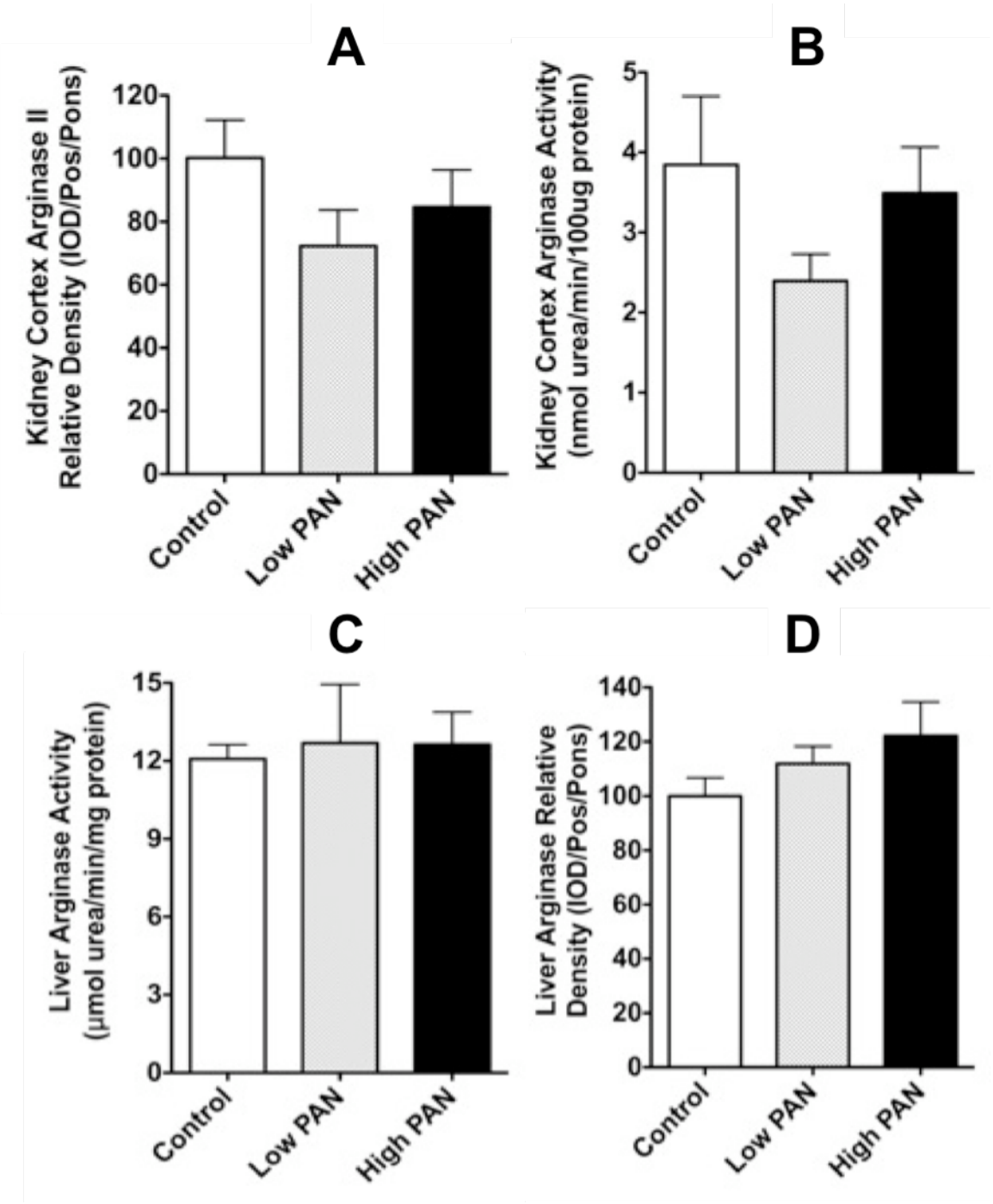

Figure 4-4. L-Arginine metabolizing enzyme abundance and activity. Kidney cortex arginase II (A) protein expression measured by Western blot and (B) activity measured by urea formation (n=8 per group). Hepatic arginase I (C) protein expression and (D) activity. (E) Aortic arginase I protein expression. Statistics comparing each PAN group to controls were done with one-way ANOVA. ** $p<0.01$ vs. Controls.

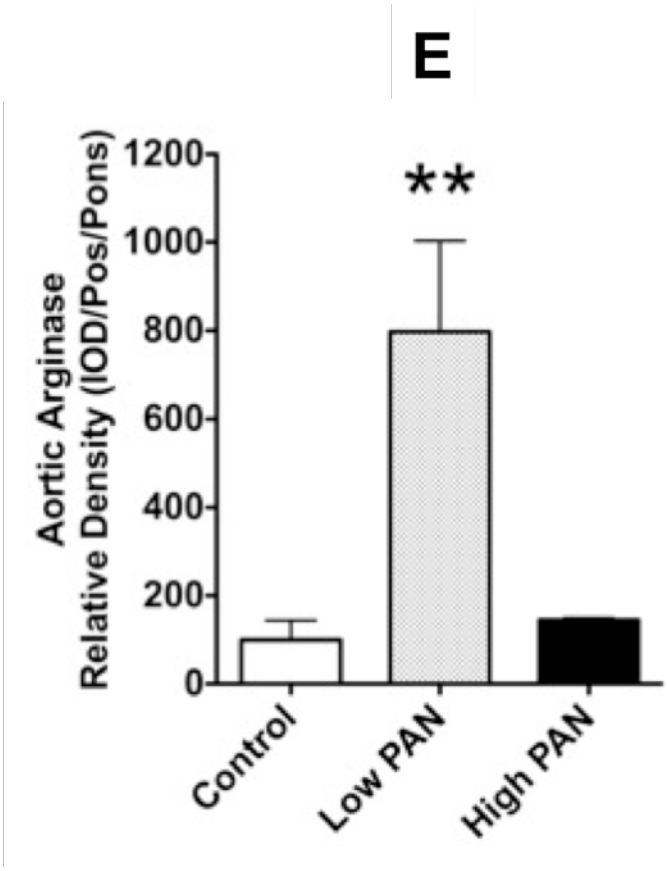

Figure 4-4. Continued

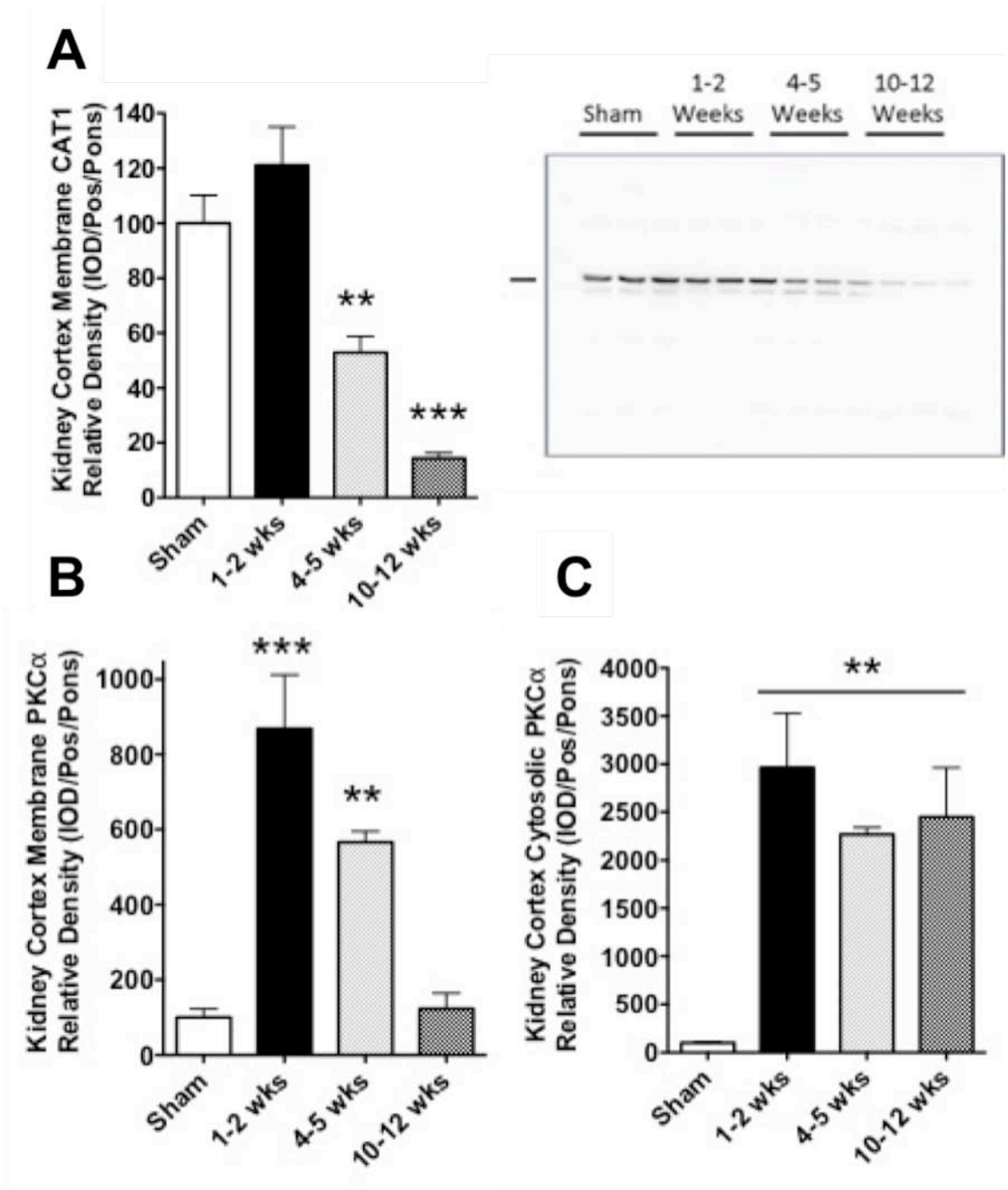

Figure 4-5. Kidney cortex CAT and cellular fractions of PKC-α expression. (A) Membrane bound CAT expression in the kidney cortex with representative blot shown. (B) Membrane bound and (C) cytosolic PKC-α abundance measured by western blot. Statistics comparing each injury to sham were done with one-way ANOVA. ** $p<0.01$, *** $p<0.001$ vs. sham.

CHAPTER 5
ARGININE/ADMA SYNTHESIS AND METABOLIC PATHWAYS IN FAWN-HOODED HYPERTENSIVE RATS: A MODEL OF SPONATENOUS CHRONIC KIDNEY DISEASE; IMPACT OF DISEASE ATTENUATION ON ARGINASE

Introduction

NO is essential to normal cardiovascular and renal function. There is a net NO deficiency in patients and animals with CKD and ERKD (2, 15). NO is produced by conversion of L-Arg by NOS. The L-Arg required for NO synthesis is produced from L-citrulline by the argininosuccinate synthetase (ASS) and argininosuccinate lyase (ASL) enzymes and the kidney provides most of the circulating L-Arg (105). Renal synthesis of L-Arg occurs primarily in the proximal tubules and a deficiency in renal L-Arg production may result in decreased substrate availability for NOS, and hence decreased L-Arg availability. There is also evidence that the arginases are elevated in several disease models (196) and may divert L-Arg away from the NOS leading to decreased NO production.

Any L-Arg that is available for NO synthesis must compete with endogenous inhibitors, such as ADMA for NOS (174). Therefore, the balance between L-Arg and ADMA is also an important determinant of NO generating ability. ADMA is generated by protein arginine methyltransferase (PRMT1) and removed mainly by hydrolysis by dimethylarginine dimethylaminohydrolase (DDAH); the kidney is an important site of ADMA breakdown (1)

The fawn-hooded hypertensive (FHH) rat provides a genetic model for spontaneous glomerulosclerosis that has been linked to several renal failure genes (99). NO deficiency may contribute to the glomerular damage since chronic NOS inhibition accelerates the development of glomerulosclerosis in the FHH rat (177) and perinatal

exposure to an NO donor attenuates hypertension and glomerular injury (77). Angiotensin II (ANGII) antagonism slows down progression of many types of CKD, including the FHH rat (180-183, 211). In this study we investigated the high-protein fed FHH with and without ANGII blockade, to test the hypothesis that attenuation of hypertension and renal injury will improve L-Arg availability and reduce ADMA.

Methods

All experiments were performed using male FHH rats (purchased at 5 weeks old, Hilltop Lab Animals, Scottsdale, PA) in accordance with the National Institutes of Health Guide for the Care and Use of Laboratory Animals and approved and monitored by the University of Florida Institutional Animal Care and Use Committee. Rats were housed in conventional cages and given free access to normal chow and water. Urine was collected overnight (16 hours) in metabolic cages with animals given free access to water only at 6weeks of age then all animals were switched to a 40% casein (Hill's Science Diet, Topeka, KS) diet and were divided into 2 groups (n=10/group): high protein diet alone (HP) and HP plus irbesartan (an ANG receptor type 1, AT1, blocker) in the diet (~100mg/kg BW/day, HP+Irb). All rats were maintained on the respective diet for 13 weeks, and body weight and UpV (by Bradford method (BioRad, Hercules, CA), were measured at weeks 2, 4, 7, 10, and 13. At week 13, rats were anesthetized with isofluorane and mean arterial pressure (MAP) was measured by an abdominal aortic puncture, blood was collected, and plasma was stored at -80^{o}C. The organs were then perfused with sterile PBS, the left kidney was removed, weighed and fixed in 10% formalin for histology and the aorta, liver, and right kidney were harvested and flash frozen in liquid nitrogen and stored at -80∞C.

Renal Function

Week 13 overnight urine collected prior to sacrifice and plasma collected at sacrifice were analyzed for creatinine by HPLC. Plasma was prepared using the method of Tsikas et al (167) with a few modifications. Plasma (80μl) was precipitated in acetonitrile at 4 times its volume and then centrifuged at 15,000 g for 15 min and dried under N_2 at 45 ^{o}C. The dried sample was dissolved in glass-distilled water at half of its original sample volume and then centrifuged for 10 minutes at 15,000xg. Urine samples (were diluted 1:200 and then prepared using the method of Tsikas et al (167). Creatinine was measured by HPLC using the chromatographic method of George et al (48). Creatinine was eluted on a 3.9x150 mm Waters AccQ-Tag C18 column in a 20mM potassium dihydrogen phosphate pH 7.4 isocratic mobile phase, followed by a 60/40 buffer/acetonitrile 12 minute column wash out and then a 5 minute reequilibration in 100% Buffer (20mM potassium dihydrogen phosphate buffer pH 7.4). Creatinine was then measured with a Perkin Elmer series 200 HPLC with series 200 UV detector.

Histology

Kidney histology was prepared as previously described in Chapter 2-Kidney Histology. The left kidney was cut along the transverse axis and fixed in 10% formalin for 48 hours then paraffin embedded. Sections were cut at 5μm onto Superfrost/Plus microscope slides (Fisher Scientific). Slides were deparaffinized and rehydrated in xylene and serial alcohol incubations and stained with Periodic Acid Schiff (PAS, Sigma, St Louis, MO) followed by Hematoxylin as the secondary stain. Up to one hundred glomeruli were scored blindly based on the following scale: 0=healthy glomeruli, +1=<25% damage, +2=25-50% damage, +3=51-75% damage, +4=>75% damage. A

glomerulosclerosis index score (GSI) was calculated using the following equation: (#of+1)+ 2(#of+2)+ 3(#of+3)+ 4(#of +4)/ total glomeruli observed.

Western Blot

Western blot analysis was made as described previously (Tain, Freshour, et al. 2007) using 12% acrylamide gels. Measurements were conducted on kidney cortex, aorta, and liver homogenates. Rabbit polyclonal antibodies (developed by Dr Masataka Mori, Kumamoto University, Kumamoto)(203) against ASS and ASL were used at 1:2000 dilutions, 1-hour incubation. Rabbit polyclonal arginase II antibody (Santa Cruz) was used at a dilution of 1:3000. A goat anti-rabbit IgG-HRP secondary antibody (Bio-Rad, 1:3000 dilution, one hour incubation) was used for detection. Chicken arginase I antibody (gift from Dr. Sidney Morris) was used at 1:10000 and a goat anti-chicken IgG-HRP secondary antibody was used for detection. For PRMT1, we used a rabbit antibody (Upstate, 1:2000 dilution, overnight incubation) and a goat anti-rabbit antibody secondary. For DDAH we used a goat anti-rat DDAH1 antibody (Santa Cruz, 1:500 dilution, overnight incubation) and a goat anti-rat DDAH2 antibody (Santa Cruz, 1:100 dilution, overnight incubation), followed by a secondary donkey anti-goat antibody (Santa Cruz, 1:2000 dilution, 1h incubation). Bands of interest were visualized using SuperSignal West Pico reagent (Pierce, Rockford, IL) and quantified using the VersaDoc imaging system and Quantity One Analysis software (Bio-Rad), as integrated optical density (IOD) after subtraction of background. The IOD was factored for Ponceau red staining to correct for any variations in total protein loading and for an internal positive control (rat liver for ASS, ASL, and arginase I; rat kidney cortex for arginase II, DDAH1/2, and PRMT1; endothelial cell lysate for eNOS). The protein

abundance was represented as IOD/Positive control/total protein by Ponceau red, relative to the HP group (set to 100).

Arginase Assay

Arginase activity in liver and kidney cortex was determined by measuring the rate of urea production in the homogenate using α-isonitrosopropriophenone (9% in absolute ethanol) as previously described (208). Tissue was homogenized in 0.5 ml of lysis buffer containing 50 mM Tris-HCl (pH 7.5), 0.1 mM EDTA, 0.1 mM EGTA, and protease inhibitors (inhibitor cocktail Set III (Calbiochem)). Homogenates were incubated with L-Arg (0.5 M; pH 9.7) at 37^{o} C for 60 min. The hydrolysis reaction of L-Arg by arginase was stopped by adding 750 ml of an acid solution mixture (H_2SO_4:H_3PO_4:H_2O, 1:3:7).

DDAH Activity Assay

DDAH activity was measured by a colorimetric assay measuring the rate of citrulline production, as optimized by us (164). Kidney cortex was homogenized in sodium phosphate buffer and was pre-incubated with urease for 15 min, and then 100µl (2mg total protein) of homogenate was incubated with 1mM ADMA for 45 min at 37ºC. After deproteinization, supernatant was incubated with color mixture at 60ºC for 110 min. The absorbance was measured by spectrophotometer at 466 nm. The DDAH activity was represented as µmol citrulline formation/g protein/min at 37ºC.

L-Arginine/ADMA/SDMA Measurements

The concentration of L-Arg/ADMA in plasma and kidney cortex homogenates was measured using reverse-phase HPLC with the Waters AccQ-Fluor fluorescent reagent kit. Samples were prepared by mixing 60µl of plasma or tissue homogenate with 350µl of borate buffer (pH=9). This was placed on an unconditioned Oasis MCX column (Waters, Milford, MA) then washed with 1ml borate buffer, 3x1 ml H_2O, and 1ml MEOH.

The sample was eluted with 1ml NH_4OH/ H_2O /MEOH (10:40:50), dried under nitrogen gas, then reconstituted with 30µl H_2O. Recovery was approximately 85%. Twenty microliters of the samples was mixed with 60µl borate buffer and 20µl of AccQ Fluor reagent (Waters, Milford, MA). 50µl of mixture was injected onto a Luna 150 x 3 mm C-18 reversed-phase column (Phenomenex, Torrance, CA). A flow rate of 1.3ml/min was attained with a PerkinElmer Series 200 Pump, and fluorescence intensity was measured using a series 200 fluorescent detector, EX 250/EM 395 (PerkinElmer Life and Analytical Sciences, Shelton, CT). Standards contained concentrations of L-Arg in the range of 200µM to 3.12µM. This method was adapted from Heresztyn et al (53).

Citrulline

Renal cortex homogenate, plasma, and urine citrulline were measured by a colorimetric assay described previously (164).

Plasma and Tissue Oxidative Stress Measures

Plasma and tissue indices of oxidative stress were measured using an OXItek thiobarbituric acid reactive substances (TBARS) assay kit (ZeptoMetrix, Buffalo, NY) and an Amplex Red Hydrogen Peroxide/Peroxidase Assay Kit (Molecular Probes, Eugene, OR),

Tissue NOx

Kidney cortex homogenates were prepared as previously described (163) and total NO content (from $NOx = NO_3^- + NO_2^-$) was measured in kidney cortex homogenates by Griess reaction (159)

Statistics

Student t-test with a two-tailed p value was used to compare between treated and untreated groups. Mann-Whitney U test was used for pathology analysis. All graphs and

statistics were done with Prism 4 software (GraphPad Software, Inc., San Diego, CA). Values are reported as means ± SE with $P<0.05$ considered statistically significant.

Results

Both groups of FHH rats had similar weight gains up to 7 weeks on the high protein diet, but by 10 weeks the irbesartan treated rats weighed slightly less than untreated rats (Figure 5-1A). Baseline UpV was similar in both groups (Figure 5-1B) and increased in untreated rats over the 13 weeks of high protein diet by a maximum of ~2.5 fold. In contrast, irbesartan treated rats on high protein diet showed no increase throughout the treatment period (Figure 5-1B). The total percent of sclerotic glomeruli was higher in untreated (~18±2%) compared to irbesartan treated rats (~8±1%) and severity of injury was lower in the irbesartan treated rats (Figure 5-1C; Table 5-1). Irbesartan treatment also reduced BP and kidney weight (Table 5-1). The GFR, measured from 24h Ccr was near normal in the irbesartan treated FHH rats (~ 0.6 ml/min/100g BW) (163) and was ~ 2x normal in the untreated animals (Table 5-1).

Kidney cortex NOx was significantly increased with irbesartan treatment (Table 5-2), suggestive of increased renal NO production. The rats were not fasted or given a low nitrate diet (since the diet was an integral part of the CKD model) thus urine and plasma NOx values cannot be used to assess total NO production (9). We measured plasma hydrogen peroxide (10.1±2.4 vs. 5.8±0.9μM) and TBARS in plasma (20.6±2.2 vs. 16.3±1.5μM) and kidney cortex homogenates (0.222±0.005 vs. 0.201±0.009pmol/mg protein) as indices of oxidative stress, untreated vs. treated. There was no difference in any of these measurements between the two groups.

Plasma L-Arg concentration was significantly higher in irbesartan treated rats but there was no difference in kidney cortex L-Arg levels (Table 5-2).

The enzymes responsible for renal and hepatic L-Arg synthesis (ASS and ASL) were similar in the 2 groups (Figure 5-2). The abundance of renal cortex arginase II and aortic arginase I was reduced with irbesartan treatment, while hepatic expression of arginase I was unchanged (Figure 5-3A). Arginase activity, measured by urea formation from excess L-Arg, matched the protein expression with reduced activity in the renal cortex with irbesartan treatment (Figure 5-3B) and no difference in activity between groups in the liver (Figure 5-3C) (there was insufficient tissue to measure arginase activity in the aorta).

There was no difference in plasma or kidney cortex citrulline or ADMA concentration between groups, although the L-Arg to ADMA ratio was higher with irbesartan treatment in plasma (Table 5-2). Renal cortex DDAH2 protein abundance was reduced, DDAH1 was increased (Figure 5-4A) and renal cortex DDAH activity was higher in rats treated with irbesartan (Figure 5-4B). PRMT1 was unchanged with irbesartan treatment (Figure 5-4C). There were no differences in the abundance of any of these proteins in the aorta (Figure 5-4D).

Discussion

The major novel findings of this study are that protection of kidney structure and function with AT-1 blockade in the FHH rat resulted in reduced arginase protein and activity in the kidney cortex. Although the abundance of the renal L-Arg synthesizing enzymes was unchanged, the plasma concentration of L-Arg was increased in the irbesartan treated group in association with the reduction in renal arginase activity. Plasma ADMA concentrations were not changed by irbesartan treatment even though

renal DDAH activity and DDAH1 expression were increased. The increased plasma L-Arg and unchanged ADMA with AT-1 receptor blockade cause an increased plasma L-Arg to ADMA ratio, which should favor NO production.

The FHH rat develops early hypertension and renal injury that is exacerbated by feeding a high protein diet. Several genes contribute to the increased susceptibility to renal disease (99) and are associated with autoregulatory failure (93, 176) in turn leading to glomerular hypertension and susceptibility to glomerular injury (153, 178). Blockade of ANGII with ACE inhibitors or AT-1 receptor blockers reduces glomerular blood pressure and preserves glomerular structure and function (211). Early and late ANGII inhibition with ACE inhibitors protects the FHH kidney from glomerular damage (181, 182). In the present study we used AT1 receptor blockade to attenuate renal damage in FHH to test the hypotheses that L-Arg availability would be preserved and ADMA would be reduced vs. untreated FHH.

The kidney is the major organ for circulating L-Arg production via citrulline uptake and conversion by ASS and ASL (196) and we have observed marked reductions in renal L-Arg synthesis in the 5/6 ablation infarction model of CKD, due to both reduced citrulline uptake and reduced ASS/ASL abundance (28). In the present study in the FHH rat we find that in contrast to other models of CKD, plasma citrulline was not elevated and that renal cortex ASS and ASL were similar to the irbesartan treated rats with preserved kidney structure. This suggests that renal L-Arg synthesis is not inevitably reduced with CKD, but may depend on the type and/or severity of the injury process. Nevertheless, we also find that irbesartan treatment and preservation of kidney function

in FHH is associated with an increase in plasma L-Arg, suggesting increased L-Arg availability.

L-Arg is a promiscuous substrate used by several metabolic enzymes, including arginase, which can consume considerable quantities of L-Arg (196). Arginase abundance and activity increases with vascular injury: Arginase contributes to vascular remodeling after arterial injury (119) and elevated arginase I expression increases rat aortic smooth muscle cell proliferation via polyamine production (191). Vascular arginases are increased in several types of hypertension including DOCA salt, Dahl salt sensitive, the spontaneously hypertensive rat and the 5/6 renal ablation infarction models (131). In the present study we find that AT1 receptor blockade (which reduces blood pressure) also leads to reduction in aortic arginase abundance, presumably because of protection vs. hypertension and vascular damage.

Activation of vascular arginase is likely to exacerbate the hypertension, due both to increasing vascular stiffness and perhaps via reduction in endothelial NO production, secondary to substrate depletion (92). Arginase knockout mice have higher aortic and endothelial NO production vs. Wild-type (92) and overexpression of arginase in cultured endothelial cells decreases NO production (90). There is less information on renal arginase activity in hypertension and CKD, but the present study demonstrates that protection from injury and hypertension (with AT1 receptor blockade) lowers renal cortex arginase activity and abundance but is without effect on liver arginase. There was insufficient tissue to measure aortic arginase activity but given the fall in abundance with antihypertensive treatment, it is likely that there is also lower vascular arginase activity in the irbesartan-treated FHH rats. This would lead to reduced L-Arg utilization,

as evidenced by the increase in plasma L-Arg in the irbesartan treated FHH. It is not clear how AT1 receptor blockade lowers renal and vascular arginase in the FHH. It may be that preventing hypertension and CKD by any method prevents arginase activation, or possibly that ANGII has specific actions to trigger arginases, as suggested by the recent observation that arginase-1 expression increased by about 70% after 14-day ANG II infusion and was prevented by AT1 blockade (55)

In addition to L-Arg availability, the endogenous NOS inhibitor ADMA will compete with L-Arg for the NOS (174). Elevated plasma ADMA causes endothelial dysfunction, and is associated with increased cardiovascular morbidity and mortality in many diseases (8, 17, 171). In ERKD there is a clear association between adverse cardiovascular events and the level of plasma ADMA (212) although there is considerable variability and some controversy about plasma ADMA levels in patients with CKD (8). While loss of renal clearance plays some role in the increased plasma ADMA in renal disease, the primary method of ADMA removal is by catabolism via the DDAH enzymes. Since the kidney contains a high density of DDAH (1) and since plasma ADMA often increases with renal disease, it is thought that renal DDAH activity contributes importantly to ADMA removal (117).

Despite moderate renal disease, in the present study we find that plasma ADMA is low in the untreated FHH, at a value similar to the normal Sprague Dawley rat (163). Plasma ADMA level remains unchanged in the FHH treated with irbesartan, despite an increase in renal DDAH activity, but the plasma L-Arg/ADMA ratio increases, due to the increased plasma L-Arg. While plasma ADMA is also low in untreated older FHH (27

weeks) the plasma L-Arg/ADMA ratio is lower than in other strains, due to lower L-Arg levels ((169).

In conclusion, we have shown that the spontaneous injury the FHH develops is independent of ADMA but is mediated, at least partially through ANGII. We have shown a novel benefit to ANGII blockade in the treatment of hypertension and CKD, which involves reductions in tissue arginase activity and abundance. It is unknown whether there is a direct interaction between ANGII and arginase or if it is a secondary effect due to attenuation of the hypertension. These questions need to be addressed in further studies.

.

Table 5-1. Functional data taken at time of sacrifice for FHH rats. Glomerulosclerosis index (GSI), mean arterial blood pressure (MAP) measured by aortic puncture, 2-kidney weight (KW), and creatinine clearance (CCr) factored for body weight. Data is shown as mean ± SE. Significance determined by t-test between treatment groups. *p<0.05, **p<0.01, ***p<0.001.

Group	n	GSI	MAP (mmHg)	KW (g)	Total CCr (ml/min/100gBW)
HP	10	0.41±0.04	140±6	3.9±0.1	1.6±0.3
HP+Irb	10	0.16±0.01***	116±4*	3.0±0.1**	0.6±0.1**

Table 5-2. L-Arginine/citrulline/ADMA concentrations and kidney cortex NOx concentrations. Data is shown as mean ± SE. Significance determined by t-test between treatment groups. *p<0.05. NA-Not Available.

Group	Plasma				
	Citrulline (μM)	Arginine (μM)	ADMA (μM)	Arginine:ADMA	NOx (nmol/mg protein)
HP	66±3	40±4	0.18±0.01	214±14	NA
HP+Irb	64±3	62±8*	0.18±0.02	295±28*	NA
	Kidney Cortex				
	(μM/g protein)	(μM/g protein)	(μM/g protein)		
HP	3.7±0.4	8.1±1.2	0.10±0.02	108±13	0.99±0.27
HP+Irb	3.8±0.3	10.7±1.4	0.11±0.03	139±21	2.56±0.62*

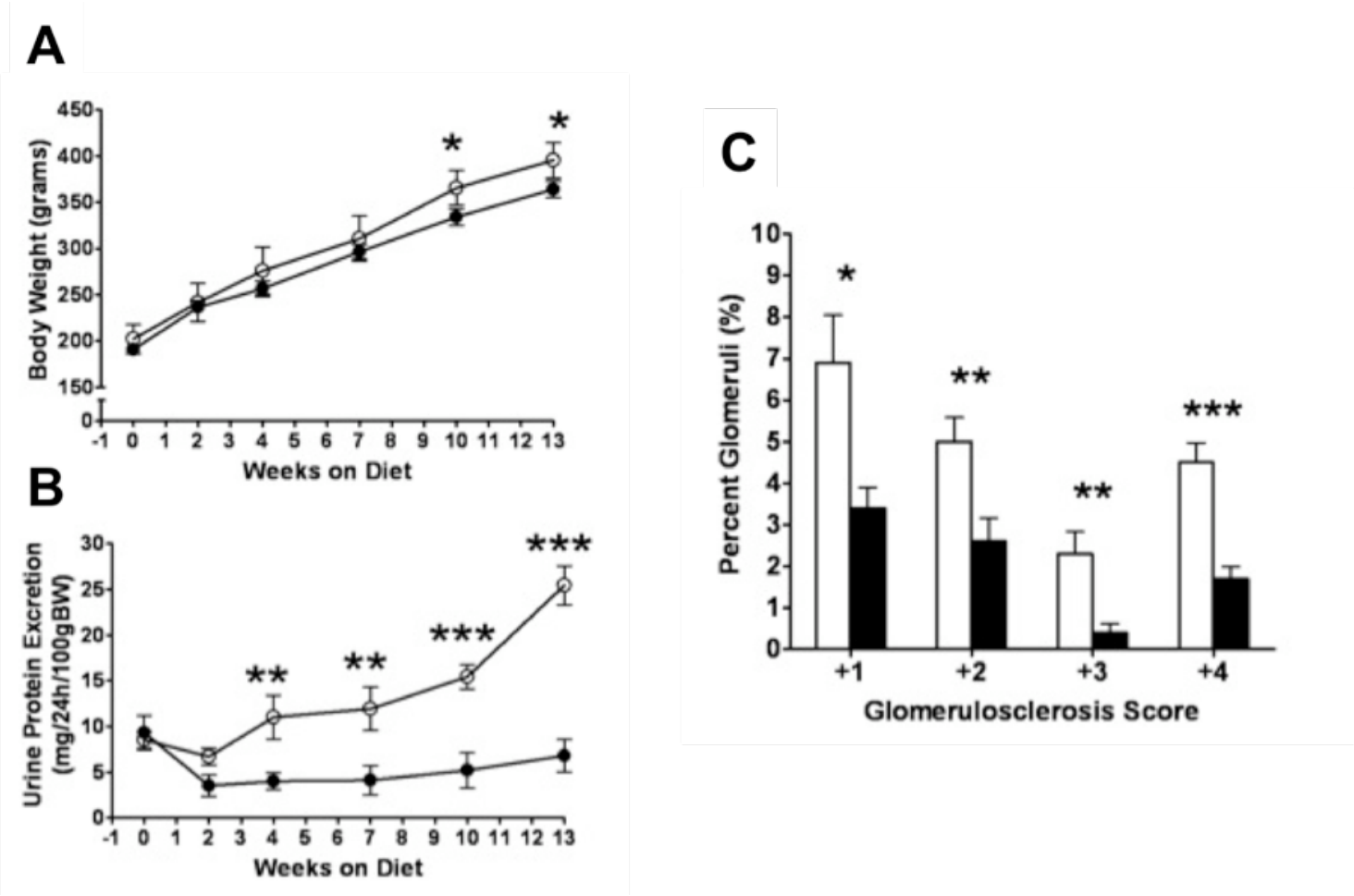

Figure 5-1. Body weight, urine protein excretion and renal pathology. (A) Fasted body weights taken at various intervals over 13 weeks from FHH rats fed a high protein diet (open circles) and rats treated with irbesartan (filled circles). (B) 24-hour urine protein adjusted per 100g bodyweights taken at various intervals. Renal pathology in kidneys taken at sacrifice shown as (C) percent glomeruli at each index score. Untreated shown in open bars, treated shown in filled bars. Significance determined by t-test between treatment groups. Pathology significance determined by Mann-Whitney U. *p<0.05, **p<0.01, ***p<0.001.

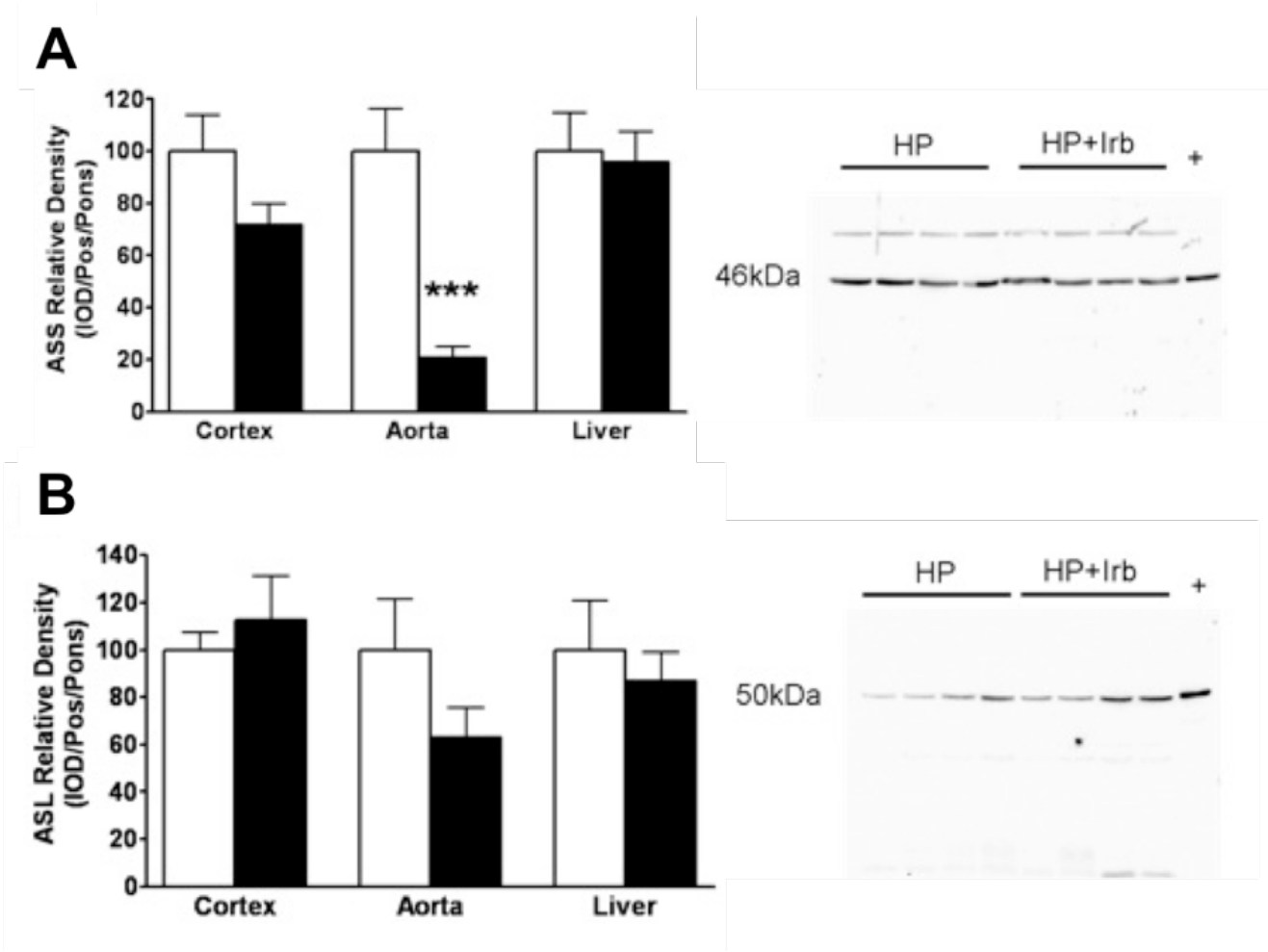

Figure 5-2. Arginine synthesizing enzyme abundance measured by western blot. (A) Argininosuccinate synthetase abundance in cortex and liver. (B) Argininosuccinate lyase abundance in cortex and liver. 100µg of total protein was loaded into each lane (n=8 per group). Untreated shown in open bars, treated shown in filled bars. Representative blot of each protein from kidney cortex is shown. Significance *p<0.05, **p<0.01, ***p<0.001.

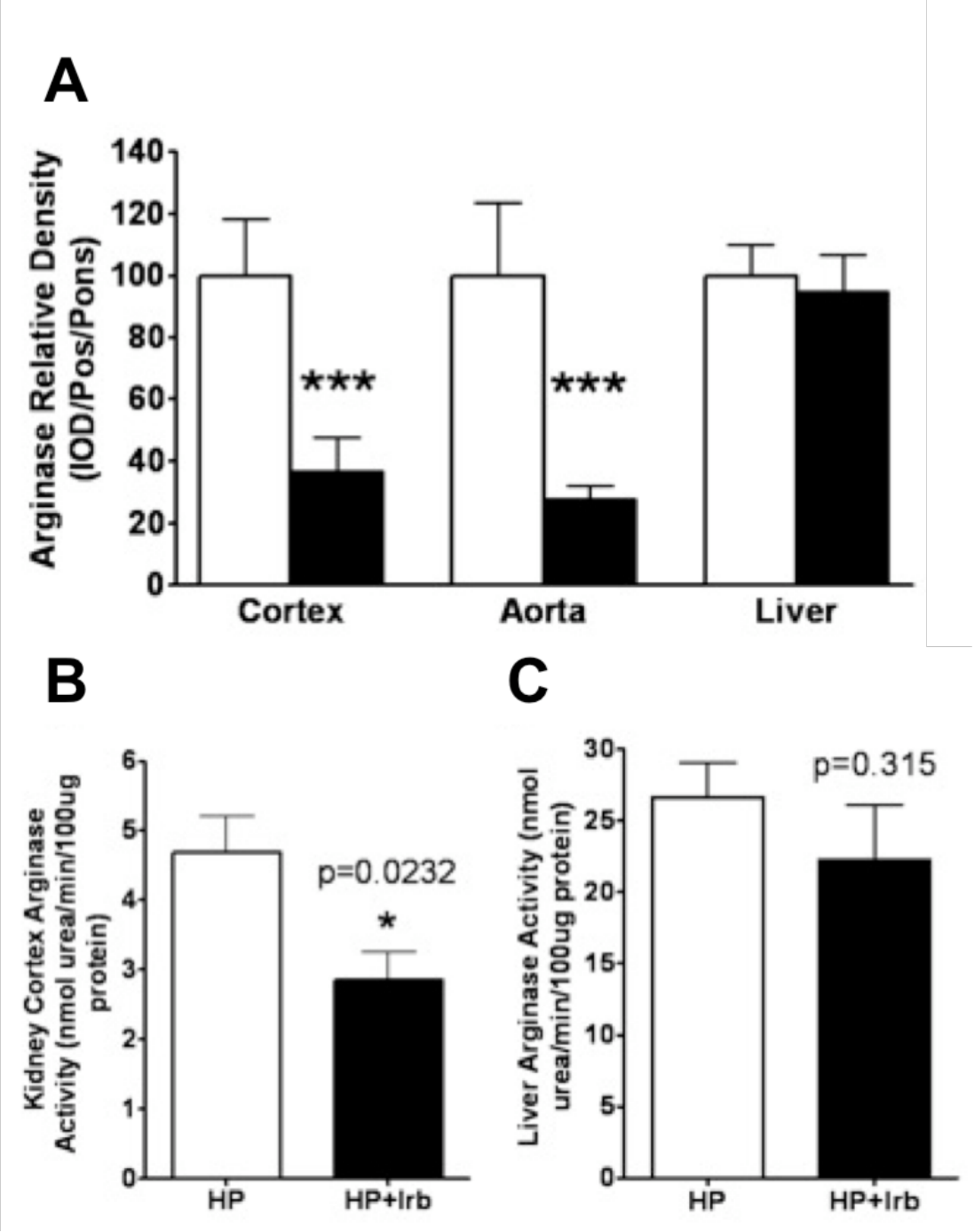

Figure 5-3. Arginase protein abundance measured by western blot. (A) Arginase II in the kidney cortex and arginase I in the aorta and liver. 100µg of total protein was loaded into each lane (n=8 per group). Representative blot of each protein from kidney cortex is shown. Untreated shown in open bars, treated shown in filled bars. (B) Kidney cortex and (C) liver arginase activity measured by urea production. Significance *p<0.05, **p<0.01, ***p<0.001.

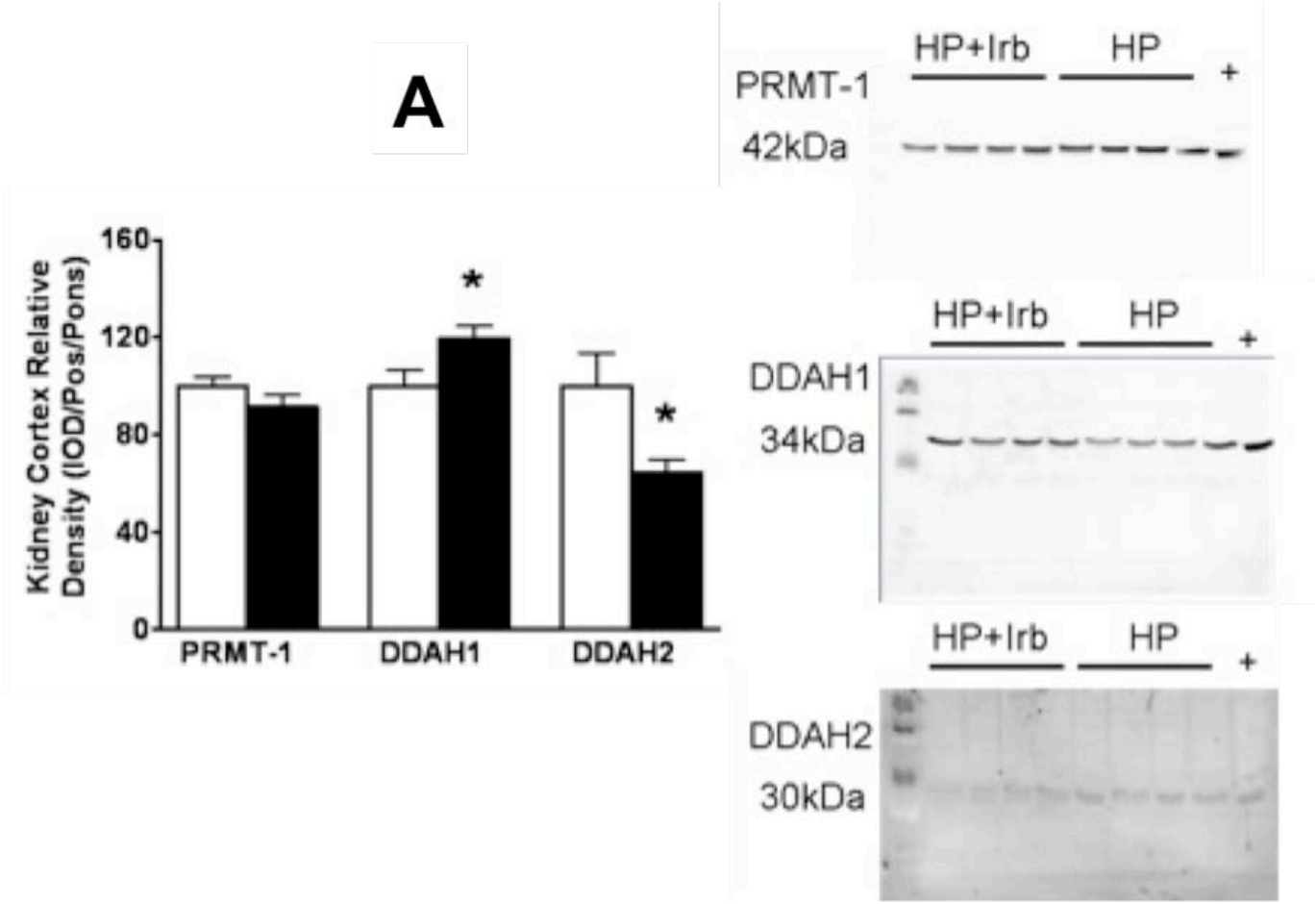

Figure 5-4. ADMA synthesizing and metabolizing enzyme abundance. (A) Kidney cortex DDAH1 and 2 expression and (B) activity assay measured by citrulline production. (C) Kidney cortex PRMT1 and (D) aorta PRMT1 and DDAH2. 100µg of total protein was loaded into each lane (n=8 per group). Representative blot of each protein from kidney cortex is shown. Significance determined by t-test between treatment groups. *p<0.05, **p<0.01, ***p<0.001.

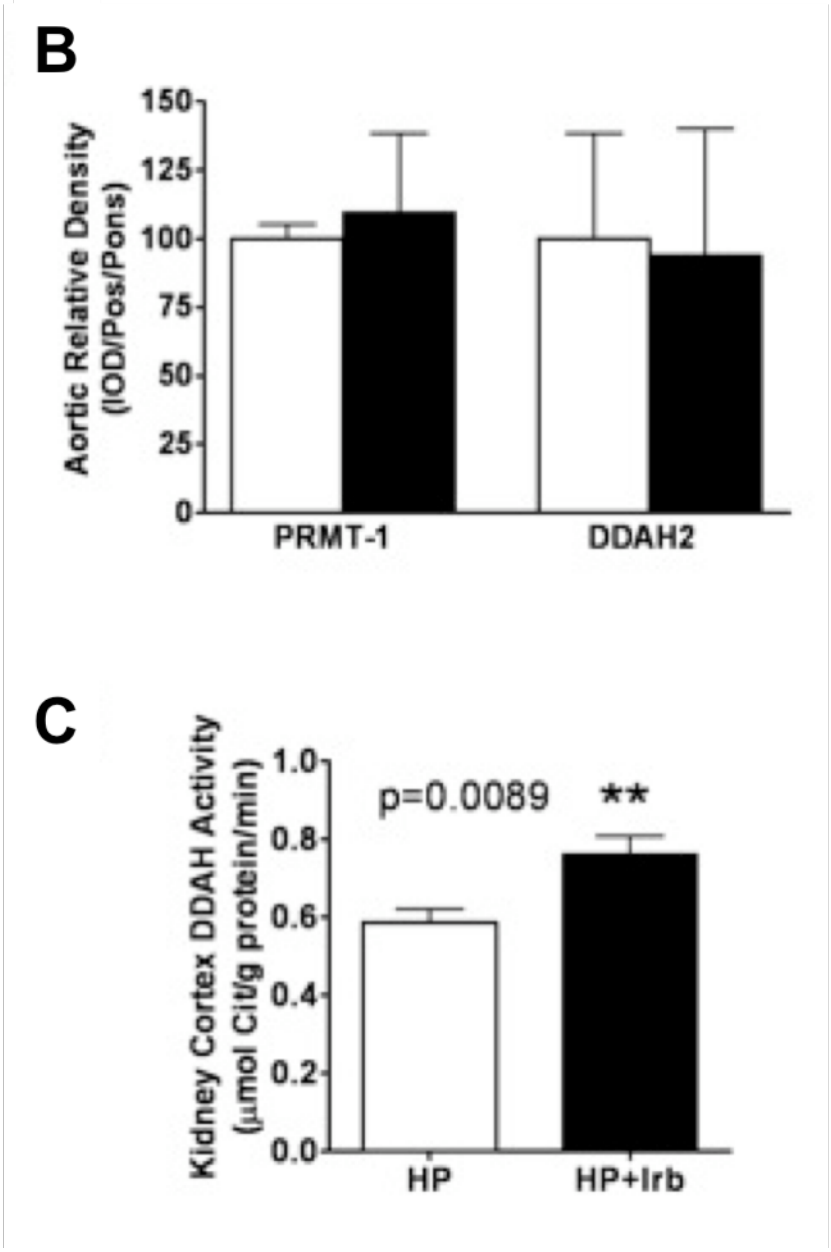

Figure 5-4. Continued

CHAPTER 6
ADMA ABUNDANCE AND REGULATION IN PUROMYCIN AND 5/6 ABLATION/INFARCTION INDUCED CHRONIC KIDNEY DISEASE

Introduction

Experimental and clinical data show a reduction in NO synthesis in CKD and ERKD. NO bioavailability can be determined by many factors including the expression/activity of the NO synthase enzyme and scavengers of NO such as reactive oxygen species. In addition, ADMA competitively inhibits NO production by competing for L-Arg transport into the cell and binding to NOS. ADMA has been reported to accumulate in patients with CKD and may contribute to the increased cardiovascular risk in these patients (173).

Sato et al demonstrated in the puromycin aminonucleoside (PAN) model of focal and segmental glomerulosclerosis (FSGS) a correlation between blood pressure (BP) and ADMA levels in endothelial cells, plasma, and urine (138). However, the regulation of ADMA, synthesis by PRMT-1 and degradation by DDAHI/II, has not been studied in the PAN model. Symmetric DMA (SDMA) is a methylation product of PRMT-2 but is cleared only by renal excretion. The PAN model is associated with increased ROS activation and ROS have been shown to negatively regulate DDAH (16, 115, 164). Additionally, since ADMA competes with L-Arg it has been suggested that the functionally relevant concentration of ADMA should more accurately be represented as the L-Arg/ADMA ratio (11).

In this study, we tested the hypothesis that PAN induced CKD reduces NO bioavailability by causing a decline in the L-Arg to ADMA ratio and a reduction in NOS enzyme expression. Using a moderate and severe model of PAN induced CKD we measured the enzyme abundance of the ADMA regulatory enzymes PRMT and DDAH.

We also measured plasma ADMA and tissue DDAH activity in the 5/6 A/I CKD model. We propose that a reduction in the plasma L-Arg/ADMA ratio due to dysfunction in ADMA metabolism may contribute to the development and progression of CKD due to reductions in NO synthesis.

Methods

Plasma L-Arginine/ADMA/SDMA

The concentration of L-Arg, ADMA, and SDMA in plasma was measured using reverse-phase HPLC with the Waters AccQ-Fluor fluorescent reagent kit. Samples were prepared by mixing 60µl of plasma with 350µl of borate buffer (pH=9). This was placed on an unconditioned Oasis MCX column (Waters, Milford, MA) then washed with 1ml borate buffer, 3x1 ml H_2O, and 1ml MEOH. The sample was eluted with 1ml NH_4OH/ H_2O /MEOH (10:40:50), dried under nitrogen gas, then reconstituted with 30µl H_2O. Recovery was approximately 85%. Twenty microliters of the samples was mixed with 60µl borate buffer and 20µl of AccQ Fluor reagent (Waters, Milford, MA). 50µl of mixture was injected onto a Luna 150 x 3 mm C-18 reversed-phase column (Phenomenex, Torrance, CA). A flow rate of 1.3ml/min was attained with a PerkinElmer Series 200 Pump, and fluorescence intensity was measured using a series 200 fluorescent detector, EX 250/EM 395 (PerkinElmer Life and Analytical Sciences, Shelton, CT). Standards contained concentrations of L-Arg in the range of 200µM to 3.12µM. This method was adapted from Heresztyn et al (53).

Oxidate Stress

Urine collected at week 11 by metabolic cage was used for TBARs and H_2O_2. Methods are decribed in Chapter 2.

Western Blot

Western blot analysis was made as described previously (163). Briefly, measurement was conducted on kidney cortex (200µg total protein) and liver (100µg total protein). Samples were probed for PRMT1, DDAH1, and DDAH2 by methods decribed in Chapter 2. Renal cortex p22-phox was measured by a goat polyclonal antibody (Santa Cruz, 1:50 dilution, overnight incubation) and a donkey anti-goat IgG-HRP secondary antibody (Santa Cruz, 1:2000 dilution, 1-hour incubation). The protein abundance was represented as IOD/Positive control/total protein by Ponceau red, relative to the HP group (set to 100).

DDAH Activity

DDAH activity was measured by a colorimetric assay measuring the rate of citrulline production, as optimized by us recently (164). Kidney cortex and liver were homogenized by sodium phosphate buffer. Tissue homogenate was pre-incubated with urease for 15 min, and then 100µl (2mg for kidney cortex and liver) of homogenate was incubated with 1mM ADMA for 45 min (kidney cortex) or 60min (liver) at 37ºC. After deproteinization, supernatant was incubated with color mixture at 60ºC for 110 min. The absorbance was measured by spectrophotometry at 466 nm. The DDAH activity was represented as µM citrulline formation/g protein/min at 37ºC.

Statistics

One-way ANOVA combined with Newman-Keuls post hoc test was used for statistical evaluation of mean values across groups. All graphs and statistics were done with Prism 4 software (GraphPad Software, Inc., San Diego, CA). Values are reported as means ± SE with $P<0.05$ was considered statistically significant.

Results

The functional data was presented in Chapter 4. Both low dose and high dose PAN injected rats exhibited significant proteinuria throughout the study. High dose PAN led to protein excretions up to ~400mg/day/100g BW at week 9, and the low dose treated rats reached a peak at week 9 of 200mg/day/100gBW. There was a fall in protein excretion at week 11 in the high dose group associated with a very low GFR, while GFR was similar to controls in the low dose group. BW of high dose PAN rats fell within 1 week of the first injection and remained low throughout the study, whereas low dose PAN animals had similar weight gain versus control until 11 weeks post injection. Blood pressure increased dose dependently in the 2 PAN groups and renal pathology revealed significant injury in the low dose PAN and marked injury in high dose PAN kidneys. Significant renal hypertrophy was also evident in the high PAN dos group.

Urinary excretion of MDA (measured by TBARs) was unchanged. Excretion of H_2O_2 was increased only in the low dose PAN group. Renal cortex content of p22-phox protein expression was unchanged (Table 6-1).

Plasma L-Arg concentration was unchanged in either PAN group (Table 6-2). High dose PAN injections resulted in a 2-fold elevation in plasma ADMA (Table 6-2). The L-Arg/ADMA ratio was significantly reduced only in the high dose group, and plasma SDMA concentration were also elevated only in this group (Table 6-2).

Renal cortex protein expression of PRMT-1 was increased in the low dose and further enhanced in the high dose (Figure 6-1A). Hepatic expression was unchanged in any of the groups (Figure 6-1B). Kidney cortex expression of DDAHI was increased in the high dose group (Figure 6-2A) and DDAHII was increased in both PAN groups (Figure 6-2B). However, total renal cortex DDAH activity was reduced in both PAN

groups (Figure 6-2C). Hepatic expression of DDAHI and II were unchanged (Figure 6-2D and E) and total activity was reduced in the high dose group only (Figure 6-2F).

Plasma ADMA was increased at all stages of 5/6 A/I and the plasma content were unchanged (shown in Chapter 3). This resulted in a lower L-Arg/ADMA ratio at all stages of CKD (Figure 6-3A). The renal activity of DDAH also reduced at all stages of CKD but there was no change in hepatic activity (Figure 6-3B and C).

Discussion

Our data of increased plasma ADMA levels in severe PAN induced CKD supports the findings of Sato et al (138). We found no change in plasma L-Arg but the increased ADMA caused a reduction in the L-Arg/ADMA ratio, which would result in reduced NO production. In fact, we do see a significant reduction in whole body synthesis of NO in the high dose PAN group. The increased ADMA levels were also associated with increased renal expression of PRMT-1and reduced activity of renal and hepatic DDAH in the high dose group. The increased ADMA was also seen in the 5/6 A/I CKD model at all stages and was associated with reduced renal DDAH activity.

Plasma ADMA is tightly regulated and even small increases above normal are associated with increased cardiovascular risk, even in “normal”, non-smoking young men (170). Plasma levels of ADMA are always elevated in patients with ERKD (173) although there is a wide range of values and are a predictor of cardiovascular complication and mortality in these patients (212). In patients with CKD increases in plasma ADMA have also been reported although these are very variable. In some studies plasma ADMA ranges from normal to elevated, in some plasma ADMA increases as renal function is lost and in others plasma ADMA is uniformly elevated at all levels of CKD irrespective of the level of renal function (7). In healthy human

subjects exogenously administered ADMA decreased renal sodium excretion (72) and has potent vasoconstrictive and pressor effects (94, 154, 173). Miyazaki et al found that plasma levels of ADMA were associated with mean BP levels in hypertensive patients (102) and plasma levels of ADMA correlated with BP levels in nephrectomized rats (98). Therefore there is an association with plasma ADMA and hypertension although whether ADMA leads to development of hypertension or increases as a result of hypertension is not known.

The regulation of plasma ADMA is complex and thought to be controlled mainly by rate of removal (117). Ogawa el at determined that only 4.6% of injected ADMA was excreted in the first 12 hour urine(114). Nijveldt et al measured renal uptake and excretion of ADMA and suggested a major for renal DDAH metabolism vs. renal excretion (112, 113). Wilcox and colleagues showed that DDAHI reductions resulted in increased plasma ADMA but DDAH2 reductions did not alter plasma ADMA levels (186). However, DDAH2 is necessary for normal vascular response to EDRF/NO.

In the present study we found that the protein expression of DDAHI and II in the renal cortex was increased with PAN injury. Despite this, there was a reduction in the total activity of DDAH measured by citrulline formation in kidney cortex homogenates. This suggests post-translational modifications of DDAH enzymes and also highlights the importance of conducting measures of enzyme activity rather than relying on protein abundance. High levels of NO are able to S-nitrosylate cysteines on DDAH leading to inhibition of DDAH activity (83). Studies have suggested the ability for ROS to negatively regulate DDAH activity and this attenuation is blunted by ANGII blockade (16, 115, 120). The activation of DDAH activity is associated with a variety of

antioxidants which would suggest superoxide reduce activity. Our lab has shown that a superoxide donor (2,3-dimethoxy-1,4 naphthoquinone) reduces DDAH activity in rat renal cortex homogenates (164). L-Arg also has been shown to exert a dose dependent inhibition of DDAH activity in liver cells (187).

Other workers have shown increased ROS in the PAN model of CKD (97, 130) although in the present study we saw no change in the p22 phox, which increases in the presence of NADPH oxidase induced oxidative stress (118).

Although ADMA formation has been largely ignored as a regulatory mechanism, a recent study suggests that that ADMA production, by protein methylation and/or rate of proteolysis is also of importance. High homocysteine levels have been reported to raise ADMA levels via DDAH inhibition but Dayal et al report that in hyperhomocysteinemic mice, ADMA is *not* elevated despite reduced DDAH transcript in liver and kidney, as well as decreased hepatic DDAH1 protein and activity (34). These workers pointed out that reductions in hepatic protein methylation occur in hyperhomocysteinemic mice (i.e. ADMA production is also decreased) could explain the relative constancy of plasma ADMA. In the present study we found that PRMT1 abundance was widely increased which could also contribute to the rise in plasma ADMA.

When the initial injury is very severe, as seen in the high dose, it is associated with massive structural damage, loss of function, hypertension, and proteinuria. The total NO production was also decreased in both groups. Interestingly, Rincon et al showed increased NO production with PAN injection but also increased superoxide production 1-2 weeks post PAN injection at 150mg/kg dose (130). Ni et al reported no change in renal NOS isoforms 1 day after 130mg/kg PAN injection but reductions in NO

productions (measured by urinary NOx) (111). It is difficult to compare these results with our present study since the initial dosage and timing is so different. However, fall in plasma L-Arg: ADMA likely contributes to the reduction in total NO production.

.

Table 6-1. Measures of oxidative stress in puromycin CKD. The measure of p22-phox is western blot data with controls set to 100%. Statistics comparing each PAN group to controls were done with one-way ANOVA. * $p<0.05$ vs. Controls.

Group	n	Urine TBARS (nmol/day)	Urine H_2O_2 (µmol/day)	p22 phox (%)
Control	8	0.11±0.02	0.042±0.005	100±10
Low Dose	8	0.11±0.01	0.090±0.019*	129±13
High Dose	7	0.12±0.01	0.048±0.007	119±23

Table 6-2. Plasma concentrations of L-Arginine, ADMA, and SDMA. Concentrations measured by HPLC and calculated L-Arg/ADMA ratio. Statistics comparing each PAN group to controls were done with one-way ANOVA. ** $p<0.01$ vs. Controls.

Group	n	L-Arg (µM)	ADMA (µM)	L-Arg/ADMA	SDMA (µM)
Control	8	97±9	0.34±0.01	283±24	0.30±0.03
Low Dose	8	127±8	0.50±0.02	248±15	0.36±0.04
High Dose	8	98±10	0.74±0.12**	159±30**	0.92±0.18**

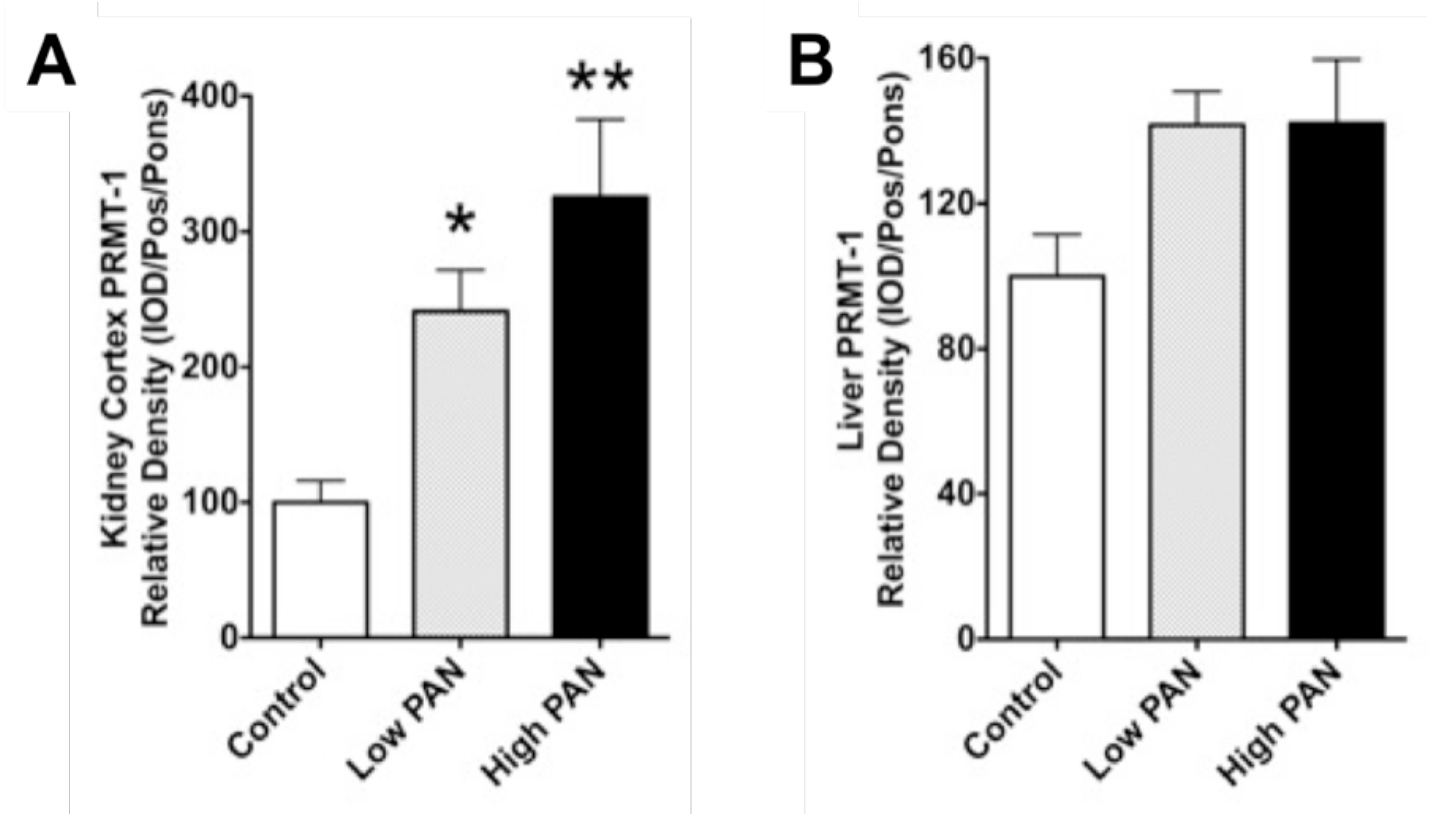

Figure 6-1. Tissue abundance of L-Arginine methylating enzyme. (A) Kidney cortex and (B) hepatic expression of PRMT-1 measured by western blot. Statistics comparing each PAN group to controls were done with one-way ANOVA. * $p<0.05$, ** $p<0.01$vs. Control

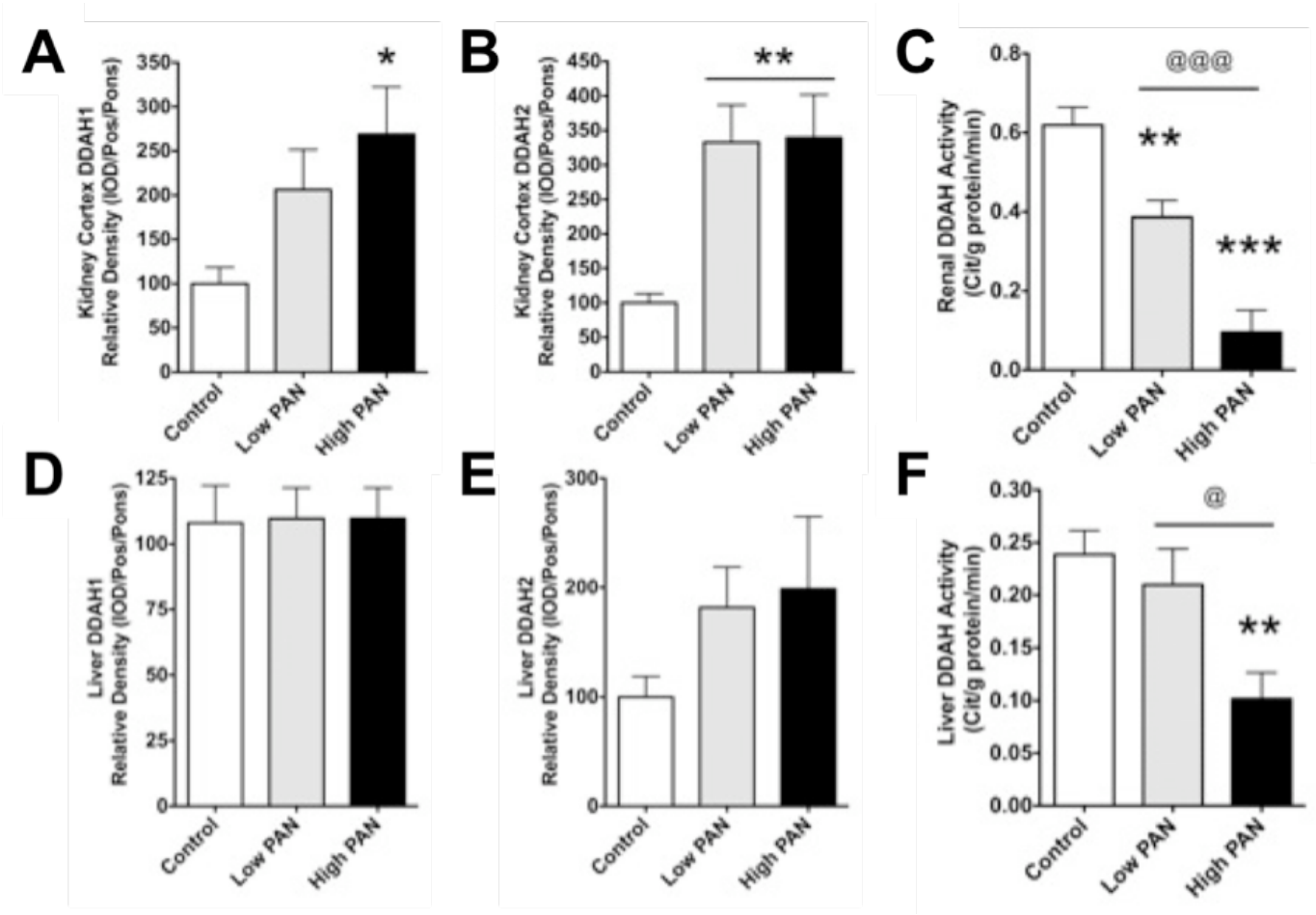

Figure 6-2. Abundance and activity of AMDA metabolizing enzymes. Kidney cortex protein abundance of (A) DDAH1 and (B) DDAH2, measured by western blot, and (C) total renal cortex DDAH activity, measured by citrulline formation. Hepatic expression of (D) DDAH1 and (E) DDAH2, and (F) total hepatic DDAH activity. Statistics comparing each PAN group to controls were done with one-way ANOVA. * $p<0.05$, ** $p<0.01$, *** $p<0.001$ vs. controls. @ $p<0.05$, @@@ $p<0.001$ vs. low dose PAN

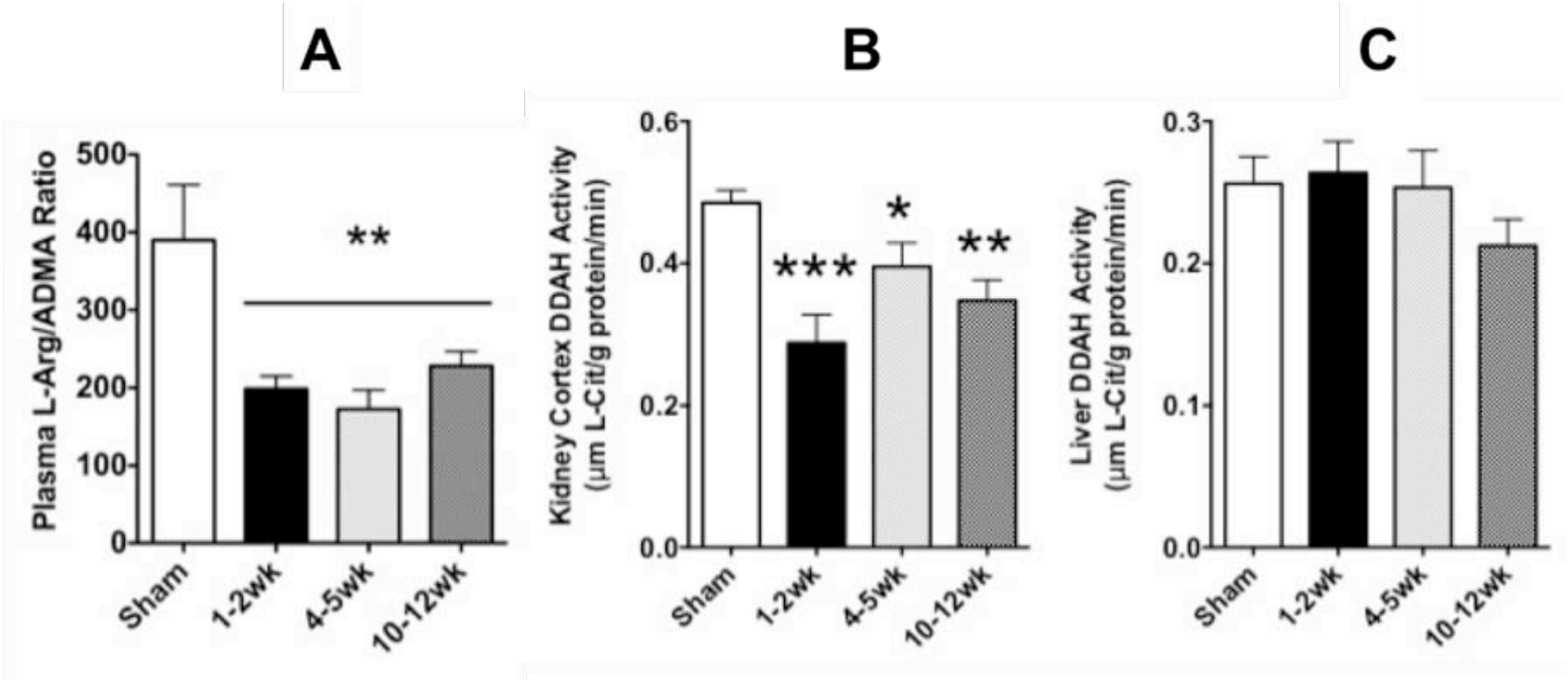

Figure 6-3. ADMA in stages of 5/6 ablation/infarction chronic kidney disease. (A) Plasma L-Arginine and ADMA measurements were made in plasma taken at time of acute terminal surgery and represented as L-Arg/ADMA ratio. (B) Renal cortex and (C) liver total DDAH activity measured by citrulline formation. Statistics comparing each injury to sham were done with one-way ANOVA. * $p<0.05$, ** $p<0.01$, *** $p<0.001$ vs. sham

CHAPTER 7
SUMMARY AND PERSPECTIVES

Summary

The data presented in this dissertation provides evidence for L-Arg deficiency in CKD and ERKD, which would explain, at least partially, the reduction in NO production seen in patients and animal models of CKD. In Chapter 1, I set forth four aims:

Aim 1

Determine the ability of the kidney to take up citrulline and release L-Arg during CKD. In Chapter 3, I have addressed the controversial topic of whether or not the injured kidney has an impaired ability to release L-Arg. As mentioned earlier, studies in patients with chronic renal insufficiency show reduced renal release of L-Arg (166). Chan et al have shown reduced ASS and ASL activity in CKD kidneys from rats (27). However, Bouby and colleagues report that renal L-Arg synthesis is preserved in CKD due to renal hypertrophy and increased plasma citrulline concentrations (18). Working in a similar model to Bouby et al, our studies have shown that a severe reduction in RPF resulted in reduced citrulline delivery to the kidney despite increased plasma concentrations in CKD. This, combined with reduced renal citrulline uptake capacity as well as reduced ASS/ASL abundance in the renal cortex, resulted in reduced L-Arg release during early, moderate, and severe CKD. When we challenged these kidneys with exogenous citrulline we found that the injured kidney does not respond with increased L-Arg synthesis as seen in kidneys from healthy shams. This was true for all stages of CKD.

Aim 2

Determine the impact of CKD on L-Arg transporter abundance and regulatory enzyme abundance. Using antibodies developed by Schwartz et al, we measured membrane abundance of CAT1, the major transporter of L-Arg, in the aorta and kidney cortex. Reductions in kidney cortex CAT1 indicated to us that the proximal tubules had a reduced ability to secrete L-Arg, thereby contributing to the reduced L-Arg release seen in the experiments described in Chapter 3.

In Chapter 4, we addressed the dilemma of maintained plasma L-Arg levels in CKD despite decreases in renal synthesis. Could the maintained plasma levels be a false indication of what is going on inside the cell? We found reductions in aortic CAT1 expression in the membrane fraction in PAN induced CKD, similar to previous work by Schwartz et al in a different CKD model (145). This decrease in CAT1 expression/activity would be expected to result with reduced L-Arg available to NOS due to transport dysfunctions.

Aim 3

Determine the changes in arginase abundance and activity in CKD. The studies performed in Chapter 5 addressed pathways of L-Arg metabolism that could divert substrate away from NOS. Previous groups have shown that arginase levels can effectively regulate NO production (6, 7, 66). We measured arginase abundance in the tissue of rats with spontaneously developing CKD (FHH) and found increased abundance and activity; however, plasma L-Arg levels were normal. These increases in arginase expression/activity were blocked by ANGII receptor blockade which also ameliorated development of

CKD. Although the direct mechanism of this interaction is unknown, the result of ANGII blockade was elevated plasma L-Arg that would increase NO production. Is this an indirect effect of lowering blood pressure and improving endothelial function or does ANGII regulate arginase expression directly? A potential link was recently presented in an abstract by Shatanawi et al (148). They found increased arginase activity/abundance in bovine aortic endothelial cells through the RhoA/MAPK pathways (one of many ANGII signaling pathways).

Aim 4

Determine the impact of various models of CKD on ADMA abundance and metabolism. Finally, in Chapter 6 we explored the correlation between levels of the endogenous NOS inhibitor (ADMA), hypertension and renal injury in the PAN model. Our findings were consistent with those of other groups (16, 44, 71) in that we saw increased plasma ADMA levels in our CKD models. Appropriately, renal DDAH activity was also reduced in the same animals lending support to the idea that the kidneys play a major role in the metabolism of ADMA via DDAH. Expression of PRMT-1 was increased in the CKD animals as well.

Plasma levels of ADMA were also elevated in the 5/6 A/I CKD injured rats and were accompanied by a reduction in renal DDAH activity.

Connecting the Pathways

I have summarized these findings in Figure 7-1 for healthy states (Figure 7-1A) versus pathological states (Figure 7-1B). Although, they are represented here in a single figure, not all these changes occur in the same animal model, and additionally, the extent of these changes varies with both model type and severity. However, what is recognized in all our models is that there is a NO

deficiency originating, at least in part, from a reduction in L-Arg bioavailability. In the kidney cortex, we have shown a reduction in citrulline delivery (due to reductions in both RPF and GFR) and in uptake in the 5/6 A/I model of renal injury (current mechanism is unknown). We have also shown a reduction in ASS/ASL enzyme abundance in the kidney cortex of the PAN and 5/6 A/I models. These data indicate lower renal L-Arg synthesis in CKD. Inhibition of arginase renal activity/abundance by ANGII blockade successfully increased plasma L-Arg levels in the FHH rat.

However, what the significance of renal arginase abundance is unknown. Levillain et al (85, 86) have demonstrated that arginase is present in the more distal portions of the proximal tubule where lower levels of L-Arg are synthesized. Additionally, arginase activity in the renal cortex was not elevated in the 5/6 A/I or PAN model.

Although the role of arginase in the kidney is not clearly define, the role in the vasculature has a significant impact on NO formation. In the PAN models we have shown increased arginase abundance in the aorta, which would consume a portion of L-Arg that enters the endothelial cell. The FHH also showed elevated aortic arginase that was reduced with ANGII blockade.

We have also shown a reduction in CAT1 transporters in the kidney cortex (presumably reflecting proximal tubules) of 5/6 A/I and PAN CKD and the aorta of the PAN animals which should result in reduced renal release and vascular uptake of L-Arg. Additionally L-Arg transport can be inhibited by the increased plasma ADMA (due to reduced DDAH activity and increased PRMT1) observed

in the PAN and 5/6 A/I models. These data indicate that even though plasma L-Arg concentrations seem normal, there may be an intracellular L-Arg deficiency due to reduced membrane transport. A dysfunction in any of these mechanisms would reduce L-Arg bioavailability and could result in NOS substrate deficiency and reduced NO production, leading to the progression of CKD and its systemic sequela.

Spanning Animal Models of CKD

In my research, I utilized three models of CKD, which cover very different mechanisms of disease. The 5/6 A/I model was a very chronic and progressive injury resulting from a removal of renal mass and a 2/3 infarction of the remaining kidney. The PAN model was again a model of chronic injury but with no renal mass removal and no infarction; renal mass was higher in the injury state than controls due to hypertrophy of both kidneys. Lastly, the FHH was a model of spontaneous injury that we exacerbated with dietary protein overloading. Although the trigger for CKD in these models may be different, we have shown that there are common pathways that result from the injury or worsen the injury.

In figure 7-2, I plotted the terminal BP, CCr, and final measured proteinuria for all the animal models. Looking at the data in this way helps us to illustrate the differences between the models used. We see that the 5/6 A/I model is associated with severe hypertension and reductions in GFR in a progressive manner, while the PAN model loses renal function only at the severe stages, despite massive proteinuria and less increases in BP.

Proteinuria was used in all our studies to follow the progression of CKD. However, the extent of the proteinuria was very model dependent, as the PAN

groups showed massive protein excretion that did not reflect the level of glomerulosclerosis (as seen in the mild PAN group). It appeared that plasma citrulline levels were a better indication of glomerular damage across all the models (Figure 7-3). This data is in support of findings by Levillain et al where they found that plasma citrulline was a better indicator for the degree of renal nephrectomy than plasma urea, or creatinine levels (87). Could this implicate that renal uptake of citrulline and L-Arg release is a greater factor in progression of CKD than previously thought? Since citrulline is not excreted and the metabolism of circulating citrulline is predominately through ASS/ASL conversion to produce L-Arg, the increase in plasma citrulline is most probably due to reduced renal metabolism. Our data in Aim 1 support these findings. Studies by Bouby et al claimed that there was maintained citrulline uptake and metabolism by 5/6 A/I kidneys but failed to explain why there would be an accumulation of citrulline in the same animals.

All CKD models seem to show a strong correlation between renal DDAH activity and plasma levels of ADMA (Figure 7-4). This is expected since the kidneys have the highest expression of DDAH compared to any other organ, although the liver also has a high abundance. What is interesting, however, is that the renal DDAH activity does not match the protein abundance of DDAHI and II. In fact, we have shown in the PAN and FHH models that DDAHI is usually upregulated in CKD states. This suggests that there is a post-translational modification of DDAH enzymes that may inactivate them. Currently there are no known phosphorylation sites on DDAHI or II that play a role in

activation or reducing activity. Other factors such as reactive oxygen species are thought to have a role in the regulation of DDAH activity based on in vitro studies (83), but the regulation of DDAH, in vivo, has not been fully characterized. Future studies should examine the factors that determine the activity of these enzymes in the kidney in both the healthy kidney and in disease states.

Limitations of Our Studies

Hindsight is 20/20, and in this case it is no different. It is the responsibility of scientists to look back critically on their research and find areas that are lacking or need more elaborate study. In the first aim we were not able to measure exact GFR using inulin infusion since the fluorescence tagged inulin used in our lab interfered with the HPLC measurements for L-Arg. There are alternate methods of labeling and probing for inulin and the true GFR, instead of relying on CCr as a cruder estimate of GFR. An improved GFR measurement would give us a more accurate representation of how much citrulline is being delivered to the proximal tubule, so that we could more accurately determine tubular uptake of citrulline.

In the FHH study we could have provided additional controls including providing the diet and drug to pair-fed German Brown rat (background strain of the FHH). Many of our measurements, including GFR and ADMA, were compared back to normal SD rat values seen in the shams of our other studies. With the additional controls we could have separated the effects of genetics vs. diet vs. ANGII blockade. In the same study, we could not fast the animals or place them on a low nitrate diet prior to sacrifice due to the method of drug

delivery and therefore, were unable to use nitrite/nitrate excretion, or plasma levels as a measure of endogenous NO production.

Clinical Implications and Future Directions

Maintained Plasma L-Arg

One of the most perplexing findings in my research is the maintenance of plasma L-Arg concentrations despite reduced renal L-Arg synthesis. Although we have suggested that this could be due to reduced systemic uptake and utilization, we cannot ignore the alternate sources of L-Arg. We know that L-Arg can be produced by protein turnover. Protein turnover is increased in several disease states including muscle wasting and in uremic states. So what role did protein turnover have in our models of CKD? There are methods for measuring the amount of protein turnover (56, 69), which may be an interesting factor to examine in exploring the mechanisms of maintenance of plasma L-Arg.

Another contributing source could be dietary L-Arg. Although in healthy states, dietary L-Arg is metabolized by arginases in the intestine and not absorbed; some studies have suggested that dietary L-Arg contributes to circulating levels in disease states. I believe it is important to fully understand the role of dietary L-Arg during CKD as a scientific interest but also for clinical implications. Current technology allows us to construct diets completely devoid of L-Arg. In states of CKD, could dietary L-Arg be compensating for the reduced renal synthesis? Would deprivation of dietary L-Arg worsen the rate of CKD progression?

L-Arginine Supplementation

If in fact L-Arg deficiency is a contributing factor to reduce NO production, can we prevent or slow the progression of CKD with L-Arg supplementation? The beneficial effects of L-Arg supplementation have been reported in several models of CKD (ablation, ureter obstruction, PAN) (4, 59, 127-129). L-Arg supplementation in the water (10g/L) for remnant kidney CKD for 6 weeks resulted in increased GFR, RPF, and improved renal structure (129). The beneficial effects of L-Arg supplementation were seen at a 1/10 of the dose used in the Reyes study (129), in the same injury model; and the normalization of hypertension, proteinuria, CCr, and NO production was equivalent to that of angiotensin converting enzyme inhibition (4). In the bilateral ureter obstruction model of CKD, administration of L-Arg reduced BP, restored GFR, and increased NO production in two separate studies (59, 127). It is important to note here that these findings are not consistent with clinical results (discussed later).

So do these findings contradict the findings seen in aim 2 of reduced transporter abundance? Actually, the increased NO production seen with supplementation of L-Arg in some animal studies strengthens our findings that there IS an L-Arg deficiency that can be overcome by exogenous L-Arg. Thus, despite the normal plasma L-Arg levels seen in all our models, there must exist an intracellular deficiency due to reduced transport into the cell AND the inability of the kidney to produce appropriate amounts of L-Arg.

These data support our findings of L-Arg deficiency leading to reductions in NO production and CKD progression. Unfortunately, clinical studies have not shown similar success (64, 144, 158, 162, 202). A large portion of the L-Arg

taken orally passes through the GI tract and the hepatic portal system, and is metabolized by arginase I (106). Furthermore, high levels of dietary or circulating L-Arg can induce arginase I and II in various tissue (63, 106, 175). Oral administration (0.2g/kg/day) for 6 months increased plasma L-Arg levels and increased NO production but did not improve proteinuria, GFR, or RPF in patients with nondiabetic glomerular disease (36). Moreover, chronic L-Arg treatment has shown the potential for adverse effects on cardiovascular function (144). Additionally, relatively large doses (50 mg/kg/day or more) appear to be required for any effect (144, 158).

So why is there a discrepancy between the animal and human studies? Could this be due to differences in handling of dietary L-Arg? Oral L-Arg stimulates arginase in animals (63) and could have a more robust effect in humans, although this has never been studied. Could this reflect a significant contribution of CAT1 defects in humans? There is evidence of reduced L-Arg transport in humans with essential hypertension and those with a family history of hypertension (140).

Citrulline Supplementation

Since there are so many mechanisms producing L-Arg metabolism during oral supplementation, is there a possibility of utilizing citrulline instead? Citrulline can bypass hepatic metabolism, and it is not a substrate of arginase. In fact, citrulline also has been reported to be a noncompetitive inhibitor of arginase (149) and can reduce arginase activity. Currently, there is no information on citrulline transporter abundance in CKD although our studies from aim 1 imply that the injured kidney has reduced transport ability.

Studies by Koeners et al (78) have shown increased renal NO production and prevention of hypertension when citrulline was given to SHR rats perinatally.

What about the effect in human studies? The ability of citrulline to increase or restore blood L-Arg was first reported by Hartman et al in patients with sickle cell disease (49). Waugh et al also reported that oral citrulline is more effective than L-Arg in raising plasma arginine levels in patients with sickle cell (188). Citrulline supplementation (0.2g/kg/day) given to patients with sickle cell disease with increased arginase activity (104), raised plasma L-Arg levels and reduced disease symptoms with no apparent side effects (188).

But what does this tell us about citrulline supplementation in kidney disease? Our data suggest that the injured kidney cannot respond to exogenous citrulline. We found no increase in renal L-Arg synthesis despite increasing plasma citrulline concentrations and delivery in the 5/6 A/I model. So why is there a benefit shown in the above studies? Simply put, the above-mentioned studies do not involve or do not provide data for significant renal damage. Koeners showed a benefit in SHRs when given prior to the occurrence of any damage to the kidneys (78). Also our experimental design was acutely delivered citrulline. What effect chronic delivery of citrulline would have on renal ASS/ASL expression and renal L-Arg synthesis is unknown and therefore, needs to be studied. There is little known about the regulators of citrulline transport in the kidney in healthy and CKD states. The injured kidney does not respond to the increase in citrulline delivery, implying that the observed fall in uptake is not due to a competitive inhibitor but rather a reduction in transporters. Would a long-

term increase in plasma citrulline (past that already seen in CKD) result in increased transporter abundance, or would it cause a negative regulation and reduce the already diminished abundance?

Here we should address the possibility that citrulline supplementation may increase plasma L-Arg through non-renal mechanisms. In Chapter 3 we showed that plasma L-Arg was increased in shams and early CKD during citrulline infusion. The shams also showed increased renal release of L-Arg, which contributed to plasma levels; however, the early CKD rats had reduced renal L-Arg release. Studies have shown that endothelial cells have the ability to produce L-Arg (52, 195) and may significantly contribute to circulating L-Arg levels in disease states.

Methods of Increasing NO Production

The most obvious and intriguing studies would be gene therapy manipulation of the L-Arg system. We have already shown that ANGII blockade may increase L-Arg levels by reducing arginase. Others have shown ANGII blockade can increase DDAH abundance and increase activity by reducing ROS-mediated DDAH inhibition (83). However, there are no known methods of manipulating CAT1 transporter abundance or activity. Schwartz et al (145, 147) and our studies have shown increased PKC-α in CKD, and this may be a simple target for therapeutics. Recent studies by Schwartz et al (146) showed PKC-α inhibition with tocopherol increased L-Arg transport and NO production in 19 month old males. What about renal synthesis of L-Arg? Can we manipulate ASS/ASL enzyme levels or increase citrulline transporters in the proximal

tubules? These may provide promising targets for therapy, but renal gene therapy is extremely difficult due to the complexity of the kidney. Perhaps there are alternate methods of increasing ASS/ASL abundance? Interestingly, ASS and ASL abundance are increased during starvation (61). Could the benefits of caloric restriction on renal disease (65, 76) occur partially through increasing ASS/ASL abundance and subsequently increasing NO production?

Mechanisms of ANGII Regulation of Arginase

In aim 3, we have shown a reduction in arginase abundance and activity in FHH rats treated with an ANGII receptor blocker. However, we have no mechanistic data regarding why this occurs. I believe that cell culture studies would help to elaborate on whether or not a correlation exists between ANGII and arginase per se or if this was a secondary effect of attenuating hypertension and CKD. Based on some preliminary data presented at a national meeting this year (148), there appears to be a direct signaling mechanism between ANGII and arginase. What occurs with this signaling pathway in animals with CKD? What happened in patients being treated with ANGII blockade in relation to their arginase levels?

Human L-Arg Deficiency

Here I would like to address the topic of the first patients documented with L-Arg deficiency (67). The patient was a 37-year old Japanese male who presented with lysinuric protein intolerance (LPI). Stemming from a dysfunction in the LAT transporter the patient was unable to release L-Arg and resulted in plasma levels ~25% of normal. His NO production was about ~1/3 normal and also he also exhibited reduced endothelium dependent vasodilation. The NO

production and vasodilation was restored with L-Arg infusion (0.67mg/min for 30min). The patient complained of chest pains but was not hypertensive and there was no reported information on renal function. This case suggests that impairment of renal L-Arg release may result in an L-Arg deficiency and reduced NO production. The fact that L-Arg infusions increased NO production implies that there was no dysfunction in L-Arg transport or increased consumption by arginase. Further studies and data are needed to address the impact of this substrate deficiency on renal functions.

Final Thoughts

In conclusion, my research over the past 3 years has helped to clarify the role of L-Arg production and utilization in CKD. In this dissertation I have presented some common themes seen across three very different models of CKD. However, by no means do I assume that restoration of L-Arg production will end the progression of CKD. Like in most studies, for every literature claiming one beneficial effect of a drug there is another study showing the adverse effects. This is most clearly seen in the L-Arg supplementations in rats versus humans, and indeed our ultimate goal is the treatment of CKD in humans. What I hope to have achieved is not a magic cure but a clarification and added importance of L-Arg in CKD.

In the current treatment of patients, the focus has been on ANGII pathways, antioxidants, and controlling BP. There is no doubt that this treatment has proven beneficial but are we neglecting alternate pathways that could lead to additional treatments? In dialysis patients we are removing the harmful products from the blood but are we also depleting these patients of the essential L-Arg?

Can we impact the reductions in NO by concentrating on increasing its substrate delivery to NOS as well as reducing NO scavenging? Perhaps through combination therapy of increasing L-Arg synthesis, delivery, reducing arginase, or improving the L-Arg/ADMA ratio in current treatments, we can improve the outcome of the patients and help to brighten the future of CKD and ERKD in America and the world.

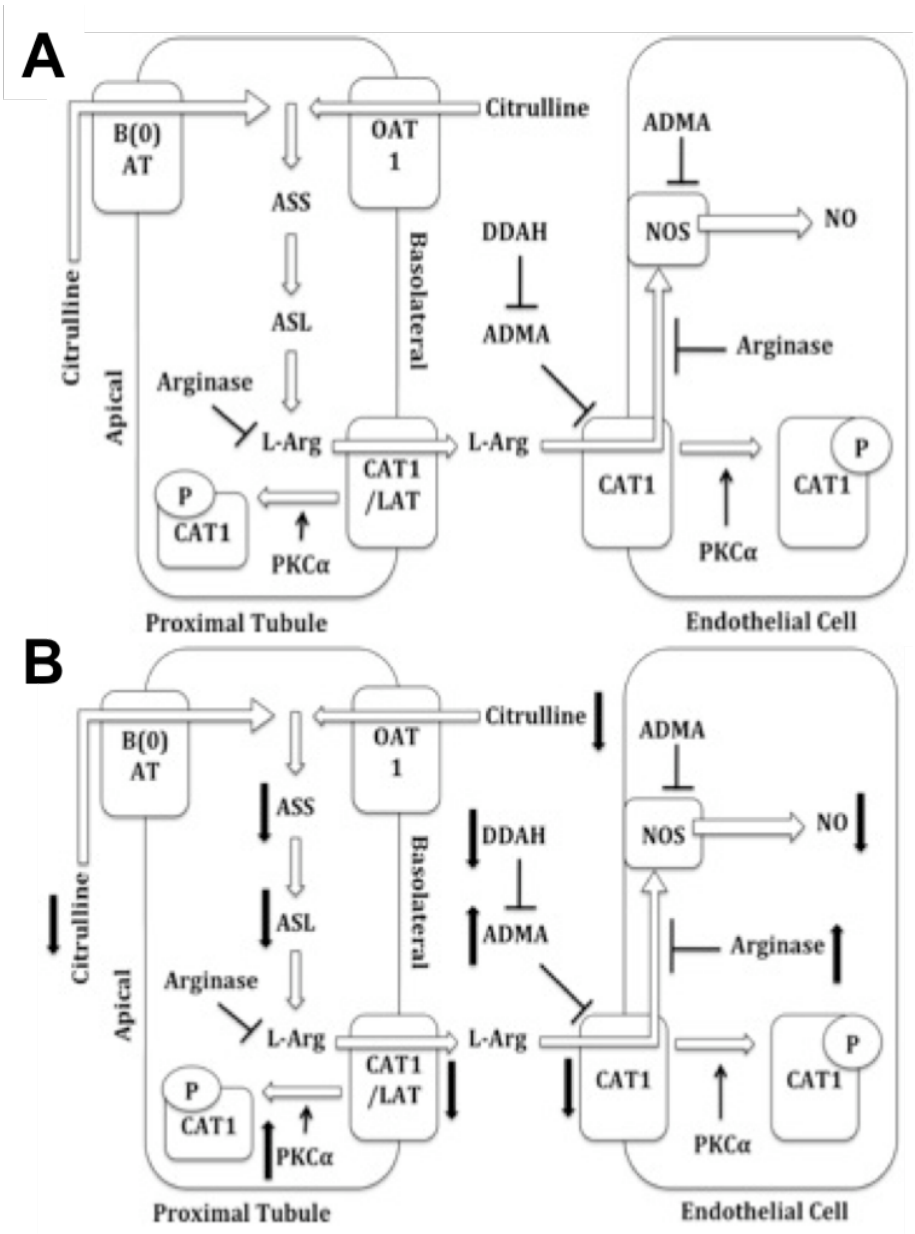

Figure 7-1. Regulation of L-Arginine and nitric oxide synthesis. The synthesis, transport, metabolism, and utilization of L-Arg in (A) normal states and in (B) kidney disease. Filled arrows indicate changes in content (↓ symbolizes a decrease and ↑ symbolizes an increase). These include only changes shown by the data presented in this dissertation. B(0)AT- basic neutral amino acid transporter, OAT- organic amino acid transporter, CAT- cationic amino acid transporter, LAT - L-type amino acid transporter, ASS- argininosuccinate synthase, ASL- argininosuccinate lyase, DDAH-dimethylarginine dimethylaminohydrolase, ADMA- asymmetric dimethylarginine, NOS- nitric oxide synthase, PKC- protein kinase C, NO- nitric oxide, P- phosphorylation.

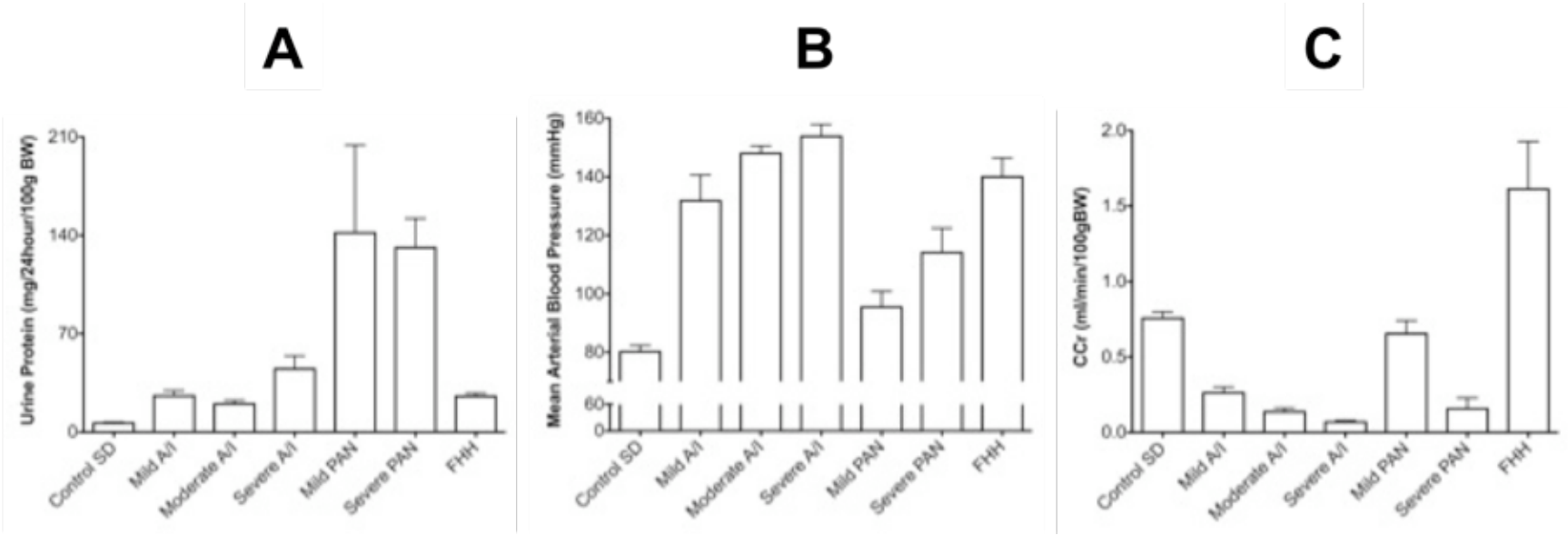

Figure 7-2. Indices of disease severity in various CKD models. (A) Mean arterial blood pressure, (B) creatinine clearance and (C) proteinuria compiled across three CKD models: 5/6 A/I at stages 1-2 weeks (mild), 4-5 weeks (moderate), and 10-12 week (severe) post injury, low (moderate) and high (severe) dose PAN injections, and spontaneously developing 18-week old FHH exacerbated with a high protein diet for 13 weeks. The 5/6 A/I and PAN models were done in male SD rats. Control SD group is compiled data from Shams from 5/6 A/I study and controls from PAN study.

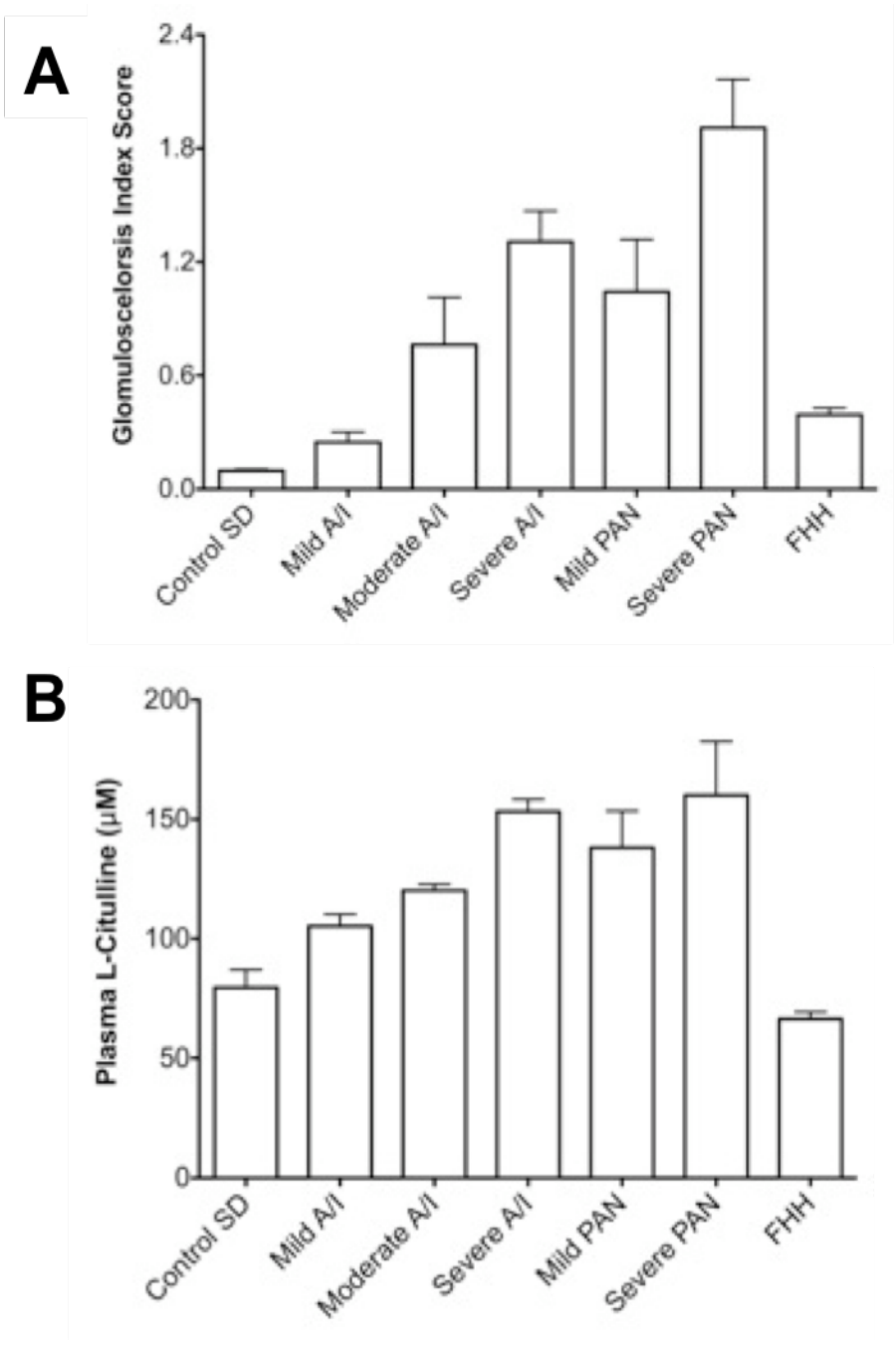

Figure 7-3. Plasma citrulline as a marker of renal injury. (A) Glomerulosclerosis index and (B) plasma citrulline concentrations compiled across three CKD models: 5/6 A/I at stages 1-2 weeks (mild), 4-5 weeks (moderate), and 10-12 week (severe) post injury, low (moderate) and high (severe) dose PAN injections, and spontaneously developing 18-week old FHH exacerbated with a high protein diet for 13 weeks. The 5/6 A/I and PAN models were done in male SD rats. Control SD group is compiled data from Shams from 5/6 A/I study and controls from PAN study.

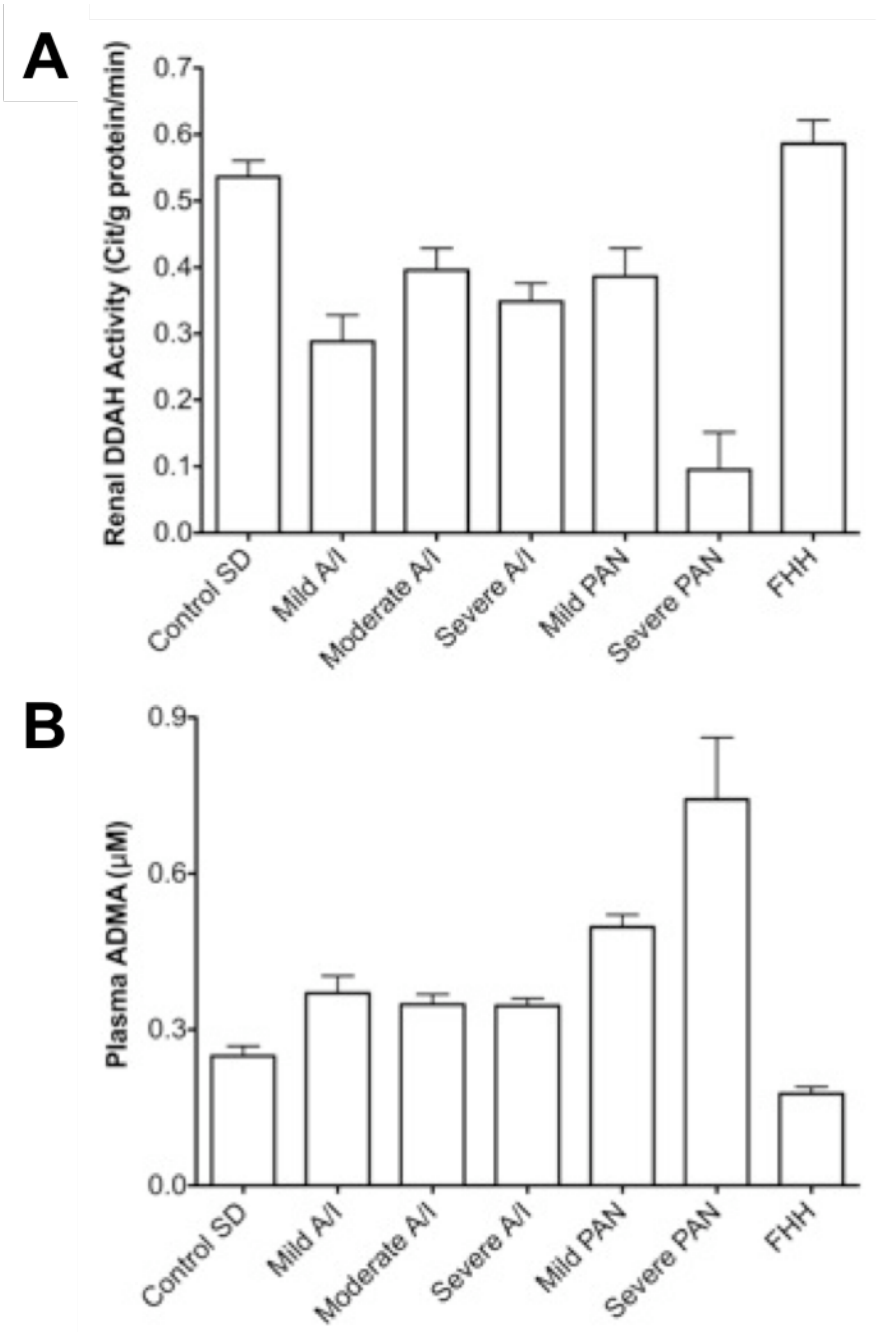

Figure 7-4. Renal DDAH activity and plasma ADMA values in various CKD models. Compilation of (A) renal DDAH activity and (B) plasma ADMA values taken across three CKD models: 5/6 A/I at stages 1-2 weeks (mild), 4-5 weeks (moderate), and 10-12 week (severe) post injury, low (moderate) and high (severe) dose PAN injections, and spontaneously developing 18-week old FHH exacerbated with a high protein diet for 13 weeks. The 5/6 A/I and PAN models were done in male SD rats. Control SD group is compiled data from Shams from 5/6 A/I study and controls from PAN study

LIST OF REFERENCES

1. **Achan V, Broadhead M, Malaki M, Whitley G, Leiper J, MacAllister R, and Vallance P**. Asymmetric dimethylarginine causes hypertension and cardiac dysfunction in humans and is actively metabolized by dimethylarginine dimethylaminohydrolase. *Arterioscler Thromb Vasc Biol* 23: 1455-1459, 2003.

2. **Aiello S, Noris M, Todeschini M, Zappella S, Foglieni C, Benigni A, Corna D, Zoja C, Cavallotti D, and Remuzzi G**. Renal and systemic nitric oxide synthesis in rats with renal mass reduction. *Kidney Int* 52: 171-181, 1997.

3. **Anderson S, Diamond JR, Karnovsky MJ, and Brenner BM**. Mechanisms underlying transition from acute glomerular injury to late glomerular sclerosis in a rat model of nephrotic syndrome. *J Clin Invest* 82: 1757-1768, 1988.

4. **Ashab I, Peer G, Blum M, Wollman Y, Chernihovsky T, Hassner A, Schwartz D, Cabili S, Silverberg D, and Iaina A**. Oral administration of L-arginine and captopril in rats prevents chronic renal failure by nitric oxide production. *Kidney Int* 47: 1515-1521, 1995.

5. **ASN**. Kidney Disease: A Growing Public Health and Economic Concern http://www.asn-online.org/facts%5Fand%5Fstatistics/kd-health-threat.pdf.

6. **Bagnost T, Berthelot A, Bouhaddi M, Laurant P, Andre C, Guillaume Y, and Demougeot C**. Treatment with the arginase inhibitor N(omega)-hydroxy-nor-L-arginine improves vascular function and lowers blood pressure in adult spontaneously hypertensive rat. *J Hypertens* 26: 1110-1118, 2008.

7. **Baylis C**. Arginine, arginine analogs and nitric oxide production in chronic kidney disease. *Nat Clin Pract Nephrol* 2: 209-220, 2006.

8. **Baylis C**. Nitric Oxide Deficiency in Chronic Kidney Disease. *AJP-Renal* 294: F1-F9, 2008.

9. **Baylis C, and Vallance P**. Measurement of nitrite and nitrate levels in plasma and urine--what does this measure tell us about the activity of the endogenous nitric oxide system? *Curr Opin Nephrol Hypertens* 7: 59-62, 1998.

10. **Bedford MT, and Richard S**. Arginine methylation an emerging regulator of protein function. *Mol Cell* 18: 263-272, 2005.

11. **Beltowski J, and Kedra A**. Asymmetric dimethylarginine (ADMA) as a target for pharmacotherapy. *Pharmacol Rep* 58: 159-178, 2006.

12. **Bennett-Richards KJ, Kattenhorn M, Donald AE, Oakley GR, Varghese Z, Bruckdorfer KR, Deanfield JE, and Rees L**. Oral L-arginine does not improve endothelial dysfunction in children with chronic renal failure. *Kidney Int* 62: 1372-1378, 2002.

13. **Bergstrom J, Alvestrand A, and Furst P**. Plasma and muscle free amino acids in maintenance hemodialysis patients without protein malnutrition. *Kidney Int* 38: 108-114, 1990.

14. **Berkowitz DE, White R, Li D, Minhas KM, Cernetich A, Kim S, Burke S, Shoukas AA, Nyhan D, Champion HC, and Hare JM**. Arginase reciprocally regulates nitric oxide synthase activity and contributes to endothelial dysfunction in aging blood vessels. *Circulation* 108: 2000-2006, 2003.

15. **Blum M, Yachnin T, Wollman Y, Chernihovsky T, Peer G, Grosskopf I, Kaplan E, Silverberg D, Cabili S, and Iaina A**. Low nitric oxide production in patients with chronic renal failure. *Nephron* 79: 265-268, 1998.

16. **Boger RH, Schwedhelm E, Maas R, Quispe-Bravo S, and Skamira C**. ADMA and oxidative stress may relate to the progression of renal disease: rationale and design of the VIVALDI study. *Vasc Med* 10 Suppl 1: 97-9102, 2005.

17. **Boger RH, and Zoccali C**. ADMA: a novel risk factor that explains excess cardiovascular event rate in patients with end-stage renal disease. *Atheroscler Suppl* 4: 23-28, 2003.

18. **Bouby N, Hassler C, Parvy P, and Bankir L**. Renal synthesis of arginine in chronic renal failure: in vivo and in vitro studies in rats with 5/6 nephrectomy. *Kidney Int* 44: 676-683, 1993.

19. **Brosnan JT, Wijekoon EP, Warford-Woolgar L, Trottier NL, Brosnan ME, Brunton JA, and Bertolo RF**. Creatine synthesis is a major metabolic process in neonatal piglets and has important implications for amino acid metabolism and methyl balance. *J Nutr* 139: 1292-1297, 2009.

20. **Brosnan ME, and Brosnan JT**. Renal arginine metabolism. *J Nutr* 134: 2791S-2795S; discussion 2796S-2797S, 2004.

21. **Cardounel AJ, Xia Y, and Zweier JL**. Endogenous methylarginines modulate superoxide as well as nitric oxide generation from neuronal nitric-oxide synthase: differences in the effects of monomethyl- and dimethylarginines in the presence and absence of tetrahydrobiopterin. *J Biol Chem* 280: 7540-7549, 2005.

22. **Carritt B, and Povey S**. Regional asssignments of the loci AK3, ACONS, and ASS on human chromosome 9. *Cytogenet Cell Genet* 23: 171-181, 1979.

23. **Castillo L, Beaumier L, Ajami AM, and Young VR**. Whole body nitric oxide synthesis in healthy men determined from [15N] arginine-to-[15N]citrulline labeling. *Proc Natl Acad Sci U S A* 93: 11460-11465, 1996.

24. **Castillo L, Chapman TE, Sanchez M, Yu YM, Burke JF, Ajami AM, Vogt J, and Young VR**. Plasma arginine and citrulline kinetics in adults given adequate and arginine-free diets. *Proc Natl Acad Sci U S A* 90: 7749-7753, 1993.

25. **Castillo L, Sanchez M, Chapman TE, Ajami A, Burke JF, and Young VR**. The plasma flux and oxidation rate of ornithine adaptively decline with restricted arginine intake. *Proc Natl Acad Sci U S A* 91: 6393-6397, 1994.

26. **Ceballos I, Chauveau P, Guerin V, Bardet J, Parvy P, Kamoun P, and Jungers P**. Early alterations of plasma free amino acids in chronic renal failure. *Clin Chim Acta* 188: 101-108, 1990.

27. **Chan W, Wang M, Kopple JD, and Swendseid ME**. Citrulline levels and urea cycle enzymes in uremic rats. *J Nutr* 104: 678-683, 1974.

28. **Chen G-F, and Baylis C**. Exogenous Citrulline on Renal Uptake in Various Stages of 5/6 Ablation/Infarction Chronic Kidney Disease. *FASEB J* 23: 2009.

29. **Closs EI, Boissel JP, Habermeier A, and Rotmann A**. Structure and function of cationic amino acid transporters (CATs). *J Membr Biol* 213: 67-77, 2006.

30. **Closs EI, Graf P, Habermeier A, Cunningham JM, and Forstermann U**. Human cationic amino acid transporters hCAT-1, hCAT-2A, and hCAT-2B: three related carriers with distinct transport properties. *Biochemistry* 36: 6462-6468, 1997.

31. **Crombez EA, and Cederbaum SD**. Hyperargininemia due to liver arginase deficiency. *Mol Genet Metab* 84: 243-251, 2005.

32. **Cross JM, Donald AE, Kharbanda R, Deanfield JE, Woolfson RG, and MacAllister RJ**. Acute administration of L-arginine does not improve arterial endothelial function in chronic renal failure. *Kidney Int* 60: 2318-2323, 2001.

33. **Curis E, Nicolis I, Moinard C, Osowska S, Zerrouk N, Benazeth S, and Cynober L**. Almost all about citrulline in mammals. *Amino Acids* 29: 177-205, 2005.

34. **Dayal S, Rodionov RN, Arning E, Bottiglieri T, Kimoto M, Murry DJ, Cooke JP, Faraci FM, and Lentz SR**. Tissue-specific downregulation of dimethylarginine dimethylaminohydrolase in hyperhomocysteinemia. *Am J Physiol Heart Circ Physiol* 295: H816-825, 2008.

35. **Dayoub H, Achan V, Adimoolam S, Jacobi J, Stuehlinger MC, Wang B-y, Tsao PS, Kimoto M, Vallance P, Patterson AJ, and Cooke JP**. Dimethylarginine dimethylaminohydrolase regulates nitric oxide synthesis: genetic and physiological evidence. *Circulation* 108: 3042-3047, 2003.

36. **De Nicola L, Bellizzi V, Minutolo R, Andreucci M, Capuano A, Garibotto G, Corso G, Andreucci VE, and Cianciaruso B**. Randomized, double-blind, placebo-controlled study of arginine supplementation in chronic renal failure. *Kidney Int* 56: 674-684, 1999.

37. **Demougeot C, Prigent-Tessier A, Marie C, and Berthelot A**. Arginase inhibition reduces endothelial dysfunction and blood pressure rising in spontaneously hypertensive rats. *J Hypertens* 23: 971-978, 2005.

38. **Dhanakoti SN, Brosnan JT, Herzberg GR, and Brosnan ME**. Renal arginine synthesis: studies in vitro and in vivo. *Am J Physiol* 259: 437-442, 1990.

39. **Di Giusto G, Anzai N, Endou H, and Torres AM**. Elimination of organic anions in response to an early stage of renal ischemia-reperfusion in the rat: role of basolateral plasma membrane transporters and cortical renal blood flow. *Pharmacology* 81: 127-136, 2008.

40. **El Nahas M**. The global challenge of chronic kidney disease. *Kidney Int* 68: 2918-2929, 2005.

41. **Erdely A, Freshour G, Smith C, Engels K, Olson JL, and Baylis C**. Protection against puromycin aminonucleoside-induced chronic renal disease in the Wistar-Furth rat. *Am J Physiol Renal Physiol* 287: 81-89, 2004.

42. **Erdely A, Greenfeld Z, Wagner L, and Baylis C**. Sexual dimorphism in the aging kidney: Effects on injury and nitric oxide system. *Kidney Int* 63: 1021-1026, 2003.

43. **Erdely A, Wagner L, Muller V, Szabo A, and Baylis C**. Protection of wistar furth rats from chronic renal disease is associated with maintained renal nitric oxide synthase. *J Am Soc Nephrol* 14: 2526-2533, 2003.

44. **Fleck C, Janz A, Schweitzer F, Karge E, Schwertfeger M, and Stein G**. Serum concentrations of asymmetric (ADMA) and symmetric (SDMA) dimethylarginine in renal failure patients. *Kidney Int Suppl* 78: 14-18, 2001.

45. **Fogo AB**. Animal models of FSGS: lessons for pathogenesis and treatment. *Semin Nephrol* 23: 161-171, 2003.

46. **Foley RN, Parfrey PS, and Sarnak MJ**. Epidemiology of cardiovascular disease in chronic renal disease. *J Am Soc Nephrol* 9: 16-23, 1998.

47. **Galea E, Regunathan S, Eliopoulos V, Feinstein DL, and Reis DJ**. Inhibition of mammalian nitric oxide synthases by agmatine, an endogenous polyamine formed by decarboxylation of arginine. *Biochem J* 316 (Pt 1): 247-249, 1996.

48. **George SK, Dipu MT, Mehra UR, Singh P, Verma AK, and Ramgaokar JS**. Improved HPLC method for the simultaneous determination of allantoin, uric acid and creatinine in cattle urine. *J Chromatogr B Analyt Technol Biomed Life Sci* 832: 134-137, 2006.

49. **Hartman WJ, Torre PM, and Prior RL**. Dietary citrulline but not ornithine counteracts dietary arginine deficiency in rats by increasing splanchnic release of citrulline. *J Nutr* 124: 1950-1960, 1994.

50. **Hasegawa K, Wakino S, Tatematsu S, Yoshioka K, Homma K, Sugano N, Kimoto M, Hayashi K, and Itoh H**. Role of asymmetric dimethylarginine in vascular injury in transgenic mice overexpressing dimethylarginie dimethylaminohydrolase 2. *Circ Res* 101: 2-10, 2007.

51. **Hatzoglou M, Fernandez J, Yaman I, and Closs E**. Regulation of cationic amino acid transport: the story of the CAT-1 transporter. *Annu Rev Nutr* 24: 377-399, 2004.

52. **Hecker M, Sessa WC, Harris HJ, Anggard EE, and Vane JR**. The metabolism of L-arginine and its significance for the biosynthesis of endothelium-derived relaxing factor: cultured endothelial cells recycle L-citrulline to L-arginine. *Proc Natl Acad Sci U S A* 87: 8612-8616, 1990.

53. **Heresztyn T, Worthley MI, and Horowitz JD**. Determination of l-arginine and NG, NG - and NG, NG' -dimethyl-L-arginine in plasma by liquid chromatography as AccQ-Fluor fluorescent derivatives. *J Chromatogr B Analyt Technol Biomed Life Sci* 805: 325-329, 2004.

54. **Hosokawa H, Sawamura T, Kobayashi S, Ninomiya H, Miwa S, and Masaki T**. Cloning and characterization of a brain-specific cationic amino acid transporter. *J Biol Chem* 272: 8717-8722, 1997.

55. **Hultstrom M, Helle F, and Iversen BM**. AT1 receptor activation regulates the mRNA expression of CAT-1, CAT-2, Arginase-1 and DDAH-2 in preglomerular vessels from angiotensin II hypertensive rats. *Am J Physiol Renal Physiol* 2009.

56. **Humphrey TJ, and Davies DD**. A sensitive method for measuring protein turnover based on the measurement of 2-3H-labelled amino acids in protein. *Biochem J* 156: 561-568, 1976.

57. **Husson A, Brasse-Lagnel C, Fairand A, Renouf S, and Lavoinne A**. Argininosuccinate synthetase from the urea cycle to the citrulline-NO cycle. *Eur J Biochem* 270: 1887-1899, 2003.

58. **Ito A, Tsao PS, Adimoolam S, Kimoto M, Ogawa T, and Cooke JP**. Novel mechanism for endothelial dysfunction: dysregulation of dimethylarginine dimethylaminohydrolase. *Circulation* 99: 3092-3095, 1999.

59. **Ito K, Chen J, Vaughan ED, Jr., Seshan SV, Poppas DP, and Felsen D**. Dietary L-arginine supplementation improves the glomerular filtration rate and renal blood flow after 24 hours of unilateral ureteral obstruction in rats. *J Urol* 171: 926-930, 2004.

60. **Iyer RK, Yoo PK, Kern RM, Rozengurt N, Tsoa R, O'Brien WE, Yu H, Grody WW, and Cederbaum SD**. Mouse model for human arginase deficiency. *Mol Cell Biol* 22: 4491-4498, 2002.

61. **Jackson MJ, Allen SJ, Beaudet AL, and O'Brien WE**. Metabolite regulation of argininosuccinate synthetase in cultured human cells. *J Biol Chem* 263: 16388-16394, 1988.

62. **Jacobi J, Sydow K, von Degenfeld G, Zhang Y, Dayoub H, Wang B, Patterson AJ, Kimoto M, Blau HM, and Cooke JP**. Overexpression of dimethylarginine dimethylaminohydrolase reduces tissue asymmetric dimethylarginine levels and enhances angiogenesis. *Circulation* 111: 1431-1438, 2005.

63. **Jean C, Rome S, Mathe V, Huneau JF, Aattouri N, Fromentin G, Achagiotis CL, and Tome D**. Metabolic evidence for adaptation to a high protein diet in rats. *J Nutr* 131: 91-98, 2001.

64. **Jeremy RW, McCarron H, and Sullivan D**. Effects of dietary L-arginine on atherosclerosis and endothelium-dependent vasodilatation in the hypercholesterolemic rabbit. Response according to treatment duration, anatomic site, and sex. *Circulation* 94: 498-506, 1996.

65. **Jiang T, Liebman SE, Lucia MS, Phillips CL, and Levi M**. Calorie restriction modulates renal expression of sterol regulatory element binding proteins, lipid accumulation, and age-related renal disease. *J Am Soc Nephrol* 16: 2385-2394, 2005.

66. **Johnson FK, Johnson RA, Peyton KJ, and Durante W**. Arginase inhibition restores arteriolar endothelial function in Dahl rats with salt-induced hypertension. *Am J Physiol Regul Integr Comp Physiol* 288: 1057-1062, 2005.

67. **Kamada Y, Nagaretani H, Tamura S, Ohama T, Maruyama T, Hiraoka H, Yamashita S, Yamada A, Kiso S, Inui Y, Ito N, Kayanoki Y, Kawata S, and Matsuzawa Y**. Vascular endothelial dysfunction resulting from L-arginine deficiency in a patient with lysinuric protein intolerance. *J Clin Invest* 108: 717-724, 2001.

68. **Karim Z, Defontaine N, Paillard M, and Poggioli J**. Protein kinase C isoforms in rat kidney proximal tubule: acute effect of angiotensin II. *Am J Physiol* 269: C134-140, 1995.

69. **Kasperek GJ, and Snider RD**. The effect of exercise on protein turnover in isolated soleus and extensor digitorum longus muscles. *Experientia* 41: 1399-1400, 1985.

70. **Kawamoto S, Amaya Y, Murakami K, Tokunaga F, Iwanaga S, Kobayashi K, Saheki T, Kimura S, and Mori M**. Complete nucleotide sequence of cDNA and deduced amino acid sequence of rat liver arginase. *J Biol Chem* 262: 6280-6283, 1987.

71. **Kielstein JT, Frolich JC, Haller H, and Fliser D**. ADMA (asymmetric dimethylarginine): an atherosclerotic disease mediating agent in patients with renal disease? *Nephrol Dial Transplant* 16: 1742-1745, 2001.

72. **Kielstein JT, Simmel S, Bode-Boger SM, Roth HJ, Schmidt-Gayk H, Haller H, and Fliser D**. Subpressor dose asymmetric dimethylarginine modulates renal function in humans through nitric oxide synthase inhibition. *Kidney Blood Press Res* 27: 143-147, 2004.

73. **Kimoto M, Miyatake S, Sasagawa T, Yamashita H, Okita M, Oka T, Ogawa T, and Tsuji H**. Purification, cDNA cloning and expression of human NG,NG-dimethylarginine dimethylaminohydrolase. *Eur J Biochem* 258: 863-868, 1998.

74. **Kizhatil K, and Albritton LM**. System y+ localizes to different membrane subdomains in the basolateral plasma membrane of epithelial cells. *Am J Physiol Cell Physiol* 283: C1784-1794, 2002.

75. **Knipp M**. How to control NO production in cells: N(omega),N(omega)-dimethyl-L-arginine dimethylaminohydrolase as a novel drug target. *Chembiochem* 7: 879-889, 2006.

76. **Kobayashi S, and Venkatachalam MA**. Differential effects of calorie restriction on glomeruli and tubules of the remnant kidney. *Kidney Int* 42: 710-717, 1992.

77. **Koeners MP, Braam B, van der Giezen DM, Goldschmeding R, and Joles JA**. A perinatal nitric oxide donor increases renal vascular resistance and ameliorates hypertension and glomerular injury in adult fawn-hooded hypertensive rats. *Am J Physiol Regul Integr Comp Physiol* 294: R1847-1855, 2008.

78. **Koeners MP, van Faassen EE, Wesseling S, de Sain-van der Velden M, Koomans HA, Braam B, and Joles JA**. Maternal supplementation with citrulline increases renal nitric oxide in young spontaneously hypertensive rats and has long-term antihypertensive effects. *Hypertension* 50: 1077-1084, 2007.

79. **Kreisberg JI, and Karnovsky MJ**. Focal glomerular sclerosis in the fawn-hooded rat. *Am J Pathol* 92: 637-652, 1978.

80. **Krotova KY, Zharikov SI, and Block ER**. Classical isoforms of PKC as regulators of CAT-1 transporter activity in pulmonary artery endothelial cells. *Am J Physiol Lung Cell Mol Physiol* 284: 1037-1044, 2003.

81. **Kuijpers MH, and Gruys E**. Spontaneous hypertension and hypertensive renal disease in the fawn-hooded rat. *Br J Exp Pathol* 65: 181-190, 1984.

82. **Lau T, Owen W, Yu YM, Noviski N, Lyons J, Zurakowski D, Tsay R, Ajami A, Young VR, and Castillo L**. Arginine, citrulline, and nitric oxide metabolism in end-stage renal disease patients. *J Clin Invest* 105: 1217-1225, 2000.

83. **Leiper J, Murray-Rust J, McDonald N, and Vallance P**. S-nitrosylation of dimethylarginine dimethylaminohydrolase regulates enzyme activity: further interactions between nitric oxide synthase and dimethylarginine dimethylaminohydrolase. *Proc Natl Acad Sci U S A* 99: 13527-13532, 2002.

84. **Leiper JM, Santa Maria J, Chubb A, MacAllister RJ, Charles IG, Whitley GS, and Vallance P**. Identification of two human dimethylarginine dimethylaminohydrolases with distinct tissue distributions and homology with microbial arginine deiminases. *Biochem J* 343 Pt 1: 209-214, 1999.

85. **Levillain O, Balvay S, and Peyrol S**. Localization and differential expression of arginase II in the kidney of male and female mice. *Pflugers Arch* 449: 491-503, 2005.

86. **Levillain O, Hus-Citharel A, Morel F, and Bankir L**. Localization of arginine synthesis along rat nephron. *Am J Physiol* 259: 916-923, 1990.

87. **Levillain O, Parvy P, and Hassler C**. Amino acid handling in uremic rats: citrulline, a reliable marker of renal insufficiency and proximal tubular dysfunction. *Metabolism* 46: 611-618, 1997.

88. **Li C, Huang W, Harris MB, Goolsby JM, and Venema RC**. Interaction of the endothelial nitric oxide synthase with the CAT-1 arginine transporter enhances NO release by a mechanism not involving arginine transport. *Biochem J* 386: 567-574, 2005.

89. **Li G, Regunathan S, Barrow CJ, Eshraghi J, Cooper R, and Reis DJ**. Agmatine: an endogenous clonidine-displacing substance in the brain. *Science* 263: 966-969, 1994.

90. **Li H, Meininger CJ, Hawker JR, Haynes TE, Kepka-Lenhart D, Mistry SK, Morris SM, and Wu G**. Regulatory role of arginase I and II in nitric oxide, polyamine, and proline syntheses in endothelial cells. *Am J Physiol Endocrinol Metab* 280: 75-82, 2001.

91. **Li H, Meininger CJ, Kelly KA, Hawker JR, Jr., Morris SM, Jr., and Wu G**. Activities of arginase I and II are limiting for endothelial cell proliferation. *Am J Physiol Regul Integr Comp Physiol* 282: R64-69, 2002.

92. **Lim HK, Ryoo S, Benjo A, Shuleri K, Miriel V, Baraban E, Camara A, Soucy K, Nyhan D, Shoukas A, and Berkowitz DE**. Mitochondrial arginase II constrains endothelial NOS-3 activity. *Am J Physiol Heart Circ Physiol* 293: H3317-3324, 2007.

93. **Lopez B, Ryan RP, Moreno C, Sarkis A, Lazar J, Provoost AP, Jacob HJ, and Roman RJ**. Identification of a QTL on chromosome 1 for impaired autoregulation of RBF in fawn-hooded hypertensive rats. *Am J Physiol Renal Physiol* 290: F1213-1221, 2006.

94. **MacAllister R, and Vallance P**. Nitric oxide in essential and renal hypertension. *J Am Soc Nephrol* 5: 1057-1065, 1994.

95. **MacAllister RJ, Parry H, Kimoto M, Ogawa T, Russell RJ, Hodson H, Whitley GS, and Vallance P**. Regulation of nitric oxide synthesis by dimethylarginine dimethylaminohydrolase. *Br J Pharmacol* 119: 1533-1540, 1996.

96. **Mackie FE, Campbell DJ, and Meyer TW**. Intrarenal angiotensin and bradykinin peptide levels in the remnant kidney model of renal insufficiency. *Kidney Int* 59: 1458-1465, 2001.

97. **Marshall CB, Pippin JW, Krofft RD, and Shankland SJ**. Puromycin aminonucleoside induces oxidant-dependent DNA damage in podocytes in vitro and in vivo. *Kidney Int* 70: 1962-1973, 2006.

98. **Matsuguma K, Ueda S, Yamagishi S-i, Matsumoto Y, Kaneyuki U, Shibata R, Fujimura T, Matsuoka H, Kimoto M, Kato S, Imaizumi T, and Okuda S**. Molecular mechanism for elevation of asymmetric dimethylarginine and its role for hypertension in chronic kidney disease. *J Am Soc Nephrol* 17: 2176-2183, 2006.

99. **Mattson DL, Dwinell MR, Greene AS, Kwitek AE, Roman RJ, Cowley AW, Jr., and Jacob HJ**. Chromosomal mapping of the genetic basis of hypertension and renal disease in FHH rats. *Am J Physiol Renal Physiol* 293: F1905-1914, 2007.

100. **McDonald KK, Zharikov S, Block ER, and Kilberg MS**. A caveolar complex between the cationic amino acid transporter 1 and endothelial nitric-oxide synthase may explain the "arginine paradox". *J Biol Chem* 272: 31213-31216, 1997.

101. **Mitsuoka K, Shirasaka Y, Fukushi A, Sato M, Nakamura T, Nakanishi T, and Tamai I**. Transport characteristics of L-citrulline in renal apical membrane of proximal tubular cells. *Biopharm Drug Dispos* 30: 126-137, 2009.

102. **Miyazaki H, Matsuoka H, Cooke JP, Usui M, Ueda S, Okuda S, and Imaizumi T**. Endogenous nitric oxide synthase inhibitor: a novel marker of atherosclerosis. *Circulation* 99: 1141-1146, 1999.

103. **Moradi H, Kwok V, and Vaziri ND**. Effect of chronic renal failure on arginase and argininosuccinate synthetase expression. *Am J Nephrol* 26: 310-318, 2006.

104. **Morris CR, Morris SM, Jr., Hagar W, Van Warmerdam J, Claster S, Kepka-Lenhart D, Machado L, Kuypers FA, and Vichinsky EP**. Arginine therapy: a new treatment for pulmonary hypertension in sickle cell disease? *Am J Respir Crit Care Med* 168: 63-69, 2003.

105. **Morris SM**. Arginine: beyond protein. In: *Am J Clin Nutr*2006, p. 508S-512S.

106. **Morris SM, Jr.** Regulation of enzymes of the urea cycle and arginine metabolism. *Annu Rev Nutr* 22: 87-105, 2002.

107. **Munger KA, Blantz RC, and Lortie MJ**. Acute renal response to LPS: impaired arginine production and inducible nitric oxide synthase activity. *Am J Physiol Regul Integr Comp Physiol* 291: R684-691, 2006.

108. **Nakagawa I, Takahashi T, Suzuki T, and Kobayashi K**. Amino acid requirements of children: minimal needs of tryptophan, arginine and histidine based on nitrogen balance method. *J Nutr* 80: 305-310, 1963.

109. **Nakakariya M, Shima Y, Shirasaka Y, Mitsuoka K, Nakanishi T, and Tamai I**. Organic Anion Transporter OAT1 Is Involved in Renal Handling of Citrulline. *Am J Physiol Renal Physiol* 2009.

110. **Naylor SL, Klebe RJ, and Shows TB**. Argininosuccinic aciduria: assignment of the argininosuccinate lyase gene to the pter to q22 region of human chromosome 7 by bioautography. *Proc Natl Acad Sci U S A* 75: 6159-6162, 1978.

111. **Ni Z, and Vaziri ND**. Downregulation of nitric oxide synthase in nephrotic syndrome: role of proteinuria. *Biochim Biophys Acta* 1638: 129-137, 2003.

112. **Nijveldt RJ, Teerlink T, Van Der Hoven B, Siroen MP, Kuik DJ, Rauwerda JA, and van Leeuwen PA**. Asymmetrical dimethylarginine (ADMA) in critically ill patients: high plasma ADMA concentration is an independent risk factor of ICU mortality. *Clin Nutr* 22: 23-30, 2003.

113. **Nijveldt RJ, Van Leeuwen PA, Van Guldener C, Stehouwer CD, Rauwerda JA, and Teerlink T**. Net renal extraction of asymmetrical (ADMA) and symmetrical (SDMA) dimethylarginine in fasting humans. *Nephrol Dial Transplant* 17: 1999-2002, 2002.

114. **Ogawa T, Kimoto M, Watanabe H, and Sasaoka K**. Metabolism of NG,NG-and NG,N'G-dimethylarginine in rats. *Arch Biochem Biophys* 252: 526-537, 1987.

115. **Onozato ML, Tojo A, Leiper J, Fujita T, Palm F, and Wilcox CS**. Expression of NG,NG-dimethylarginine dimethylaminohydrolase and protein arginine N-methyltransferase isoforms in diabetic rat kidney: effects of angiotensin II receptor blockers. *Diabetes* 57: 172-180, 2008.

116. **Pahlich S, Zakaryan RP, and Gehring H**. Protein arginine methylation: Cellular functions and methods of analysis. *Biochim Biophys Acta* 1764: 1890-1903, 2006.

117. **Palm F, Onozato ML, Luo Z, and Wilcox CS**. Dimethylarginine dimethylaminohydrolase (DDAH): expression, regulation, and function in the cardiovascular and renal systems. *Am J Physiol Heart Circ Physiol* 293: H3227-3245, 2007.

118. **Perianayagam MC, Liangos O, Kolyada AY, Wald R, MacKinnon RW, Li L, Rao M, Balakrishnan VS, Bonventre JV, Pereira BJ, and Jaber BL**. NADPH oxidase p22phox and catalase gene variants are associated with biomarkers of oxidative stress and adverse outcomes in acute renal failure. *J Am Soc Nephrol* 18: 255-263, 2007.

119. **Peyton KJ, Ensenat D, Azam MA, Keswani AN, Kannan S, Liu XM, Wang H, Tulis DA, and Durante W**. Arginase promotes neointima formation in rat injured carotid arteries. *Arterioscler Thromb Vasc Biol* 29: 488-494, 2009.

120. **Pope AJ, Druhan L, Guzman JE, Forbes SP, Murugesan V, Lu D, Xia Y, Chicoine LG, Parinandi NL, and Cardounel AJ**. Role of DDAH-1 in lipid peroxidation product-mediated inhibition of endothelial NO generation. *Am J Physiol Cell Physiol* 293: C1679-1686, 2007.

121. **Prescott LM, and Jones ME**. Modified methods for the determination of carbamyl aspartate. *Anal Biochem* 32: 408-419, 1969.

122. **Prins HA, Nijveldt RJ, Gasselt DV, van Kemenade F, Teerlink T, van Lambalgen AA, Rauwerda JA, and van Leeuwen PA**. The flux of arginine after ischemia-reperfusion in the rat kidney. In: *Kidney International*2002, p. 86-93.

123. **Provoost AP, Shiozawa M, Van Dokkum RP, and Jacob HJ**. Transfer of the Rf-1 region from FHH onto the ACI background increases susceptibility to renal impairment. *Physiol Genomics* 8: 123-129, 2002.

124. **Purkerson ML, Hoffsten PE, and Klahr S**. Pathogenesis of the glomerulopathy associated with renal infarction in rats. *Kidney Int* 9: 407-417, 1976.

125. **Racusen LC, Whelton A, and Solez K**. Effects of lysine and other amino acids on kidney structure and function in the rat. *Am J Pathol* 120: 436-442, 1985.

126. **Raij L, Azar S, and Keane W**. Mesangial immune injury, hypertension, and progressive glomerular damage in Dahl rats. *Kidney Int* 26: 137-143, 1984.

127. **Reyes AA, Martin D, Settle S, and Klahr S**. EDRF role in renal function and blood pressure of normal rats and rats with obstructive uropathy. *Kidney Int* 41: 403-413, 1992.

128. **Reyes AA, Porras BH, Chasalow FI, and Klahr S**. L-arginine decreases the infiltration of the kidney by macrophages in obstructive nephropathy and puromycin-induced nephrosis. *Kidney Int* 45: 1346-1354, 1994.

129. **Reyes AA, Purkerson ML, Karl I, and Klahr S**. Dietary supplementation with L-arginine ameliorates the progression of renal disease in rats with subtotal nephrectomy. *Am J Kidney Dis* 20: 168-176, 1992.

130. **Rincon J, Romero M, Viera N, Pedreanez A, and Mosquera J**. Increased oxidative stress and apoptosis in acute puromycin aminonucleoside nephrosis. *Int J Exp Pathol* 85: 25-33, 2004.

131. **Rodriguez S, Richert L, and Berthelot A**. Increased arginase activity in aorta of mineralocorticoid-salt hypertensive rats. *Clin Exp Hypertens* 22: 75-85, 2000.

132. **Rotmann A, Strand D, Martine U, and Closs EI**. Protein kinase C activation promotes the internalization of the human cationic amino acid transporter hCAT-1. A new regulatory mechanism for hCAT-1 activity. *J Biol Chem* 279: 54185-54192, 2004.

133. **Rotmann A, Vekony N, Gassner D, Niegisch G, Strand D, Martine U, and Closs EI**. Activation of classical protein kinase C reduces the expression of human cationic amino acid transporter 3 (hCAT-3) in the plasma membrane. *Biochem J* 395: 117-123, 2006.

134. **Ryoo S, Gupta G, Benjo A, Lim HK, Camara A, Sikka G, Lim HK, Sohi J, Santhanam L, Soucy K, Tuday E, Baraban E, Ilies M, Gerstenblith G, Nyhan D, Shoukas A, Christianson DW, Alp NJ, Champion HC, Huso D, and Berkowitz DE**. Endothelial arginase II: a novel target for the treatment of atherosclerosis. *Circ Res* 102: 923-932, 2008.

135. **Sabbatini M, Pisani A, Uccello F, Fuiano G, Alfieri R, Cesaro A, Cianciaruso B, and Andreucci VE**. Arginase inhibition slows the progression of renal failure in rats with renal ablation. *Am J Physiol Renal Physiol* 284: 680-687, 2003.

136. **Safar ME, London GM, Asmar R, and Frohlich ED**. Recent advances on large arteries in hypertension. *Hypertension* 32: 156-161, 1998.

137. **Sasser JM, and Baylis C**. The natriuretic and diuretic response to dopamine is maintained during rat pregnancy. In: *American Journal of Physiology- Renal Physiology*2008.

138. **Sato J, Masuda H, Tamaoki S, Hamasaki H, Ishizaka K, Matsubara O, and Azuma H**. Endogenous asymmetrical dimethylarginine and hypertension associated with puromycin nephrosis in the rat. *Br J Pharmacol* 125: 469-476, 1998.

139. **Scalera F, Kielstein JT, Martens-Lobenhoffer J, Postel SC, Tager M, and Bode-Boger SM**. Erythropoietin increases asymmetric dimethylarginine in endothelial cells: role of dimethylarginine dimethylaminohydrolase. *J Am Soc Nephrol* 16: 892-898, 2005.

140. **Schlaich MP, Parnell MM, Ahlers BA, Finch S, Marshall T, Zhang WZ, and Kaye DM**. Impaired L-arginine transport and endothelial function in hypertensive and genetically predisposed normotensive subjects. *Circulation* 110: 3680-3686, 2004.

141. **Schmidlin A, Fischer S, and Wiesinger H**. Transport of L-citrulline in neural cell cultures. *Dev Neurosci* 22: 393-398, 2000.

142. **Schmidt RJ, and Baylis C**. Total nitric oxide production is low in patients with chronic renal disease. *Kidney Int* 58: 1261-1266, 2000.

143. **Schmidt RJ, Domico J, Samsell LS, Yokota S, Tracy TS, Sorkin MI, Engels K, and Baylis C**. Indices of activity of the nitric oxide system in hemodialysis patients. *Am J Kidney Dis* 34: 228-234, 1999.

144. **Schulman SP, Becker LC, Kass DA, Champion HC, Terrin ML, Forman S, Ernst KV, Kelemen MD, Townsend SN, Capriotti A, Hare JM, and Gerstenblith G**. L-arginine therapy in acute myocardial infarction: the Vascular Interaction With Age in Myocardial Infarction (VINTAGE MI) randomized clinical trial. *JAMA* 295: 58-64, 2006.

145. **Schwartz IF, Ayalon R, Chernichovski T, Reshef R, Chernin G, Weinstein T, Litvak A, Levo Y, and Schwartz D**. Arginine uptake is attenuated through modulation of cationic amino-acid transporter-1, in uremic rats. *Kidney Int* 69: 298-303, 2006.

146. **Schwartz IF, Chernichovski T, Krishtol N, Grupper A, Laron I, and Schwartz D**. Sexual dimorphism in glomerular arginine transport affects nitric oxide generation in old male rats. *Am J Physiol Renal Physiol* 297: F80-84, 2009.

147. **Schwartz IF, Ingbir M, Chernichovski T, Reshef R, Chernin G, Litvak A, Weinstein T, Levo Y, and Schwartz D**. Arginine uptake is attenuated, through post-translational regulation of cationic amino acid transporter-1, in hyperlipidemic rats. *Atherosclerosis* 194: 357-363, 2007.

148. **Shatanawi A, Romero MJ, Iddings JA, Caldwell RB, and Caldwell RW**. Angiotensin II elevates endothelial arginase activity via RhoA/MAPK pathways *FASEB J* 23: 2009.

149. **Shearer JD, Richards JR, Mills CD, and Caldwell MD**. Differential regulation of macrophage arginine metabolism: a proposed role in wound healing. *Am J Physiol* 272: E181-190, 1997.

150. **Shen L-J, Beloussow K, and Shen W-C**. Accessibility of endothelial and inducible nitric oxide synthase to the intracellular citrulline-arginine regeneration pathway. *Biochem Pharmacol* 69: 97-9104, 2005.

151. **Shi O, Morris SM, Zoghbi H, Porter CW, and O'Brien WE**. Generation of a mouse model for arginase II deficiency by targeted disruption of the arginase II gene. *Mol Cell Biol* 21: 811-813, 2001.

152. **Simon A, Plies L, Habermeier A, Martine U, Reining M, and Closs EI**. Role of neutral amino acid transport and protein breakdown for substrate supply of nitric oxide synthase in human endothelial cells. *Circ Res* 93: 813-820, 2003.

153. **Simons JL, Provoost AP, De Keijzer MH, Anderson S, Rennke HG, and Brenner BM**. Pathogenesis of glomerular injury in the fawn-hooded rat: effect of unilateral nephrectomy. *J Am Soc Nephrol* 4: 1362-1370, 1993.

154. **Smith CL, Birdsey GM, Anthony S, Arrigoni FI, Leiper JM, and Vallance P**. Dimethylarginine dimethylaminohydrolase activity modulates ADMA levels, VEGF expression, and cell phenotype. *Biochem Biophys Res Commun* 308: 984-989, 2003.

155. **Stuehr DJ, and Marletta MA**. Mammalian nitrate biosynthesis: mouse macrophages produce nitrite and nitrate in response to Escherichia coli lipopolysaccharide. *Proc Natl Acad Sci U S A* 82: 7738-7742, 1985.

156. **Stuhlinger MC, Tsao PS, Her JH, Kimoto M, Balint RF, and Cooke JP**. Homocysteine impairs the nitric oxide synthase pathway: role of asymmetric dimethylarginine. *Circulation* 104: 2569-2575, 2001.

157. **Su Y, and Block ER**. Hypoxia inhibits the induction of argininosuccinate synthetase by endotoxin in lung endothelial cells. *Am J Physiol* 272: L934-938, 1997.

158. **Susic D, Francischetti A, and Frohlich ED**. Prolonged L-arginine on cardiovascular mass and myocardial hemodynamics and collagen in aged spontaneously hypertensive rats and normal rats. *Hypertension* 33: 451-455, 1999.

159. **Suto T, Losonczy G, Qiu C, Hill C, Samsell L, Ruby J, Charon N, Venuto R, and Baylis C**. Acute changes in urinary excretion of nitrite + nitrate do not necessarily predict renal vascular NO production. *Kidney Int* 48: 1272-1277, 1995.

160. **Swendseid ME, Wang M, Vyhmeister I, Chan W, Siassi F, Tam CF, and Kopple JD**. Amino acid metabolism in the chronically uremic rat. *Clin Nephrol* 3: 240-246, 1975.

161. **Szabo AJ, Wagner L, Erdely A, Lau K, and Baylis C**. Renal neuronal nitric oxide synthase protein expression as a marker of renal injury. *Kidney Int* 64: 1765-1771, 2003.

162. **Taddei S, Virdis A, Mattei P, Ghiadoni L, Sudano I, and Salvetti A**. Defective L-arginine-nitric oxide pathway in offspring of essential hypertensive patients. *Circulation* 94: 1298-1303, 1996.

163. **Tain Y-L, Freshour G, Dikalova A, Griendling K, and Baylis C**. Vitamin E reduces glomerulosclerosis, restores renal neuronal NOS, and suppresses oxidative stress in the 5/6 nephrectomized rat. *Am J Physiol Renal Physiol* 292: 1404-1410, 2007.

164. **Tain YL, and Baylis C**. Determination of dimethylarginine dimethylaminohydrolase activity in the kidney. *Kidney Int* 72: 886-889, 2007.

165. **Thambyrajah J, Landray MJ, McGlynn FJ, Jones HJ, Wheeler DC, and Townend JN**. Abnormalities of endothelial function in patients with predialysis renal failure. *Heart* 83: 205-209, 2000.

166. **Tizianello A, De Ferrari G, Garibotto G, Gurreri G, and Robaudo C**. Renal metabolism of amino acids and ammonia in subjects with normal renal function and in patients with chronic renal insufficiency. *J Clin Invest* 65: 1162-1173, 1980.

167. **Tsikas D, Wolf A, and Frolich JC**. Simplified HPLC method for urinary and circulating creatinine. *Clin Chem* 50: 201-203, 2004.

168. **Ueda S, Kato S, Matsuoka H, Kimoto M, Okuda S, Morimatsu M, and Imaizumi T**. Regulation of cytokine-induced nitric oxide synthesis by asymmetric dimethylarginine: role of dimethylarginine dimethylaminohydrolase. *Circ Res* 92: 226-233, 2003.

169. **Ulu N, Schoemaker RG, Henning RH, Buikema H, Teerlink T, Zijlstra FJ, Bakker SJ, van Gilst WH, and Navis G**. Proteinuria-Associated Endothelial Dysfunction Is Strain Dependent. *Am J Nephrol* 30: 209-217, 2009.

170. **Valkonen VP, Laakso J, Paiva H, Lehtimaki T, Lakka TA, Isomustajarvi M, Ruokonen I, Salonen JT, and Laaksonen R**. Asymmetrical dimethylarginine (ADMA) and risk of acute coronary events. Does statin treatment influence plasma ADMA levels? *Atheroscler Suppl* 4: 19-22, 2003.

171. **Vallance P, and Leiper J**. Asymmetric dimethylarginine and kidney disease--marker or mediator? *J Am Soc Nephrol* 16: 2254-2256, 2005.

172. **Vallance P, and Leiper J**. Cardiovascular biology of the asymmetric dimethylarginine:dimethylarginine dimethylaminohydrolase pathway. *Arterioscler Thromb Vasc Biol* 24: 1023-1030, 2004.

173. **Vallance P, Leone A, Calver A, Collier J, and Moncada S**. Accumulation of an endogenous inhibitor of nitric oxide synthesis in chronic renal failure. *Lancet* 339: 572-575, 1992.

174. **Vallance P, Leone A, Calver A, Collier J, and Moncada S**. Endogenous dimethylarginine as an inhibitor of nitric oxide synthesis. *J Cardiovasc Pharmacol* 20 Suppl 12: S60-62, 1992.

175. **van de Poll MCG, Soeters PB, Deutz NEP, Fearon KCH, and Dejong CHC**. Renal metabolism of amino acids: its role in interorgan amino acid exchange. *Am J Clin Nutr* 79: 185-197, 2004.

176. **Van Dijk SJ, Specht PA, Lutz MM, Lazar J, Jacob HJ, and Provoost AP**. Interaction between Rf-1 and Rf-4 quantitative trait loci increases susceptibility to renal damage in double congenic rats. *Kidney Int* 68: 2462-2472, 2005.

177. **Van Dokkum RP, Jacob HJ, and Provoost AP**. Genetic differences define severity of renal damage after L-NAME-induced hypertension in rats. *J Am Soc Nephrol* 9: 363-371, 1998.

178. **van Dokkum RP, Sun CW, Provoost AP, Jacob HJ, and Roman RJ**. Altered renal hemodynamics and impaired myogenic responses in the fawn-hooded rat. *Am J Physiol* 276: R855-863, 1999.

179. **van Rodijnen WF, van Lambalgen TA, Tangelder GJ, van Dokkum RP, Provoost AP, and ter Wee PM**. Reduced reactivity of renal microvessels to pressure and angiotensin II in fawn-hooded rats. *Hypertension* 39: 111-115, 2002.

180. **Verseput GH, Braam B, Provoost AP, and Koomans HA**. Tubuloglomerular feedback and prolonged ACE-inhibitor treatment in the hypertensive fawn-hooded rat. *Nephrol Dial Transplant* 13: 893-899, 1998.

181. **Verseput GH, Koomans HA, Braam B, Weening JJ, and Provoost AP**. ACE inhibition delays development of terminal renal failure in the presence of severe albuminuria. *Am J Kidney Dis* 35: 202-210, 2000.

182. **Verseput GH, Provoost AP, Braam BB, Weening JJ, and Koomans HA**. Angiotensin-converting enzyme inhibition in the prevention and treatment of chronic renal damage in the hypertensive fawn-hooded rat. *J Am Soc Nephrol* 8: 249-259, 1997.

183. **Verseput GH, Provoost AP, van Tol A, Koomans HA, and Joles JA**. Hyperlipidemia is secondary to proteinuria and is completely normalized by angiotensin-converting enzyme inhibition in hypertensive fawn-hooded rats. *Nephron* 77: 346-352, 1997.

184. **Visek WJ**. Arginine needs, physiological state and usual diets. A reevaluation. *J Nutr* 116: 36-46, 1986.

185. **Wagner L, Riggleman A, Erdely A, Couser W, and Baylis C**. Reduced nitric oxide synthase activity in rats with chronic renal disease due to glomerulonephritis. *Kidney Int* 62: 532-536, 2002.

186. **Wang D, Gill PS, Chabrashvili T, Onozato ML, Raggio J, Mendonca M, Dennehy K, Li M, Modlinger P, Leiper J, Vallance P, Adler O, Leone A, Tojo A, Welch WJ, and Wilcox CS**. Isoform-specific regulation by N(G),N(G)-dimethylarginine dimethylaminohydrolase of rat serum asymmetric dimethylarginine and vascular endothelium-derived relaxing factor/NO. *Circ Res* 101: 627-635, 2007.

187. **Wang J, Sim AS, Wang XL, and Wilcken DE**. L-arginine regulates asymmetric dimethylarginine metabolism by inhibiting dimethylarginine dimethylaminohydrolase activity in hepatic (HepG2) cells. *Cell Mol Life Sci* 63: 2838-2846, 2006.

188. **Waugh WH, Daeschner CW, 3rd, Files BA, McConnell ME, and Strandjord SE**. Oral citrulline as arginine precursor may be beneficial in sickle cell disease: early phase two results. *J Natl Med Assoc* 93: 363-371, 2001.

189. **Wei LH, Jacobs AT, Morris SM, Jr., and Ignarro LJ**. IL-4 and IL-13 upregulate arginase I expression by cAMP and JAK/STAT6 pathways in vascular smooth muscle cells. *Am J Physiol Cell Physiol* 279: C248-256, 2000.

190. **Wei LH, Wu G, Morris SM, and Ignarro LJ**. Elevated arginase I expression in rat aortic smooth muscle cells increases cell proliferation. *Proc Natl Acad Sci U S A* 98: 9260-9264, 2001.

191. **Wei LH, Wu G, Morris SM, Jr., and Ignarro LJ**. Elevated arginase I expression in rat aortic smooth muscle cells increases cell proliferation. *Proc Natl Acad Sci U S A* 98: 9260-9264, 2001.

192. **Wever R, Boer P, Hijmering M, Stroes E, Verhaar M, Kastelein J, Versluis K, Lagerwerf F, van Rijn H, Koomans H, and Rabelink T**. Nitric oxide production is reduced in patients with chronic renal failure. *Arterioscler Thromb Vasc Biol* 19: 1168-1172, 1999.

193. **Windmueller HG, and Spaeth AE**. Source and fate of circulating citrulline. *Am J Physiol* 241: 473-480, 1981.

194. **Wu F, Cholewa B, and Mattson DL**. Characterization of L-arginine transporters in rat renal inner medullary collecting duct. *Am J Physiol Regul Integr Comp Physiol* 278: R1506-1512, 2000.

195. **Wu G, and Meininger CJ**. Regulation of L-arginine synthesis from L-citrulline by L-glutamine in endothelial cells. *Am J Physiol* 265: H1965-1971, 1993.

196. **Wu G, and Morris SM, Jr.** Arginine metabolism: nitric oxide and beyond. *Biochem J* 336 (Pt 1): 1-17, 1998.

197. **Xia Y, Roman LJ, Masters BS, and Zweier JL**. Inducible nitric-oxide synthase generates superoxide from the reductase domain. *J Biol Chem* 273: 22635-22639, 1998.

198. **Xiao S, Schmidt RJ, and Baylis C**. Plasma from ESRD patients inhibits nitric oxide synthase activity in cultured human and bovine endothelial cells. *Acta Physiol Scand* 168: 175-179, 2000.

199. **Xiao S, Wagner L, Mahaney J, and Baylis C**. Uremic levels of urea inhibit L-arginine transport in cultured endothelial cells. *Am J Physiol Renal Physiol* 280: 989-995, 2001.

200. **Xiao S, Wagner L, Schmidt RJ, and Baylis C**. Circulating endothelial nitric oxide synthase inhibitory factor in some patients with chronic renal disease. *Kidney Int* 59: 1466-1472, 2001.

201. **Yin Q-F, and Xiong Y**. Pravastatin restores DDAH activity and endothelium-dependent relaxation of rat aorta after exposure to glycated protein. *J Cardiovasc Pharmacol* 45: 525-532, 2005.

202. **Yoon YS, Uchida S, Masuo O, Cejna M, Park JS, Gwon HC, Kirchmair R, Bahlman F, Walter D, Curry C, Hanley A, Isner JM, and Losordo DW**. Progressive attenuation of myocardial vascular endothelial growth factor expression is a seminal event in diabetic cardiomyopathy: restoration of microvascular homeostasis and recovery of cardiac function in diabetic cardiomyopathy after replenishment of local vascular endothelial growth factor. *Circulation* 111: 2073-2085, 2005.

203. **Yu Y, Terada K, Nagasaki A, Takiguchi M, and Mori M**. Preparation of recombinant argininosuccinate synthetase and argininosuccinate lyase: expression of the enzymes in rat tissues. *J Biochem* 117: 952-957, 1995.

204. **Zani BG, and Bohlen HG**. Transport of extracellular l-arginine via cationic amino acid transporter is required during in vivo endothelial nitric oxide production. *Am J Physiol Heart Circ Physiol* 289: 1381-1390, 2005.

205. **Zatz R, and Baylis C**. Chronic nitric oxide inhibition model six years on. *Hypertension* 32: 958-964, 1998.

206. **Zhang C, Hein TW, Wang W, Miller MW, Fossum TW, McDonald MM, Humphrey JD, and Kuo L**. Upregulation of vascular arginase in hypertension decreases nitric oxide-mediated dilation of coronary arterioles. *Hypertension* 44: 935-943, 2004.

207. **Zhang XZ, Ardissino G, Ghio L, Tirelli AS, Dacco V, Colombo D, Pace E, Testa S, and Claris-Appiani A**. L-arginine supplementation in young renal allograft recipients with chronic transplant dysfunction. *Clin Nephrol* 55: 453-459, 2001.

208. **Zharikov S, Krotova K, Hu H, Baylis C, Johnson RJ, Block ER, and Patel J**. Uric acid decreases NO production and increases arginase activity in cultured pulmonary artery endothelial cells. *Am J Physiol Cell Physiol* 295: C1183-1190, 2008.

209. **Zharikov SI, Herrera H, and Block ER**. Role of membrane potential in hypoxic inhibition of L-arginine uptake by lung endothelial cells. *Am J Physiol* 272: 78-84, 1997.

210. **Zharikov SI, Krotova KY, Belayev L, and Block ER**. Pertussis toxin activates L-arginine uptake in pulmonary endothelial cells through downregulation of PKC-alpha activity. *Am J Physiol Lung Cell Mol Physiol* 286: 974-983, 2004.

211. **Ziai F, Ots M, Provoost AP, Troy JL, Rennke HG, Brenner BM, and Mackenzie HS**. The angiotensin receptor antagonist, irbesartan, reduces renal injury in experimental chronic renal failure. *Kidney Int Suppl* 57: S132-136, 1996.

212. **Zoccali C, Bode-Boger S, Mallamaci F, Benedetto F, Tripepi G, Malatino L, Cataliotti A, Bellanuova I, Fermo I, Frolich J, and Boger R**. Plasma concentration of asymmetrical dimethylarginine and mortality in patients with end-stage renal disease: a prospective study. *Lancet* 358: 2113-2117, 2001.

BIOGRAPHICAL SKETCH

Gin-Fu “Peter” Chen was born in Taipei, Taiwan on January 3rd. He attended the University of Florida in Gainesville, Florida, where he graduated with this Bachelors of Science in microbiology in 2003. In the fall of 2003, he began graduate school in the Interdisciplinary Program in Biomedical Sciences at the University of Florida.

Peter began his career in 1999 in the laboratory of Dr. Janet Yamamoto, at the University of Florida, as a technician working on feline immunodeficiency virus for over 2 years. Then in 2000 he joined the laboratory of Dr. Hazel Jones and studied the genetics of hydrocephalus at the University of Florida. In 2003 he joined Dr. Zhongjie Sun’s laboratory to begin his doctoral work studying the role of endothelin in cold induced hypertension. Dr. Sun left the University of Florida to join Oklahoma University and Peter was unable to follow due to personal reason. So in late 2006 he joined the laboratory of Dr. Chris Baylis studying the role of chronic kidney disease on nitric oxide synthase substrate availability.

On August 3, 2009 Peter successfully defended his dissertation and obtained his Doctorate of Philosophy. Peter continued his career in scientific research as a postdoctoral research associated in the laboratory or Dr. Tohru Fukai at the University of Illinois in Chicago.